

https://dspace.org/

The supply of ecosystem services along an urban-rural gradient, in Johannesburg, South Africa

Jaxa, Busisiwe

2024

University of the Witwatersrand, Johannesburg

https://hdl.handle.net/10539/42003

Jaxa, Busisiwe. (2024). The supply of ecosystem services along an urban-rural gradient, in Johannesburg, South Africa [Master's dissertation, University of the Witwatersrand, Johannesburg]. WireDSpace.

Downloaded from a DSpace repository. https://dspace.org/



The supply of ecosystem services along an urban-rural gradient, in Johannesburg, South Africa

Busisiwe Jaxa (1433341)

Supervisor: Dr U. Schwaibold

School of Animal, Plant and Environmental Sciences

A dissertation submitted to the Faculty of Science, University of the Witwatersrand, Johannesburg in fulfilment of the requirements of the degree of Master of Science

10 June 2023

DECLARATION

I declare that this is my own, unaided work. It is being submitted for the degree of Master of Science as applicable at the University of the Witwatersrand, Johannesburg. It has not been submitted before for any degree or examination at any other University.



Busisiwe Jaxa

10 June 2024

ABSTRACT

Currently, the entire world is experiencing an unparalleled process of urbanisation, which is marked by an increase in population, economic progress, and the spread of urban areas. Although urbanisation presents opportunities such as economic advancement, enhanced infrastructure, and improved living conditions, it also brings about adverse effects on the natural environment. Ecosystem services vary along urban-rural gradients as they are largely affected by land use and land cover change. There is an increasing focus on urban ecosystem services that enhance urban resilience. Nonetheless, there has been minimal research conducted in South Africa regarding the effects of urbanisation on the provision of ecosystem services. This study aimed to investigate the impact of urbanisation on ecosystem services in the greater Johannesburg area and provide a deeper understanding of how the provision of three specific ecosystem services has evolved. These ecosystem services included temperature regulation, flood regulation and carbon sequestration. The land surface temperature (LST) along each gradient was derived from the Landsat (5 TM, 7 ETM+, 8 OLI) datasets available in the Google Earth Engine. Carbon storage was determined by estimating biomass using basic tree measurements. Soil compaction was measured as a proxy for the flood regulation ecosystem service. Lasty, land cover change was also assessed with the use of the ArcGIS software. The findings revealed that the supply of ecosystem services increased with an increasing distance from the city centre. Temperature and soil compaction were found to be high at the urban end of the gradient and carbon storage was found to be low at the urban end of the gradient. The land cover assessment revealed that the City of Johannesburg has suffered a substantial loss of green spaces over the 20 years, as the area covered by built-up surfaces increased. This study, therefore, has how how green spaces in urban areas enhance the sustainability of cities by supporting the supply of various ecosystem services including flood and climate regulation, carbon sequestration and storage. It has also shown that, the rapid urbanisation that the city experienced has led to a reduction in the overall supply of ecosystem services, whilst rural landscapes on the other hand continue to maintain the provision of these services. In order to enhance the green infrastructure in urban areas, it is recommended that, the urban natural systems are integrated in the urban planning and infrastructure initiatives.

Keywords: Ecosystem services; urban green spaces, urban-rural gradient; temperature regulation; flood regulation; carbon sequestration; land cover change.

ACKNOWLEDGEMENTS

Thank you, God Almighty, for granting me the strength and grace to navigate through this journey and reach its completion. I am very grateful to Dr Ute Schwaibold for her assistance and counsel throughout this dissertation. Her encouragement to believe in myself and my potential is greatly appreciated. I would want to convey my gratitude for the time she dedicated to thoroughly assessing my work without voicing complaints. I will remain thankful for the privilege of being under her supervision. I am thankful to the Animal, Plant, and Environmental Sciences staff for facilitating my academic journey in different ways. Thank you to my fellow Master's student Mr Joseph Freimond for your willingness to teach me land surface temperature retrieval, I appreciate the skill I learned from you. I convey deep appreciation to Nthabiseng Jaxa and Rivoningo Maphanga for their invaluable support, dedication, and aid throughout the fieldwork and data collection process. Lastly, I would like to express my gratitude to my mother, Zukiswa Jaxa, for her unwavering support throughout my academic pursuits.

TABLE OF CONTENTS

DECLARATION **2**

ABSTRACT **3**

TABLE OF CONTENTS **5**

LIST OF FIGURES **7**

LIST OF TABLES **9**

CHAPTER 1: INTRODUCTION **10**

1.1 Research gap 12

1.2 Aim and Objectives 12

1.3 Dissertation layout 13

CHAPTER 2: LITERATURE REVIEW **14**

2.1 Urbanisation and its environmental impacts 14

2.2 Urban ecosystem services 17

2.3 Ecological connectivity in urban areas 21

2.4 Global climate change and urban ecosystems 23

2.5 Ecosystem service assessments along urban-rural gradients 24

2.6 Johannesburg and its surroundings 26

CHAPTER 3: METHODOLOGY **28**

3.1 Study area 28

3.2 Site selection 34

3.3 Objective 1: Temperature regulation 37

3.3.1 Fractional vegetation cover 38

3.4 Objective 2: Carbon sequestration 39

3.5 Objective 3: Flood regulation 41

3.6 Objective 4: Land cover change 41

CHAPTER 4: RESULTS **45**

4.1 Objective 1: Temperature regulation 45

4.2 Objective 2: Carbon sequestration 62

4.3 Objective 3: Flood regulation 68

4.4 Objective 4: Land cover change 73

CHAPTER 5: DISCUSSION **78**

5.1 Temperature regulation 78

5.2 Carbon sequestration 81

5.3 Flood regulation 84
5.4 Landcover change. 85
CHAPTER 6: CONCLUSION AND RECOMMENDATIONS 88
REFERENCE LIST 90

LIST OF FIGURES

Figure 1: The Gauteng province, City of Johannesburg and its urban edge, South Africa. 29
Figure Google 2: The city of Johannesburg and the land cover in the city. 30
Figure 3: The two urban-rural gradients of the study, from Johannesburg CBD, the urban extreme to Hartbeespoort (gradient (A)) and Vaal (gradient (B)), the rural extremes (Google Earth Pro, 2024). 33
Figure 4: Gradient A, from Johannesburg CBD, the urban extreme to Hartbeespoort the rural extreme (Earth Pro, 2024). 34
Figure 5: Gradient B, from Johannesburg CBD, the urban extreme to the Vaal, the rural extreme (Google Earth Pro, 2024). 35
Figures 6a-c: Land Surface Temperature (LST) maps of the city of Johannesburg, South Africa for the years 2001 (a), 2006 (b), and 2011 (c). 46
Figures 6d-e: Land Surface Temperature (LST) maps of the city of Johannesburg, South Africa for the years 2016 (d) and 2021 (e) 47
Figure 7: Mean (± SE) land surface temperature along the urban-rural gradient, over a period of two decades. 48
Figure 8: The relationship between the land surface temperature (°C) and the distance from the city centre (km) along gradient A. 49
Figure 9: Relationship between the land surface temperature (°C) and time along gradient A. 50
Figure 10: Mean (± SE) land surface temperature(°C) for each land use type along gradient A. ...51
Figure 11: Mean (± SE) land surface temperature difference (°C) between site 1 and all the other sites along gradient A (1= CBD, 2 = Urban Park, 3 = Urban Park, 4 = Urban Park, 5= Residential, 6=Residential, 7 = Highway, 8 = Highway, 9 = Nature Reserve, 10 = Nature Reserve, 11= Nature Reserve, 12 = Residential). 52
Figure 12: Mean (± SE) land surface temperature (°C) along the urban-rural gradient B for the years 2001, 2011 and 2021. 53
Figure 13: The relationship between the land surface temperature (°C) and the distance from the city centre (km) along gradient B. 53
Figure 14: Relationship between the land surface temperature (°C) and time along gradient B.....54
Figure 15: Mean (± SE) Land surface temperature (°C) for each land use type along gradient B. .55
Figure 16: Mean (± SE) land surface temperature difference Δ LST (°C) 56
Figure 17: Mean (± SE) fractional vegetation cover across gradient A.....57
Figure 18: Mean (± SE) fractional vegetation cover at each land use type along gradient A. 58
Figure 19: The relationship between fractional vegetation cover on the LST (°C) for gradient A. 59
Figure 20: The Mean (± SE) fractional vegetation cover across gradient B.....60

Figure 21: Mean (± SE) fractional vegetation cover for each land use type along gradient B. 61
Figure 22: The relationship between fractional vegetation cover and land surface temperature for gradient B 62
Figure 23: Mean (± SE) stored carbon (ton/ha) along gradient A 63
Figure 24: Relationship between stored carbon (ton/ha) and distance from the city centre (km) along gradient A. 63
Figure 25: Mean (± SE) stored carbon for each land use type along gradient A 64
Figure 26: Mean (± SE) stored carbon (ton/ha) for every five years, from 2001 to 2021. 65
Figure 27: Mean (± SE) stored carbon (ton/ha) along gradient B 66
Figure 28: Relationship between stored carbon (ton/ha) and distance from the city centre (km) along gradient B. 66
Figure 29: Mean (± SE) stored carbon at each land use type along gradient B. 67
Figure 30: Mean (± SE) stored carbon (ton/ha) along gradient (B) for every five years, from 2001 to 2021 68
Figure 31: Mean (± SE) soil compaction measurements (kg/cm2) along Gradient A 69
Figure 32: Relationship between soil compaction (kg/cm^2) and distance from the city centre (km) along gradient A. 69
Figure 33: Mean soil compaction readings for each land use type along gradient A. 70
Figure 34: Mean (± SE) soil compaction measurements (kg/cm2) along the urban-rural gradient (B) 71
Figure 35: Linear regression showing the change in soil compaction (kg/cm^2) over the distance from the city centre (km) along gradient B. 72
Figure 36: Mean (± SE) soil compaction readings for each land use type along gradient B. 72
Figure 37: Land cover maps of the northern gradient (gradient A), for the years a) 2001, b) 2011, and c) 2021. 74
Figure 38: Land cover maps of the southern gradient (gradient B), for the years a) 2001, b) 2011, and c) 2021. 76

LIST OF TABLES

Table 1: Land cover and land use description of the site's locations along gradient A.....35
Table 2: Land cover and land use description of the site's locations along gradient B.....36
Table 3: Description of land cover classes identified (as per Rwanga and Ndambuki, 2017). 42
Table 4: Land use classification accuracy for the year 2001. 43
Table 5: Land use classification accuracy for the year 2011. 44
Table 6: Land use classification accuracy for the year 2021. 44
Table 7: The Kruskal Wallis multiple comparisons post hoc test for LST at different land use types, at the 95% and 99% confidence level.....49
Table 8: Kruskal Wallis Multiple comparison post hoc test for Δ LST °C at a 99% and 95% confidence level. 52
Table 9: Tukey HSD multiple comparisons of means post hoc test, at 95% confidence level.....54
Table 10: Tukey HSD multiple comparisons of means post hoc test results for temperature difference, at 95% confidence level.....56
Table 11: The Kruskal Wallis multiple comparisons post hoc test for FVC, at the 95% and 99% confidence level. 58
Table 12: The Kruskal Wallis multiple comparisons post hoc test for FVC at the 95% and 99% confidence level. 60
Table 13: Kruskal Wallis multiple comparisons post hoc test, at the 95% and 99% confidence level.....64
Table 14: Kruskal Wallis multiple comparisons post hoc test, at the 95% and 99% confidence level.....67
Table 15: The Kruskal Wallis multiple comparisons post hoc test, at the 95% and 99% confidence level for FVC. 70
Table 16: The Kruskal Wallis multiple comparisons post hoc test, at the 95% and 99% confidence level.....73
Table 17: Changes in land cover area along gradient A. 75
Table 18: Area changes in the Land Cover in gradient B.....77

CHAPTER 1: INTRODUCTION

Ecosystems function as inherent support systems that protect the Earth's environment. Nevertheless, human activities, originally intended to advance economic growth and human welfare, have significantly compromised these supportive networks (Fang *et al*., 2019). Urban areas are expanding rapidly worldwide, and this expansion is exerting a notable influence on the natural ecosystems in their vicinity (Theodorou, 2022). Ecosystems in an urban context or urban ecosystems refer to the natural, semi-natural, or controlled communities of organisms and habitats located inside urban limits. These include the remaining, largely unaltered vegetated regions (for example, forests and riparian corridors), as well as properly managed urban green spaces like gardens and parks. Furthermore, this concept expands to encompass vegetation on structures like green roofs and green walls, in addition to traditional natural landscapes (Tan *et al*., 2020).

Urban green spaces, an element of urban ecosystems, are the areas that are covered with vegetation in cities, such as parks, forests, gardens, street vegetation, vacant lots, green roofs and walls, as well as wetlands (Peng *et al*., 2022). The proportion of natural, artificial, and hybrid spaces that make up urban ecosystems varies greatly from one town to the next (Threlfall and Kendal, 2018). Green spaces within urban areas are believed to enhance the sustainability of cities by providing a wide array of ecosystem services, including support for biodiversity, carbon absorption, and regulation of floods and climate (Ayala-Azcárraga *et al*., 2019). They mitigate some of the environmental degradation caused by rapid urbanisation (Peng *et al*., 2022). For instance, urban green spaces have a crucial role in conserving flora and fauna, maintaining water resources, and minimising air pollution in densely populated urban areas. Green areas are effective at improving environmental conditions, they create cool islands in congested urban areas and thus provide thermal comfort. Lastly, urban green spaces act as wildlife corridors to promote the migration of wildlife, thus minimising the fragmentation and isolation of species (Vargas-Hernández *et al*., 2018).

While urban areas offer avenues for economic growth and human progress, they also represent sources of environmental harm caused by human actions (Nhamo *et al*., 2021). Urbanisation processes, which often involve the expansion onto natural landscapes, lead to ongoing degradation and depletion of natural habitats, consequently, diminishing ecosystems' ability to provide essential ecosystem services (Cullis *et al*., 2019; Mudede *et al*., 2020; Cao *et al*., 2021). Urban pollution, for instance, affects water quality. Wetland destruction through construction and pit mining hampers flood regulation (Gupta *et al*., 2017). Deforestation affects the air and temperature regulation services that are usually supplied by trees (Cao *et al*., 2021). Furthermore, alterations in the structure

of the natural environment intensify the vulnerability of city dwellers to the risk of hazards such as floods, summer heatwaves, extreme storms and other natural disasters (Gupta *et al*., 2017).

Research to date has focused extensively on investigating the relationship between urbanisation and ecosystem service provision (Kuang *et al*., 2021), with the main point of focus being on the dynamics of the provision of ecosystem services (ES) that result from land transformation. However, the full assessment of urban characteristics, including its economy, population, and built-up land expansion, was rather limited in scope (Li *et al*., 2022). In the past few years, numerous research investigations have explored the interaction between the supply and demand of ecosystem services within the framework of urbanisation and spatial compatibility (Deng *et al*., 2021; Wang *et al*., 2022). Moreover, multiple studies have considered urban centres as an intricate network structure with notable differences in gradients and heterogeneity (Kuang *et al*., 2021; Zhang *et al*., 2021). Zhang *et al*. (2021) conducted research to analyse how urbanisation indicators influence the equilibrium between the supply and demand of ecosystem services in areas characterized by different levels of urban development. At present, the process of urbanisation is mostly focused on socioeconomic factors, as highlighted by Kuang *et al*. (2021). Nevertheless, the identification of primary function-oriented zones considers both national spatial management and the interaction between the natural ecological system and the socioeconomic system (Li *et al*., 2022).

The urban-rural gradient approach is frequently employed to describe the shift from human-influenced areas to natural environments. This method has also been acknowledged as a valuable tool for investigating the expansion of urban areas and their impacts on landscapes (Yang *et al*., 2018). Larondelle and Haase (2013) introduced an evaluation methodology for ecosystem services within urban settings, extending over both local and regional scales across various European cities. The study successfully demonstrated that core cities do not inevitably offer a lesser quantity of ecosystem services in comparison to their surrounding regions. Moreover, the findings of the study indicate that a high degree of impervious surface coverage does not lead to a complete cut-off in ecosystem service provision. This is because urban areas may contain a considerable number of mature trees that contribute to carbon storage and biodiversity. Baro *et al.* (2017) undertook a study to evaluate the ecosystem service bundles along the urban-rural gradient. The results of this research indicated that adopting land-sharing initiatives in urban and rural areas can improve the multifunctionality of the landscape. Furthermore, it is imperative to prioritise the preservation of expansive peri-urban forest regions, since they serve a vital function in delivering a wide array of local ecosystem services that are highly sought after by urban dwellers. Wang *et al*. (2022) conducted a study using the urban-rural gradient approach to examine how large-scale, dispersed

agglomeration urbanisation affects ecosystem services at different levels of urbanisation throughout a region. The research findings indicated that increased urbanisation is the main factor that influences the value of ecosystem services.

1.1 Research gap

Urban ecology and urban ecosystem services, which bolster urban resilience, have garnered increasing attention (Russo and Cirella, 2021). Nevertheless, research on the effects of urbanisation on ecosystem service provision remains sparse in South Africa. With a limited understanding of ecosystem service supply along urban-rural gradients in the region, this study aimed to shed light on urban-induced alterations in ecosystem services and to enhance comprehension of changes over time in the provisioning of three ecosystem services. Li *et al*. (2016) revealed that ecosystem services loss happens at a faster rate due to urbanisation, and the ecosystems that provide the services in urban areas are usually in poorer conditions than those in rural areas. With the knowledge that fragmentation and urbanisation are the key threats to ecosystem services and biodiversity, I tested this effect in one of the biggest cities in South Africa. South African cities have a unique urban topography as a result of their intricate and unequal growth, which has been shaped by their colonial and apartheid past (Baffi *et al*, 2018; Totaforti, 2020). This has led to a very uneven urban system, characterised by a prominent central city and an urban form and land use patterns that are influenced by a colonial past (Merwe, 2016). Although the country possesses distinctive qualities, its process of urbanisation follows worldwide trends when considering the effects it has on the destruction and fragmentation of natural habitat, which pose a threat to native species and ecosystems (Symes *et al*., 2017; Liu *et al.,* 2016; Gambe *et al*., 2023). Nevertheless, the swift urbanisation in South Africa poses notable challenges, such as overburdened infrastructure and environmental concerns (Massey, 2019).

1.2 Aim and Objectives

This research aimed to assess the supply of three ecosystem services in Johannesburg, South Africa and how they have changed over time and along two urban-to-rural (peri-urban) gradients.

To fulfil the aim, the following objectives were established:

1. to determine the supply of the temperature regulation ecosystem service from 2001 to 2021.
2. to estimate the supply of the carbon sequestration ecosystem service from 2001 to 2021’
3. to determine the current supply of flood regulation.

4. to assess the change in land cover from 2001 to 2021.

1.3 Dissertation layout

This dissertation is made of five chapters;

Chapter 1: Introduction and Literature Review, this chapter offers an overview of the research problem, the overall aim, and the specific objectives of the dissertation. Chapter 2: Urbanisation and Ecosystem Services. This chapter provides an in-depth review of urbanisation and its broad-ranging effects, particularly on ecosystem services. It includes a detailed explanation of the specific ecosystem services examined in this study and how climate change influences these services. Additionally, the urban-rural methodology used in this study is discussed. Chapter 3: Methodology, this chapter provides a comprehensive explanation of the research design and methodologies employed throughout the study. It includes the methodology used for collecting data on land surface temperature, carbon storage, and soil compaction, as well as the approach used for assessing land cover change and subsequent data analysis. Chapter 4: Results, this chapter presents the outcomes of the study in line with the objectives, featuring tables, maps, graphs, and descriptive text. Chapter 5: Discussion and Conclusion, the discussion section of the study presents the reasoning behind the results and draws upon relevant and recent literature to further explain the findings. Finally, the chapter presents an overall conclusion of the study as a whole.

CHAPTER 2: LITERATURE REVIEW

The term "urbanisation " refers to the movement of a significant number of people migrating from rural areas to towns and cities, and the consequent expansion of these cities and towns on undeveloped land (Kuddus *et al*., 2020; Warr, 2020). As a result of this, land cover attributes are altered, thus changing the composition, dynamics and functioning of ecosystems (Mao *et al*., 2019). Urban areas are defined by their compact construction, the existence of artificial structures, extensive and impermeable surfaces characterised by densely built-up spaces and the presence of man-made structures, large areas of impermeable surfaces, and high concentrations of native and non-native flora and fauna (LaPoint *et al.*, 2015).

The world is experiencing an unprecedented trend of urbanisation marked by a surge in population, economic advancement, and the expansion of urban areas and towns (Yang *et al*., 2018). The United Nations (2018) predicts that by 2050, 68% of the global population will reside in cities. This rapid growth in human population has hastened transformations in the Earth's biosphere (Pandey *et al*., 2020) due to human-induced activities, leading to climate change and a swift decline in biodiversity (Folke *et al.*, 2021). Anthropogenic actions have significantly modified the Earth's ecosystems, including the alteration and degradation of natural habitats resulting from urbanisation (Mayer-Pinto *et al*., 2018).

2.1 Urbanisation and its environmental impacts

Whilst urbanisation offers opportunities such as economic growth, improved infrastructure and better living standards (Nathaniel, 2021), it also has detrimental effects on the natural environment (Nhamo *et al*., 2021). Urbanisation is associated with the loss of habitats through significant land-use changes (Egoh *et al*., 2012). Habitat loss refers to the decrease in the physical area of natural habitats (Liu *et al*., 2016). Habitat fragmentation, on the other hand, refers to the process of separating or dividing a habitat into smaller pieces, while accounting for the effects of habitat loss (Liu *et al.*, 2016). Urbanisation has been accelerating across the world and has become a significant contributor to habitat loss and fragmentation (Nathaniel, 2021), as large areas of habitat are converted to impervious surfaces (Liu *et al.*, 2016), leading to a decline in animal and plant biodiversity (Mayer-Pinto *et al.*, 2018).

Biological invasions

Urban environments are susceptible to invasions by non-native plant and animal species, as they serve as focal points for the propagation of these species for purposes such as decoration, aquaculture, and trading of pets (Potgieter *et al*., 2020). Consequently, the diversity of native plants

and animals tends to be lower in urban areas compared to rural regions. Urban infrastructure often facilitates a higher abundance of invasive species, promoting their spread and establishment while not offering adequate habitat for indigenous species (Mayer-Pinto *et al*., 2018). For instance, *Jacaranda mimosifolia* also known as Jacaranda, is an aesthetically exceptional invasive plant that was brought to the Gauteng cities as an ornamental plant, particularly in the suburbs of Pretoria and Johannesburg, and has now spread extensively in these suburbs (Fitchett and Raik, 2021). Invasive flora in cities has been linked with the propagation of human illnesses, lowered biodiversity and infrastructure damage (Potgieter *et al.,* 2020). Over the past 150 years, urban expansion in Johannesburg and extending to the greater Gauteng metropolitan area has led to the conversion of vast grassland areas into urban woodlands. This transformation has altered the local species composition, with a notable increase in invasive species correlating positively with the rise in land transformation (Symes *et al*., 2017). Several inland impoundments in South Africa, notably the Hartebeespoort and Roodeplaat dams as well as large river systems such as the Vaal River, are infested by alien invasive populations such as Water lettuce (*Pistia stratiotes*) and Water hyacinth (*Eichhornia crassipes*) that reduce the value of waterfront properties and obstruct access to sporting and recreational areas. These effects are detrimental to the economies of communities whose livelihoods depend on fishing, tourism, and water activities (Hill *et al*., 2020).

Hydrological cycle

Urbanisation also alters the hydrological cycle, which further feeds back into water quality and quantity. Impervious surfaces result in among others, reduced groundwater filtration, and as a result increased surface runoff. Water temperatures often seem to be higher in urbanised areas than in rural regions because there is less shading due to reduced vegetation cover. The surrounding impervious surfaces which are warmer and have high thermal conductivity contribute to the warming of urban water bodies (Taka *et al.,* 2015). The surface runoff from cities also carries a variety of harmful substances such as excess nutrients, debris, heavy metals, and synthetic rubber deposits from roads (McGrane, 2016). The quantity and quality of the water are also degraded as a result of over-usage, including agricultural and industrial production. This has significant impacts on aquatic ecosystems and also limits access to safe drinking water (Khatri and Tyagi, 2015).

Warming of the local climate

Urbanisation, marked by increased population densities and land conversion, stands as the principal driver behind the urban heat island effect (Sadiq Khan *et al*., 2020; Veena *et al*., 2020). Urban areas consistently exhibit very high temperatures in relation to their surrounding rural counterparts, largely due to factors like industrialization, transportation, and reduced vegetation (Halder *et al*.,

2021). Surfaces in urban areas, such as concrete and asphalt, possess the capacity to absorb solar radiation and subsequently release it as heat into the atmosphere (Santamouris *et al*., 2019). The interplay between vegetation and buildings significantly influences land surface temperatures; areas with greater building coverage and less vegetation tend to experience higher temperatures (Alexander, 2021). Mandelmilch *et al*. (2020) demonstrated that the southern region of Tel Aviv, Israel, experienced temperatures approximately 7-9 degrees Celsius higher than its northern, vegetation-covered counterpart, attributed to a scarcity of vegetation in the southern section. In southeast Brazil, Portela *et al*. (2020) found that elevated land surface temperatures were concentrated primarily in urban and industrial regions characterized by construction structures, impermeable surfaces and pavements, and low vegetation cover. Additionally, Marcotullio *et al*. (2021) revealed a connection between dense urban configurations and elevated temperatures across the majority of tropical climate zones.

Flood risk

The expansion of urban areas heightens the risk of flooding. As impermeable surfaces increase, surface infiltration rates decrease, leading to higher peak flood discharges and soil erosion (Feng *et al*., 2021). Consequently, cities face a greater environmental flood risk compared to rural regions (Miller and Hess, 2017). Urban areas are particularly vulnerable to "pluvial" flooding, occurring when precipitation surpasses the capacity of stormwater drainage systems or the ground's ability to absorb water. This results in waterlogging and increased surface runoff within urban areas (Saurav *et al*., 2021). Soil compaction in urban areas, caused by factors like traffic and construction, reduces oxygen availability for plant roots, hindering water and nutrient transport to the roots and increasing susceptibility to floods (Clinton and Owens, 2023). Natural hydrological features such as wetlands and rivers play a critical role in flood mitigation by absorbing and retaining excess water. However, urban activities often compromise the integrity of these systems, leading to reduced water body sizes and floodplain contractions, thereby exacerbating urban flood occurrences (Singh *et al*., 2023). In many instances, unanticipated urban growth exerts excessive pressure on the city's drainage infrastructure, resulting in an increased volume of surface runoff (Singh *et al*., 2023). In addition, urban areas with low topographical relief and inadequate drainage systems become susceptible to flood events. This has a negative impact on many socio-economic systems, like the agriculture industry and infrastructure (public and private) (Pattison-William *et al.*, 2018). In a study conducted by Huang (2019), it was found that urban sprawl increases the vulnerability of urbanised areas to flood damage, even from small-scale rainfall events. In Zhengzhou, China, urbanisation exacerbates the rain island effect, resulting in earlier flood peaks and higher runoff (Wang *et al*., 2020).

Urbanisation also increases bed mobilisation, reduces retentive habitat, and lowers floodplain inundation in streams (Anim *et al*., 2018).

Air pollution

Urbanisation is widely acknowledged as a significant contributor to the global issue of air pollution, primarily due to the concentration of anthropogenic activities within a relatively small area, including infrastructure development, electricity generation, and industrial production. Anderson and Gough (2020) highlight that a considerable portion of greenhouse gas emissions stems from these urban activities. Urbanisation also impacts urban meteorology, influencing the presence and distribution of ambient air pollutants. Particulate matter (PM1.0, PM2.5, and PM10), nitrogen oxides (NOx), and ozone (O3) pollution pose significant public health concerns (Singh *et al*., 2020). The generation of electricity, a major source of greenhouse gas emissions globally, is particularly pronounced in urban areas due to their higher electricity demand compared to rural areas. This expansion of urban areas consequently increases the need for electricity, leading to substantial emissions of pollutants (Wang, 2019). Industrial zones, often located within or on the outskirts of urban areas, emit significant quantities of pollutants such as carbon monoxide, hydrocarbons, particulate matter, and various chemicals into the atmosphere, contributing significantly to air pollution (Lu *et al*., 2021; Luo *et al*., 2023).

The use of automobiles in urban settings also contributes to atmospheric emissions, releasing pollutants like carbon monoxide (CO), nitrogen oxides (NOx), sulphur oxides (SOx), particulate matter (PM10 and PM2.5), volatile organic compounds (VOCs), and ozone (Piracha and Chaudhary, 2022). Furthermore, the combustion of fossil fuels for household activities such as cooking, heating, and cleaning in residential settings significantly impacts air quality (Yun *et al*., 2020). A study in China indicated that around 30% of premature deaths associated with ambient air pollution in 2010 were linked to residential emissions (Lelieveld *et al*., 2015). Additionally, rapid urbanisation often results in the clearance of vegetation, which provides crucial air regulation services that are lost with the disappearance of green spaces.

2.2 Urban ecosystem services

The many benefits human beings and animals derive from ecosystems are known as ecosystem services that are functioning effectively (Costanza *et al*., 2017). The following are four clearly defined categories of ecosystem services, specifically; provisioning services refer to tangible goods that are derived from the ecosystem. Supporting ecosystem services refers to services that facilitate the generation of other services, such as the production of primary productivity and the cycling of nutrients. Cultural services refer to intangible advantages derived from ecosystems, including

educational, spiritual, and aesthetic benefits that contribute to human well-being. The final category encompasses the regulatory ecosystem services, which refer to the services that govern the natural environment, including the regulation of floods, temperature, and air quality (Weiskopf *et al*., 2020). Different urban environments provide unique ecological services (Milliken, 2018). Community farms, private gardens, and allotments serve as vital sources of sustenance, including food, medicinal plants, and certain raw materials. Street trees and urban park trees play a crucial role in providing important regulating functions such as temperature control, enhancement of air quality, and storage of carbon (Milliken., 2018). Urban parks offer cultural services through the provision of recreational and educational advantages (Cheng *et al*., 2019). Urban green patches also function as supplementary ecosystems by offering habitats for other species and facilitating nutrient cycling (Milliken, 2018).

In cities, ecosystem services are supplied by various landcover types, including green areas such as urban parks, household and community gardens as well as urban forests, as well as blue spaces (part of blue infrastructure) which include lakes, rivers and ponds. The green and blue infrastructure in cities supports numerous services that assist in attenuating or combating some of the impacts that are associated with urbanisation. For instance, green spaces regulate the local climate (Elmqvist *et al*., 2015). The process of collecting rainwater by plant foliage and permeable soils in towns and cities can alleviate the strain on urban drainage systems and mitigate the risk of floods (Feng *et al*., 2021). Urban vegetation also helps to cleanse the air by removing contaminants such as carbon monoxide (CO), ozone (O_3) and sulphur dioxide (SO_2) (Gómez-Baggethun and Barton, 2013a). Mangroves, for example, act as natural barriers protecting coastal cities from severe weather conditions such as thunderstorms and floods (Gómez-Baggethun and Barton, 2013b). Urban ecosystem services have the potential to increase an urban area's resilience by protecting it from various climatic impacts (Elmqvist *et al*., 2015). Numerous ecosystem services are deemed crucial in urban settings due to their role in enhancing the city's ability to adapt to the impacts of climate change (IPCC, 2013). Green spaces offer essential ecosystem services such as flood control, temperature regulation, and carbon sequestration (Elmqvist *et al*., 2015), which are pivotal for urban ecological security (Peng *et al*., 2020). With urban areas projected to expand rapidly in the future (Yang *et al*., 2018), it becomes imperative to comprehend urban ecosystem services and safeguard the ecosystems that supply them.

2.2.1 Temperature regulation

In urban areas, elevated temperatures are a common occurrence, largely due to impermeable surfaces contributing to the urban heat island effect (Pace *et al*., 2021). However, green

infrastructure plays a crucial role in mitigating these temperature extremes by enhancing cooling, providing shade, and promoting evapotranspiration from trees and vegetation (Tiwari *et al*., 2021). Urban tree shade lowers the total heat energy, thus adjusting the city's energy balance and cooling the urban canopy (Upreti *et al*., 2017). Shading changes the radiation energy balance by reducing the short-wave radiation input, thereby decreasing the temperature in shaded areas. Trees play a significant role in blocking the sun's rays from reaching buildings in cities, thereby reducing the need for air conditioning and decreasing energy consumption. Additionally, trees offer comfort to both humans and animals during hot days (Cao *et al*., 2021). A study conducted in Rosebank, a suburb located in the northern suburbs of Johannesburg with abundant street trees, and Soweto, a township in the west of Johannesburg with fewer roadside trees and green spaces, found that land surface temperatures in Soweto were 2.58 °C higher than in Rosebank. This suggests that densely populated areas with limited greenery tend to experience higher temperatures compared to less densely populated suburbs with more green spaces and street trees (Mudede *et al*., 2020).

Evapotranspiration is the loss of water from plants in the form of vapour, which results in the cooling of the leaf and reduces local temperatures; for the water to be transformed into vapour, the ambient heat is absorbed, causing the air temperature to drop (Gkatsopoulos, 2017). A 30% increase in the tree layer might cause a 5 - 6 °C temperature reduction in the surrounding area (Gkatsopoulos, 2017). This could therefore save on energy that goes into air conditioning. City trees provide cooling, and this can, as a result, lead to a cut in carbon emissions through lower energy demand (Elmqvist *et al*., 2015).

1.3.2 Flood regulation

Floods, often resulting from extreme storm and rainfall events exacerbated by climate change, pose significant risks of property damage and loss of life (Gupta *et al*., 2017). The built-up infrastructure and impervious urban surfaces make cities even more vulnerable to flooding, however, urban forests, parks, gardens and other vegetated areas reduce runoff through infiltration as the roots of the vegetation allow the water to percolate through the soil layer (Locatelli, 2016). Bera *et al*. (2022) utilized the Natural Resources Conservation Service Curve Number model to analyze changes in surface runoff across an Indian city. Their study revealed a notable increase in surface runoff on impermeable surfaces, whereas areas with higher proportions of urban green spaces experienced reduced surface runoff. The research identified a significant 54% increase in impermeable surfaces and a corresponding decrease in permeable areas between 1986 and 2016, attributed to the unplanned and unregulated expansion of metropolitan areas. This surge in impervious surfaces has been linked to the exacerbation of floods in the city. A study conducted by Abass *et al*. (2020) investigated the impact of urbanisation on the depletion of green spaces and its consequences for

urban flood occurrence in a town in Ghana. The research revealed a notable increase of 54% in impermeable surfaces between 1986 and 2016, accompanied by a corresponding drop in permeable areas at the same rate. This phenomenon can be attributed to the unplanned and unregulated expansion of metropolitan areas over the specified time frame. The exacerbation of floods in the town can be linked to the significant increase in impervious surfaces resulting from urban growth.

Flood regulation refers to the attenuation of floods by vegetated areas and wetlands as well as the groundwater recharge by the vegetative cover (Turpie *et al.,* 2017). Flood-controlling ecosystems are those that assist with absorbing excess water in times of flood and prevent cities from flooding. Floodplains and wetlands retain excess water during times of high rainfall, thus they attenuate floods (Feng *et al*., 2021). Wetlands, for example, play an ecological role in flood attenuation by holding excess water, and wetland plants have a sponge-like function, trapping and slowly distributing the water over the floodplain. Wetlands within and downstream of cities are then beneficial as they help to mitigate the high rate of surface runoff from impermeable surfaces (Balwan and Kour, 2021). Urban landscapes with impermeable surfaces can lose approximately 40-80% of rainwater to surface runoff, while forests only lose approximately 13% of the rainfall input to surface runoff, the rest is absorbed by the ground. Green roofs, depending on factors such as root length, roof angle, and rainfall intensity, can retain 25% to 100% of rainwater, thereby alleviating pressure on sewer systems (Pataki *et al*., 2011). Kim's study (2021) suggests that a higher proportion of green spaces within urban areas may reduce the likelihood of flooding events. A one-square-kilometre increase in green space could potentially lead to a $44,099 reduction in financial insurance payments related to flooding, while the absence of green spaces could result in an increased insurance cost of $691,094. Wu *et al*. (2020) utilized a distributed hydrological modelling platform to assess the impact of wetlands on flood events in a river basin in Northeast China. Their findings indicated that wetlands could reduce peak and mean flows, event duration, and runoff volume by up to 24% (equivalent to 12.14 mm). These results underscore the importance of flood regulation services provided by wetlands and their role in enhancing resilience against flood occurrences in large river basins.

1.3.3 Carbon sequestration

In addressing the impacts of climate change, carbon sequestration and storage in soils and vegetation emerge as vital ecosystem services (Davies *et al*., 2013). Carbon dioxide, a prevalent greenhouse gas and a major contributor to global climate change, primarily stems from the combustion of fossil fuels and deforestation (Udara Willhelm Abeydeera *et al*., 2019). Urbanisation has been linked to

elevated atmospheric carbon dioxide concentrations, attributed to increased transportation and industrialization, both heavily reliant on fossil fuels like oil and coal (Ma *et al*., 2019).

Carbon sequestration is crucial in mitigating emissions (Ma *et al*., 2019). Urban trees and other vegetation types are pivotal for carbon sequestration and storage (Tak and Kakde, 2020). In a study by Sharma *et al*. (2020), the capacity of carbon sequestration in 1997 trees across 45 species was assessed. The findings revealed that trees not only possess aesthetically pleasing qualities but also act as significant carbon reservoirs, storing a substantial amount of 139.9 tonnes of carbon. Carbon sequestration involves actively removing carbon from the atmosphere in the form of carbon dioxide, while carbon storage refers to the mechanism by which a carbon sink retains carbon as part of itself over time (Arehart *et al*., 2021).

Urban green spaces serve as carbon sinks by capturing carbon dioxide through photosynthesis and storing the excess carbon in plant components such as wood (Tak and Kakde, 2020). South African studies have demonstrated that thickets and forests exhibit a high potential for carbon storage, making urban forests crucial for carbon dioxide removal from the atmosphere and sequestering significant amounts of carbon as urban areas expand (Pataki *et al*., 2011; Tak and Kakde, 2020). Additionally, Shafique *et al*. (2020) showed that green roofs, as part of urban green infrastructure, contribute to carbon emission reduction in urban areas. They achieve this by absorbing carbon dioxide through photosynthesis and storing it in plant tissues and roots for the duration of the green roof's existence. Furthermore, Klein *et al*. (2021) discovered that trees in New York City's borough of Manhattan sequestered a total of 52,000 tons of carbon, underscoring the substantial carbon sequestration potential of urban trees.

2.3 Ecological connectivity in urban areas

Ecosystem services are progressively being assessed by various disciplines (Mandle *et al*., 2021). Nevertheless, a comprehension of the spatial attributes of the physical environmental attributes has not been sufficiently developed (Mandle *et al*., 2021). Ecosystem connectivity is the degree to which an ecosystem facilitates or hinders the movement of species between different habitat areas, enables the exchange of energy, and supports the maintenance of biodiversity. This connectivity is crucial for the continued provision of ecosystem services (Pelorosso *et al*., 2016).

In urban areas, ecological functions and biological diversity are sustained in the habitat patches that are spared during development, these are known as urban green spaces, habitat patches or natural areas. Green spaces within cities play a critical role in providing ecosystem services. Forests, parks,

and wetlands support biodiversity, help stabilize the local climate, sequester carbon from the atmosphere, and facilitate groundwater recharge (Semeraro *et al*., 2021). These spaces are essential for preserving both fauna and flora (McGrane, 2016). A study conducted by Vega and Kuffer (2021) found a significant positive correlation between species richness and the size of habitat patches assessed in an urban area. Additionally, it was observed that the overall biodiversity within a patch was positively influenced by its proximity to other green spaces, particularly within a range of 50-200 meters. Therefore, establishing connections between these patches could unlock their full potential as urban green spaces.

Urban green areas exhibit significant diversity due to exposure to various disturbances, but their functionality is limited when they remain isolated from each other (Paudel and States, 2023). Urbanisation, coupled with population growth, has led to a reduction in the number and size of natural habitat patches (Abutaleb *et al*., 2021). The presence of urban infrastructure, such as road networks, significantly impacts ecosystem connectivity by fragmenting habitat into smaller, disconnected areas, thus impeding wildlife movement and reducing overall ecosystem connectivity (Crookes *et al*., 2013).

A recent study conducted by Wu *et al*. (2022) in the Guangdong-Hong Kong-Macao Greater Bay Area revealed a notable negative correlation between the level of urbanisation and the ecosystem health index. This index measures changes in ecological processes to quantify the relative risk of ecosystem collapse from biotic or environmental degradation. The researchers also observed a decline over time in the ecosystem health index of the city. Overall, urbanisation has had a significant adverse impact on the health of ecosystems, particularly in the central urban areas of the greater Bay Area.

In Africa, rapid urbanisation, population growth, pollution, and unsustainable land use are posing significant threats to urban green spaces (McKay and Tantoh, 2021). Despite this trend, South Africa, being the most urbanized country in Africa, faces challenges of physical disconnection between its urban populations and nature. However, Johannesburg stands out as home to the largest urban forest globally, renowned for its diverse array of native and non-native tree species (Fitchett and Raik, 2021). Over the past century, approximately 16.1% of the Johannesburg area has been covered by trees, interconnected by green spaces (Fitchett and Raik, 2021).

The preservation and strategic arrangement of green spaces play a crucial role in fostering biodiversity within urban environments. However, the significance of urban biophysical networks in providing essential ecosystem services for enhancing urban resilience has been largely overlooked in academic research (Fitchett and Raik, 2021).

2.4 Global climate change and urban ecosystems

Climate change is characterized by variations in the state of the climate, including changes in mean and variability of temperature, precipitation, and other factors (IPCC, 2013). These changes in average weather conditions, such as rising temperatures and altered rainfall patterns, are indicative of climate change impacts (City of Tshwane, 2015). Urban centres, due to their industrial activities emitting greenhouse gases like methane, chlorofluorocarbons, carbon dioxide, and nitrous oxide, are significant contributors to climate change (Govindarajulu, 2014; Onur and Tezer, 2015). However, they are also highly susceptible to its effects, including increased temperatures, extreme weather events, altered precipitation patterns, and sea-level rise in coastal cities (Onur and Tezer, 2015). The severity of these effects is influenced by the extent and quality of ecosystem services within cities (Mngumi, 2020). Urbanisation exacerbates these vulnerabilities by impeding temperature regulation and stormwater absorption, leading to increased local temperatures and surface runoff (Onur and Tezer, 2015).

Africa is particularly susceptible to climate change due to its high exposure and low adaptive capacity (Niang *et al*., 2014). The IPCC's sixth assessment report predicts average temperature increases of at least 2°C in Africa by the mid-21st century, with much of the continent already experiencing warming and increased heatwaves (IPCC, 2021). Additionally, southern Africa is experiencing decreased mean precipitation and is projected to face drier conditions and increased droughts by mid-century (IPCC, 2021).

Urban regions must cultivate resilience to diverse shocks in order to adequately prepare for the repercussions of climate change (Borsekova *et al*., 2018). Urban resilience involves the capacity of cities to withstand and mitigate shocks while safeguarding their social, economic, and infrastructural systems (Büyüközkan *et al*., 2022). Incorporating ecosystem services into urban development plans can enhance resilience by strengthening adaptive capacity (Büyüközkan *et al*., 2022; McPhearson *et al*., 2015). The resilience of urban infrastructure and ecosystems is critical for rapid response and a community's and economy's rapid recovery (Gupta *et al*., 2017). Ecosystems within and around cities can help to buffer against many of the climate change impacts (McPhearson *et al*., 2015). Resilience to specific events may arise through ecosystem services where benefits occur during or shortly after the event, for example, wetlands can improve nearby communities' resilience by providing a buffer to the effects of storm surges (McPhearson *et al*., 2015). Urban ecosystems can help buffer against climate change impacts and improve resilience through services like carbon sequestration, climate regulation, water and air purification, and improved rainwater infiltration (Locatelli, 2016). However, these ecosystem services are also vulnerable to climate change, unsustainable use, and degradation, posing threats to human well-being (Bustamante *et al*., 2019).

2.5 Ecosystem service assessments along urban-rural gradients

Ecosystem services vary across urban-rural gradients due to the influence of land transformation (Tao *et al*., 2015). Urban areas are distinguished by their dense population, minimal greenery, and extensive impermeable surfaces. In contrast, rural areas generally exhibit a low concentration of people, a significant amount of untouched or farmed land, and porous surfaces. Rural areas are typically classified by various attributes that are distinct from metropolitan areas (Kaminski *et al*., 2021).

The gradient approach is employed to analyze patterns and trends of urbanisation and their impacts on ecosystems (Wang *et al*., 2022). This approach assumes that land transformation depends on the patterns of land development across various areas within a metropolitan region. Thus, an increase in population size is expected to have different effects on land cover in cities and rural areas (Güneralp *et al*., 2020). Research using this approach has shown significant variations in ecosystem services along urban-rural gradients, but there is no standardized model for these gradients across different regions (Wang *et al*., 2022).

The urban-rural system of classification has been used to analyse the geographical effects of land use change and the alterations in ecological patterns resulting from urban development (Feng *et al*., 2021; Larondelle and Haase, 2013). Urban-rural gradients provide an important basis for studying the provision of urban and rural ecosystem services, which are connected to the well-being of societies (Herrero-Jáuregui *et al*., 2019). The use of gradients has allowed scholars to quantitatively assess the spatial patterns of environmental change and investigate the impact of urbanisation on ecosystems (Herrero-Jáuregui *et al*., 2019). The worldwide enthusiasm towards studying the gradient of ecosystem services has been limited. However, there exists a lack of attention and research on this topic in Africa (Mngumi, 2020a).

Wang *et al*. (2022) examined the effects of extensive urban growth on ecosystem services throughout a continuum from urban to rural areas. The results showed that the ecosystem services provided by various kinds and forms of land use vary across urban-rural gradients. This suggests the need for a thorough assessment of land uses and their effects on ecosystem services. Peng *et al*. (2022) assessed the temporal and spatial distribution of ecosystem services provided by urban parks and gardens. The findings indicated that alterations in land use had a significant impact on these patterns; as the extent of urban areas expanded, there was a considerable drop in the quality of ecosystem services. Megacities had the lowest value for ecological services.

The provision of ecosystem services can undergo both spatial and temporal fluctuations (Rau *et al*., 2020). Understanding these temporal changes is crucial for assessing whether an ecosystem service

has deteriorated or recovered from past states (Jaligot *et al*., 2019). For instance, Herrero-Jáuregui *et al*. (2019) analyzed how landscape structure and ecosystem service provision changed over two decades along an urban-rural gradient in Spain. They observed a shift from uniform to diverse landscapes, with a loss of provisioning and regulatory services in favour of cultural services to support tourism. Assessing temporal changes sheds light on trends in ecosystem service provision and the factors driving change (Jaligot *et al*., 2019), although research in this area remains limited.

It's important to note that urban-rural gradients vary globally due to differences in urbanisation patterns, population densities, and industrialization trajectories among cities (Tian *et al*., 2022). While one end of this gradient may be highly urbanized and the other rural, some cities may exhibit peri-urban characteristics on one end. In such cases, the supply of ecosystem services is influenced by the unique characteristics of each area within the gradient, shaped by land cover and land use changes resulting from development (Tian *et al*., 2022). Studies have shown that ecosystems offer diverse services, which vary in quality and quantity depending on the specific land cover and land use circumstances (Belay *et al*., 2022).

Hou *et al.* (2015), assessed spatial gradients in China and Germany. The findings of their study revealed a notable disparity in the patterns of change in habitat quality within the areas under investigation. Additionally, it was shown that the carbon removal ecosystem service exhibited variations between the two regions. In general, various regions demonstrate distinct spatial variations in the ecosystems and ecosystem services from the urban core to the periphery. Similarly, Larondelle and Haase (2013) selected four cities in Europe, with a population gradient ranging from the densely populated urban interior to the rural outskirts. This research indicated variations in the provision of urban ecosystem services across different cities, with the central city typically offering fewer ecosystem services compared to the surrounding region. As impervious cover decreased a few kilometres away from the city centre, there were notable extremely high levels of the supply of ecosystem service provision, particularly in terms of tree temperature regulation.

A study conducted by Baro *et al*. (2017) on a city in Spain found that urbanisation is likely to be linked to a reduced capacity for providing ecosystem services. In contrast, forest landscapes exhibit a significant level of multifunctionality, especially in terms of controlling ecosystem services. However, the demand for these ecosystem services in these areas is generally low. Urbanisation is a factor that drives demand, as higher population densities and pressures connected to urban areas (such as air pollution) inevitably lead to an increased need for providing, managing, and cultural ecosystem services.

From the previously described case studies, it can be deduced that land cover and the underlying social-ecological variables play a crucial role in determining the patterns of supply and demand for ecosystem services (Belay *et al*., 2022). Typically, places with low impermeable cover tend to have a high potential for providing ecosystem services, as ecosystems are necessary for the provision of these services. The ecosystem provisioning potentials vary based on the landscape's characteristics and level of urbanisation (Milliken, 2018).

2.6 Johannesburg and its surroundings

South Africa's Gauteng Province was originally characterised as a grassland biome before the discovery of gold (Bobbins *et al*., 2019). Since then, Gauteng has been characterised by rapid spatial transformation and urban development. For this reason, many areas within the province saw a transformation from grassland to impermeable surfaces, leading to a variety of adverse consequences for the ecological environment. Areas that are predominantly inhabited by historically marginalised population groups, including Alexandra, Soweto, Mamelodi, and Diepsloot, exhibit very low vegetation cover. This is primarily attributed to the unjust urban planning practices of the apartheid era. This is a trend even in other townships which were developed after apartheid; many of these areas have developed rapidly due to the demand for land and are characterised by informality. As a result, these places suffer from a lack of sustainable green spaces, which means they do not have access to the full range of ecosystem services found in more affluent places (Bobbins *et al*., 2019). Currently, the City of Johannesburg harbours an expansive urban forest, ranking among the largest globally, covering approximately 16.1% of the entire terrestrial extent within the vicinity (Symes *et al*., 2017). According to Schäffler and Swilling (2013), the city has documented a population of more than 10 million trees, with a significant number located in the extensive suburban regions, including green belts, city parks, walkways, and private and community gardens. The urban forest has a vital role in delivering key environmental services, such as climate control and managing stormwater (Salbitano *et al*., 2017). Approximately one-third of the Johannesburg municipality remains in a natural state, some of which are protected in the city's ten nature reserves (CoJ, 2016). The remaining 67% of the city's composition consists of heavy industry, commercial enterprises, diverse residential districts, and numerous mining activities, notably featuring the world's deepest gold mines, some of which have been in operation since the early 1900s (CoJ, 2016; Peberdy *et al*., 2017). The outer edges of the city include small towns, commercial farming areas, townships, and remote industrial and mining areas (Peberdy, 2017).

The City of Johannesburg serves as the financial and economic hub of South Africa, contributing around 16% to the country's Gross Domestic Product (Beall *et al*., 2014). Despite the relatively small geographical extent of the city, which spans roughly 1 645 km^2, it stands as the most densely

populated urban centre in the country, with a population of approximately 4.5 million people (Statistics South Africa, 2021). The city is the fastest-growing municipality in South Africa with an annual growth rate of 3.18%, resulting in rapid urbanisation and population densification in the municipality (Statistics South Africa, 2021). The City of Johannesburg experiences a temperate climate with a mean daily temperature of 18 – 20 °C during summer months and 10 – 13 °C during winter months. The region experiences summer rainfall with a mean annual rainfall ranging from 85 – 100 mm in winter and 600 – 700 mm in summer (South African Weather Service, 2020; Fitchett and Raik, 2021).

Concluding remarks on literature

As highlighted in the literature section, the majority of cities are experiencing unprecedented levels of urbanisation. Despite the aim of enhancing the quality of life, urbanisation has several adverse effects on the environment. The urban environment features blue and green infrastructure which enables them to provide ecosystem services, also known as urban ecosystems services. The maintenance of these ecosystem services is highly dependent on the ecological connectivity in the urban areas. Connected ecosystems exert a beneficial influence on the biodiversity. Urban areas contribute largely to climate change, while also being particularly vulnerable to the impacts of climate change. The severity of these impacts is influenced by the extent and quality of ecosystem services within cities. The supply of ecosystem services varies across urban to rural gradients due to the influence of land transformation. A gradient approach can then be used understand the patterns of urbanisation and their impacts on the ecosystems and the services they generate.

CHAPTER 3: METHODOLOGY

To assess the ecosystem services along an urban-rural gradient, two gradients were chosen. The spatial and (where possible) temporal changes to three ecosystem services, namely temperature regulation, carbon sequestration, and flood regulation. These ecosystem services are crucial for regulating the natural environment. These elements have been seen as crucial in urban settings because they enhance the ability of cities to withstand the effects of climate change. An evaluation of spatial patterns was conducted using the urban-to-rural/peri-urban gradient method, together with an evaluation of temporal changes using the change-over-time method.

3.1 Study area

The assessment of the ecosystem services was based in Gauteng, South Africa, with a focus on the City of Johannesburg (CoJ) and its surrounding peri-urban and rural areas. Johannesburg is located at approximately 26.204978° S, 28.046377°E in the Gauteng province of the Republic of South Africa (Figure 1). In terms of the natural environment, the City of Johannesburg is characterised by its remarkable urban forest (~5 million trees) and extensive wetland system (CoJ, 2016). Nearly 33% of the Johannesburg municipality remains in a natural state, some of which are protected in the city's ten nature reserves (CoJ, 2016). The city is home to a section of the country's mining activities, heavy industry, commercial enterprise, and urban population. It is prone to rapid urbanisation and urban sprawl, there is a rapid loss of open spaces due to the urban sprawl (Totaforti, 2020; Katumba and Everatt, 2021) (Figures 1 and 2).

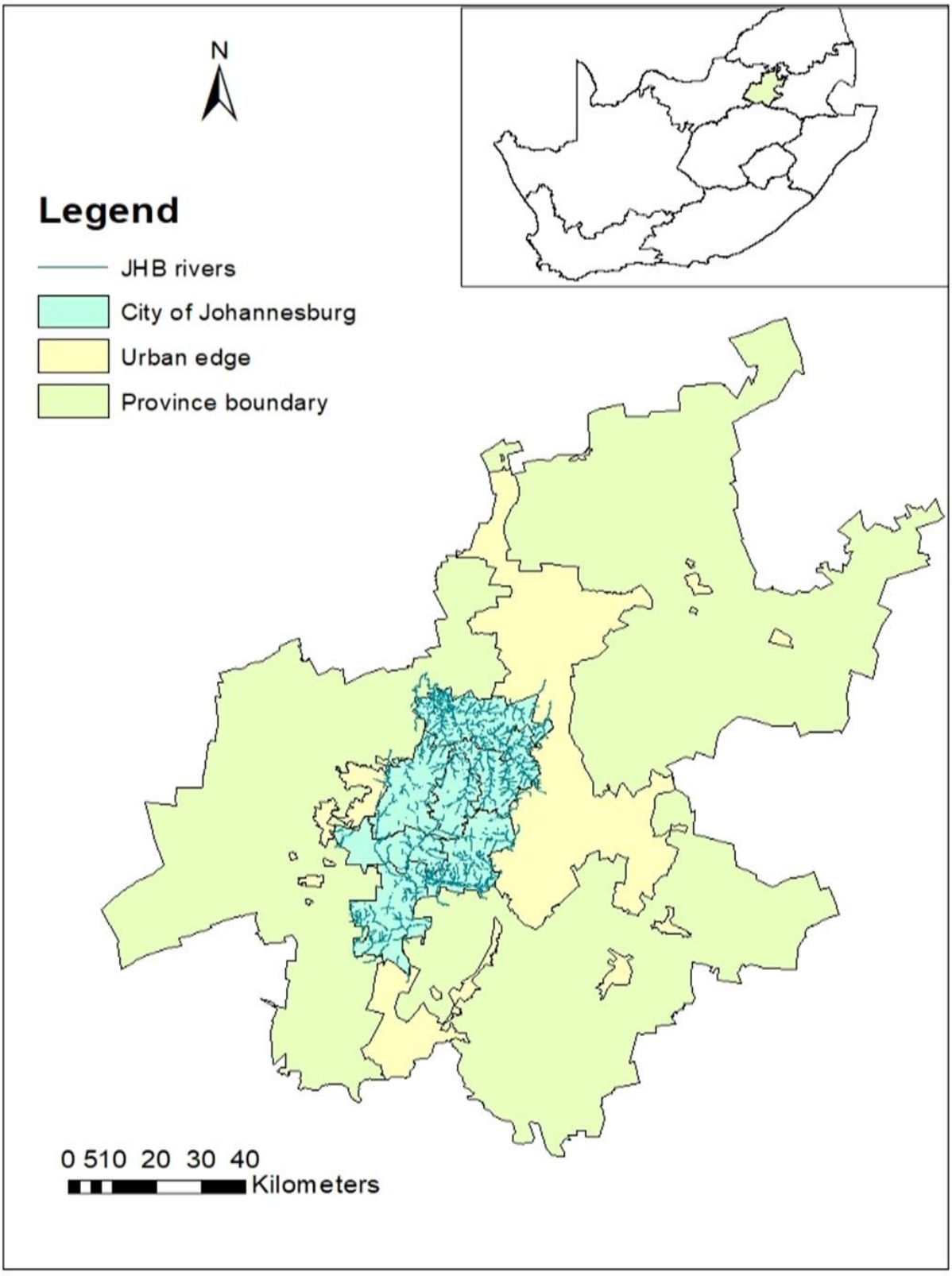

Figure 1: The Gauteng province, City of Johannesburg and its urban edge, South Africa

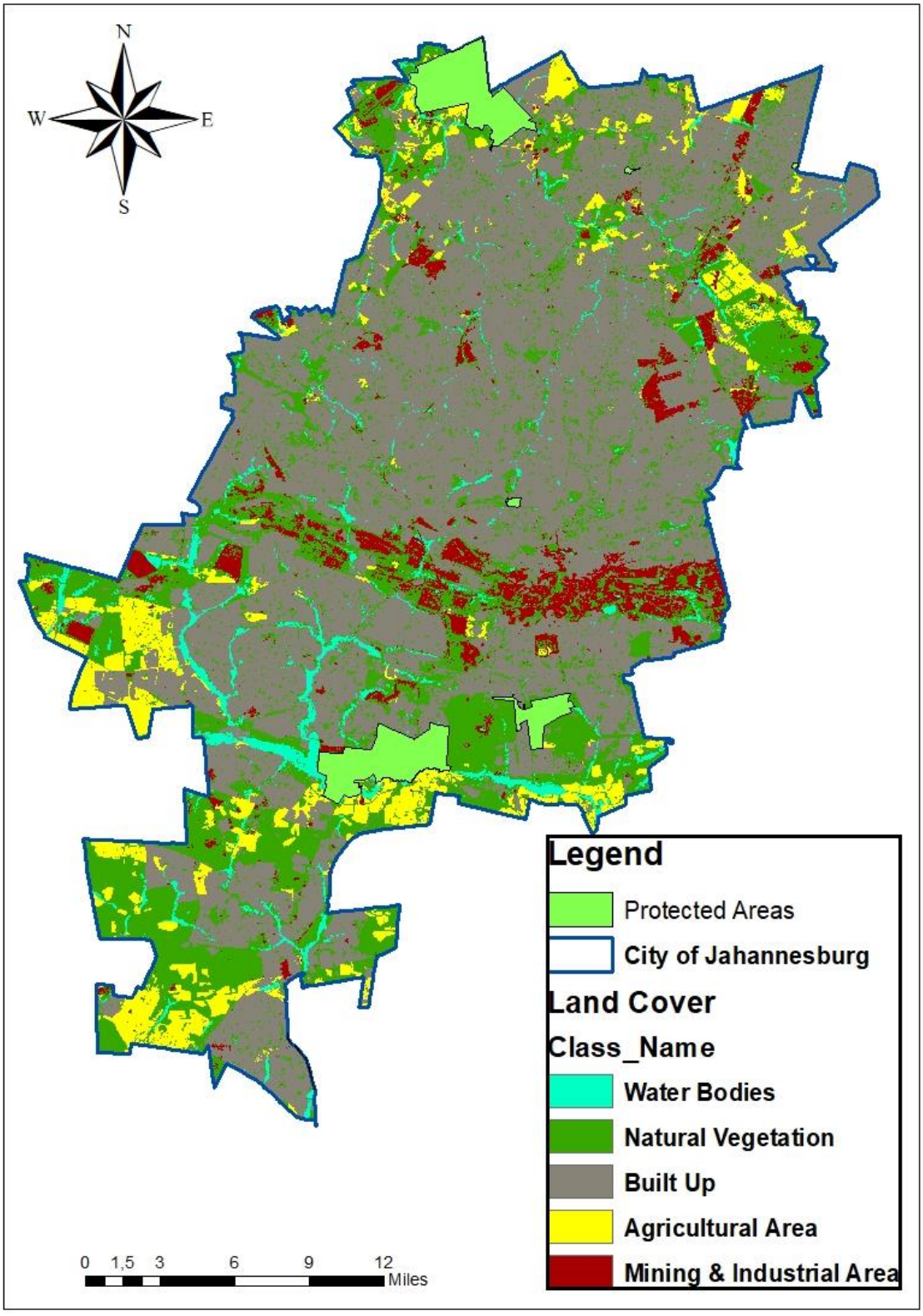

Figure 2: The city of Johannesburg and the land cover in the city

The first gradient (gradient A) under investigation ran from the Johannesburg central business district (CBD) in a northerly direction towards the Hartbeespoort dam (25.756916° S, 27.885146°E) At the start of the gradient, the landscape is more urban, characterised by numerous manmade structures, roads, impervious surfaces and commercial districts. Moving out of the CBD, towards the north, the landscape then gradually transforms into a mixture of a vast residential area (northern suburban area), commercial zones, many pockets of greenspaces, as well as continuous tree cover. From the northern suburbs, the landscape is then comprised of a less dense residential area, with a farm or plot-like structure; this area has more grass and tree cover, with sparse housing. The landscape then transitions into a more open landscape, with some commercial. There is low grass cover, sparse tree cover, small pockets of bare land and some sections of inactive agricultural lands. From there, the land cover is composed of protected areas, with tourism centres. At the very end of the gradient, there is the Hartbeespoort Dam, which is surrounded by affluent suburban houses with a few commercial zones, tourist attraction areas and agricultural lands. Hartbeespoort is a small area located in South Africa's Northwest Province. It is surrounded by extensive rural crop farming which, along with mining, manufacturing, and tourism, are the main economic sectors in the area (Tseane-Gumbi *et al*., 2019).

The second gradient, gradient B, ran from the Johannesburg CBD (-26,208835° S, long 28.045136° E) in a southerly direction through Johannesburg towards the Vaal Dam (-26.840655° S, 28.160073° E). Johannesburg South encompasses a diverse landscape that combines urban areas, suburban neighbourhoods, as well as natural areas such as nature reserves and vast farmlands. From the starting point, Johannesburg CBD, to the end of the gradient there are various landscape types. The landscape is arranged in an urban area, then residential areas at the outskirts of the city, then open grasslands, extensive agricultural grounds, then low dense residential area, lastly followed by open grasslands all the way to the Vaal Dam.

As mentioned above, the CBD is comprised of impervious surfaces, manmade structures, commercial activities, as well as numerous high-rise buildings. From the CBD, there are a few mine dumps leading to residential areas. At this point, the landscape is a mixture of residential and commercial zones, with different housing styles. There are numerous urban parks, recreational areas and one nature reserve (Klipriviersberg Nature Reserve) within the vast residential area. From the residential area, the landscape transitions into a vast open land with scattered sections of agricultural land, highways, and cemeteries, and there is one river (Kliprivier) along the gradient. The gradient then transitions into a matrix of residential areas, vast farmlands, open unoccupied land, suburb areas, a few large manufacturing facilities on the way, and then a start of residential areas again. This area is informally known as the Vaal, it includes various residential areas, some with a township

structure of high-density housing and some with a farmland structure with sparse housing and a continuous layer of vegetation cover. Along this gradient, there is the second nature reserve, known as the Suikerbosrand Nature Reserve. From then the landscape is just openly vegetated lands with discontinuous tree cover until the Vaal Dam, which is the peri-urban end of the second gradient.

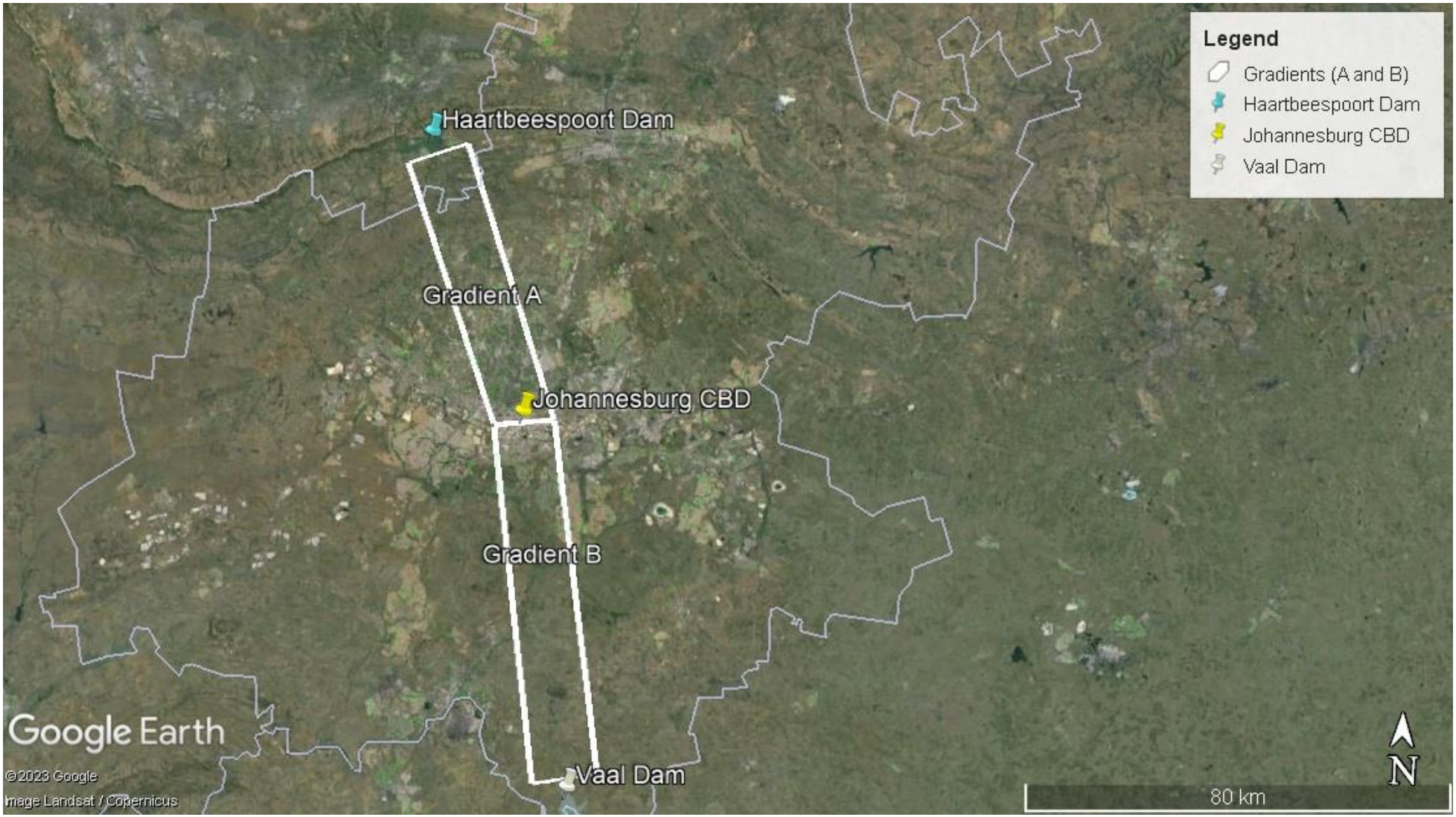

Figure 3: The two urban-rural gradients of the study, from Johannesburg CBD, the urban extreme to Hartbeespoort (gradient (A)) and Vaal (gradient (B)), the rural extremes (Google Earth Pro, 2024)

3.2 Site selection

Using Google Earth Pro, a place marker was dropped at every 5 km starting Johannesburg city centre (location) to Hartbeespoort (distance ~60 km; gradient A), and again from Johannesburg city centre towards the Vaal Damn (distance ~65 km; gradient B). Each place marker represented a study site, and thus in total, there were 12 sites in gradient A and 13 sites in gradient B (Figure 4). Each place marker marked the centre of a 100 x 100m plot, where all the assessments were done. Where a place marker was located in an inaccessible area, the nearest accessible area was selected as the study site.



Figure 4: Gradient A, from Johannesburg CBD, the urban extreme to Hartbeespoort the rural extreme (Google Earth Pro, 2024)

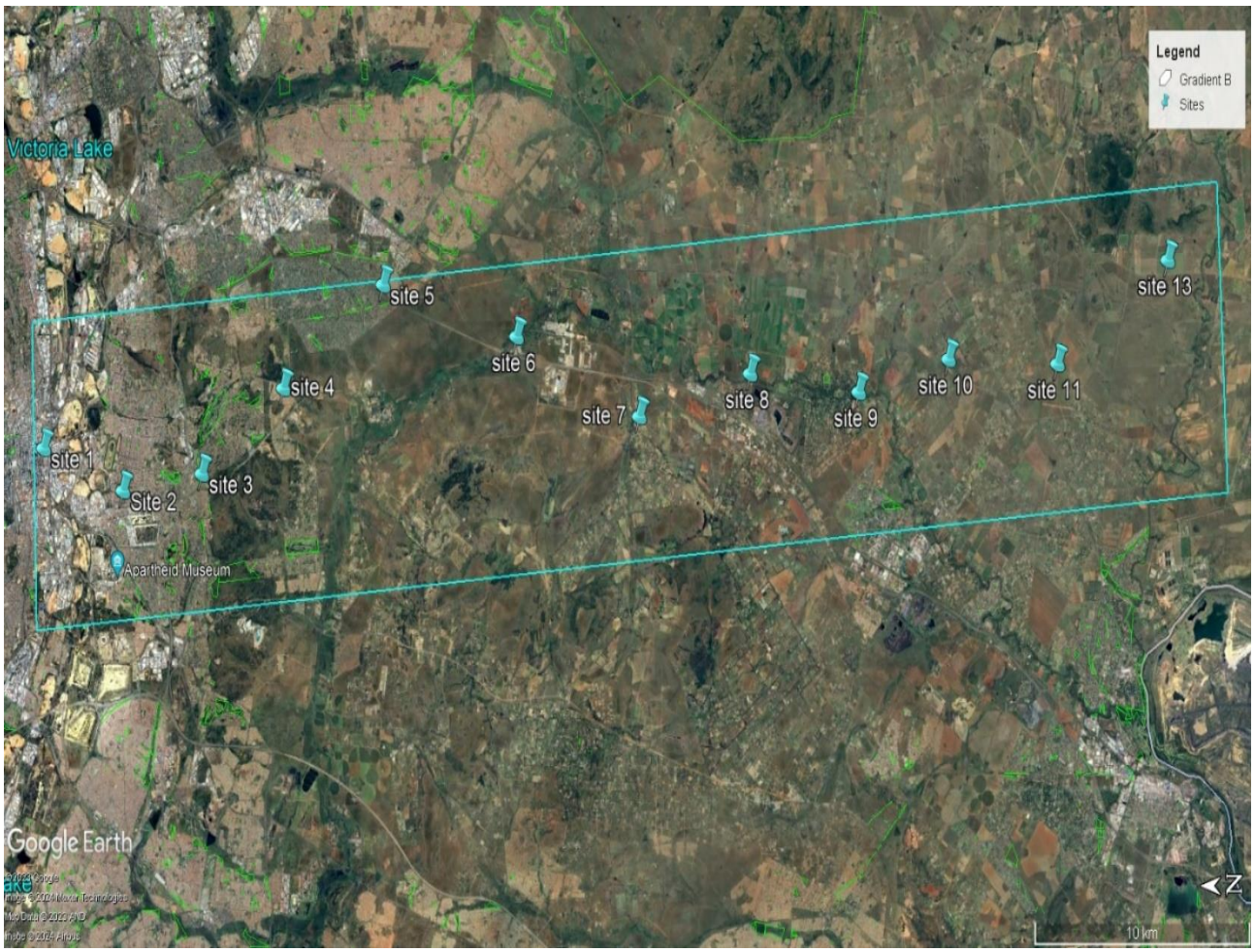

Figure 5: Gradient B, from Johannesburg CBD, the urban extreme to the Vaal, the rural extreme (Google Earth Pro, 2024)

Tables 1 and 2 present the characteristics of the gradients' landscape, the land cover, which is the physical surface cover of the land and land use, and the functional purpose of the land at the time of assessment of the sites (Ackerman, 2011).

Table 1: Land cover and land use description of the site's locations along gradient A

Site	Site name	Description
1	Central Business District (CBD)	Built-up: commercial and industrial land uses.
2	Urban Park	Built-up: mainly residential and partly commercial land use.
3	Urban Park	Built-up: mainly residential and partly commercial land use.
4	Urban Park	Built-up: mainly residential and partly commercial land use.

5	Residential	Built-up: commercial, residential (formal and informal settlements) land use.
6	Residential	Built-up: commercial, residential (formal and informal settlements) land use.
7	Highway	Sparse vegetation: partly built up (airport), wooded trees mixed with grasses.
8	Highway	Sparse vegetation: partly cultivated, wooded trees mixed with grasses, and patches of dryland.
9	Nature Reserve	Intact vegetation: partly cultivated, and natural landscaping.
10	Nature Reserve	Intact vegetation: protected area, covered with dense vegetation.
11	Nature Reserve	Intact vegetation: protected area, covered with dense vegetation.
12	Residential	Partly built up, mostly intact vegetation: Residential and partly commercial.

Table 2: Land cover and land use description of the site's locations along gradient B

Site	Site name	Description
1	Central Business District	Built-up: commercial and industrial land uses.
2	Roadside	Built-up: mainly residential and partly commercial land use.
3	Roadside	Built-up: mainly residential and partly commercial land use.
4	Urban Park	Intact Vegetation: Natural landscaping with a sparse tree cover.
5	Highway	Intact Vegetation: Natural landscaping with a sparse tree cover.
6	Highway	Intact vegetation: partly cultivated, and natural landscaping.
7	Residential	Sparse vegetation: a partly built-up low-density residential area and few commercial activities.
8	Residential	Sparse vegetation: a mixture of agricultural land, low-density residential area, there's a river crossing by, as well as small scale industrial zone.

9	Residential	Sparse vegetation: a low-density residential area, near a river, with numerous pockets of green spaces. A mixture of agricultural land, and low-density residential area, there's a river crossing by, as well as a small-scale industrial zone.
10	Open Land	Intact vegetation: Extensive agricultural land with very sparse owners' households
11	Open Land	Intact vegetation: Large agricultural area and dense vegetation on the opposite side.
12	Open Land	Intact vegetation: Large agricultural area and dense vegetation on the opposite side.
13	Open Land	Intact vegetation: Large agricultural area surrounded by open grasslands.

3.3 Objective 1: Temperature regulation

The land surface temperature (LST) along each gradient was derived from the Landsat (5 TM, 7 ETM+, 8 OLI) datasets available in Google Earth Engine (GEE), following the methods by Ermida *et al*. (2020). Ermida *et al*. (2020) provided a code (see Appendix 1) that is written in Java scripts, for application on the GEE, to obtain land surface temperatures from the Landsat dataset. This method is based on an algorithm that uses simple linear regression to assess the relationship between the top of atmosphere brightness and land surface temperatures (Li *et al*., 2013; Duguay-Tezlaff *et al*., 2015). The code uses a variety of inputs from the GEE's collection of geospatial data and satellite imagery, particularly Landsat imagery, as well as datasets on total column water vapour and emissivity. These data were used to assess temperature differences along each gradient (Figure 3) over 20 years (2001 to 2021). Only the summer months (October - March) were focused on, as this is the hottest time of the year. Many summer months were chosen to increase the sample size as some months would have high cloud cover, which would in turn render most of the images to be invalid, because of cloud masking.

To produce the LST maps along each gradient, and for each time interval, the coordinates of the study sites and the dates for the required time interval were added into the code, which was then run. The maps produced from the Google Earth Engine were downloaded as GeoTIFF files and then uploaded to the Arc Geographic Information System (ArcGIS) for the extraction of the actual temperature values using the extraction toolset, specifically, the Extract Multi Values to Point tool within ArcGIS. With this tool, I defined the locations (30 points in each site) from where I wanted to extract cell values from the downloaded raster/GeoTIFF file. When the extraction of LST from the GeoTIFF files

was done, ArcGIS produced a spreadsheet with 30 temperature values for each month that was put into the code. Months with less than 6 temperature values due to cloud masking were removed as they would skew the data. The LST values were presented in degrees Kelvin (K) and manually transformed from degrees Kelvin (K) to degrees Celsius (°C) in Microsoft (MS) Excel.

The mean annual LST of each site was computed and graphically presented against time as well as against the distance from the city centre. The LST data was not normally distributed, and thus, a non-parametric alternative to the one-way analysis of variance (ANOVA), the Kruskal Wallis test was used to test if differences existed between variables. The LST difference between the urban extreme site (site 1) and all the other sites along the urban–rural gradient was computed and graphically presented. This LST difference data was normally distributed, as a result, an ANOVA test was done, as well as the complementary post hoc test, Tuckey's HSD Test for multiple comparisons. All statistical analyses were done on the statistical software R version 4.0.3 (R Core Team, 2022). The significance level was set at $p<0.05$.

3.3.1 Fractional vegetation cover

In addition to the generation of LST from the Landsat satellites, the code repository following the methods by Ermida *et al*., (2020), offers the following outputs: Fractional Vegetation Cover (FCV), TIR Brightness Temperature, Surface Emissivity, Total Column Water Vapor (TCWV). FVC was extracted for each study site and the 2001 – 2021 time frame. Summer months were the focal point of this data collection because winter months would result in under presentation of the actual vegetation cover. Many summer months were chosen to increase the sample size as some months would have high cloud cover, which would in turn render most of the images to be invalid, because of cloud masking. The images were then transferred to the ArcGIS software, for extraction of the actual FVC values using the extraction toolset, particularly the Extract Multi Values to Point tool. Similar to the LST assessment, I defined the locations (30 points in each site) from where I wanted to extract extracted cell values from the downloaded raster/GeoTIFF file.

The output was an Excel spreadsheet of 30 FVC values (each ranging from 0 – 1) for each month that was put into the code. Months with less than 6 FVC values due to cloud masking were removed as they would skew the data. The mean annual FVC was computed for each site, and graphically presented. A linear regression model was then fitted to test for the relationship between the FVC and the LST.

3.4 Objective 2: Carbon sequestration

Carbon storage was estimated following the methods by Lembani (2015) and then verified using the methods by Schäffler and Swilling (2013). All sites had to be an area with a combination of trees and open spaces to represent urban tree arrangement. As per Lembani (2015), basic tree measurements were taken on thirty randomly selected trees across each 100 x 100 m plot along both gradients. For each tree, the circumference at breast height was obtained (cm) using a measuring tape. Circumference at breast height was ideal, as it is more precise for stems with irregular shapes than stem diameter (Lembani, 2015). From the circumference measurements, the following variables were calculated:

diameter at breast height DBH (in cm):

$$(a): DBH = \frac{CBH}{\pi}$$

the radius (r) of the stem:

$$(b): r = \frac{DBH}{2}$$

the above-ground biomass (Y):

$$(c): Y = a(\pi r^2)^b$$

where; a (constant) = 0.1936, b (constant) = 1.1654 and π (pi) = 3.142

and finally, the amount of above-ground carbon stored (in kg) for each tree:

$$(d):\ Stored\ carbon = Y \times 45\%$$
$$(e): Total\ stored\ carbon\ for\ the\ site = Stored\ carbon\ \times n$$

where; n = number of trees in the entire site

For the stored carbon equation (d), an assumption was made, that 45% is the average carbon content value for dry terrestrial biomass (as per Thomas and Malczewski, 2007). To calculate the total stored carbon for the entire site, the total number of trees was counted on site and the average stored carbon value was multiplied by the total number of trees in each site.

To estimate the historical carbon stock (2001 - 2021), Google Earth imagery of the sites was used to visually determine the total tree cover area (ha) at each site. This area was multiplied by the estimated carbon stock (tonnes), which produced the carbon stock for the year of interest.

The carbon data were checked for normality, thereafter a non-parametric test, the Kruskal Wallis test as well as the complementary post hoc test, the Kruskal Wallis Multiple comparison post hoc test at a 95% confidence level, was performed to test for the variation in the average carbon stock across the sites and over time. The average stored carbon was then graphically presented in tons across the sites and over time (Chapter 4.2). To improve confidence in the data obtained, the data was again collected following the methods proposed by Schäffler and Swilling (2013), a 50×50 m large area was selected at each site; Thirty trees were randomly selected, and the tree circumference at breast height was measured, from which the tree diameter (cm) was calculated (a):

$(f)\ DBH = CBH/\pi$

For each tree, the stem length from the ground to the main branches was measured using a RYOBI laser distance measurer. The percentage (%) of the branch volume measured as a proportion of the total tree volume = B, was estimated on site (e.g., 70%=0.7). The above measurements allowed me to calculate the basal area (g), stem volume (h), total tree volume (i), biomass (j), volume per ha (k), biomass per ha (l), carbon stock (m) and the carbon stock for the entire site (n):

(g): $Basal\ Area = \pi \times DBH \times \frac{DBH}{40000}$

(h): $Stem\ volume = BA \times stem\ length\ \times\ 0.7$

(i):. $Total\ tree\ volume = \frac{Stem\ volume}{(1 - B)}$

(j):. $Biomass\ = tree\ volume \times\ 0.7$

(k): $Volume\ per\ ha = \frac{biomass}{0.25\ (metric\ tonnes\ per\ ha)}$

(l): $Biomass\ per\ ha = volume\ per\ ha \times\ 0.7$

(m): $Carbon\ stock = biomass\ per\ ha \times\ 0.5\ (metric\ tonnes\ per\ ha)$

(n): $Carbon\ stock\ of\ the\ entire\ site =\ carbon\ stock\ per\ ha \times\ total\ tree\ cover\ area\ (ha)$.

From these calculations, the number of metric tonnes of carbon stored for each site in the current year was determined. To estimate the historical carbon stock (2001 - 2021), Google Earth imagery of the sites was used to visually determine the total tree cover area (ha) at each site. This area was multiplied by the estimated carbon stock (tonnes), which produced the carbon stock for the year of interest.

3.5 Objective 3: Flood regulation

The soil's unconfined compressive strength (kg/cm^2) was determined using a pocket soil penetrometer. A minimum of 30 measurements were taken by pressing the piston into the soil's surface at various points across each 100 x 100 m plot. From the integrated scale engraved on the penetrometer barrel, the penetration resistance from the calibrated spring was recorded. To obtain each measurement, the transparent plastic ring on the barrel of the penetrometer was read directly in kg/cm^2. The average readings on each site were calculated, and soils with a mean soil compression strength of and above 4.4 kg/cm^2 were classified as compact (as per Steber *et al*., 2007). This provided a quantitative estimate of soil compaction. Areas with less compact soil have a higher flow retention ability (Steber *et al*., 2007). Impermeable and highly compacted soils have reduced levels of water infiltration, whereas less compacted soil with macropores has better water drainage (Schüler, 2006).

Using the statistical program R version 4.0.3 (R Core Team, 2020), the data for soil compaction were first checked for normality. The average of the 30 soil compaction measurements in each site was then calculated and graphically presented. Since the data was not normally distributed, and thus, a Kruskal Wallis rank sum test, as well as a posthoc test, were done to test for differences in the average soil compaction of the site.

3.6 Objective 4: Land cover change

3.6.1 Data acquisition

To assess land cover change over time, ground truth data collected at the time of the site visits was used to later validate the land cover classification. The confirmed land cover types with georeferenced coordinates were added to ArcGIS for further analysis and aid in the creation of the land cover maps. To create the land cover maps, remotely sensed images were downloaded from the Earth Explorer website (https://earthexplorer.usgs.gov/) of the United States Geological Survey (USGS), a tool for accessing remote sensing data. Three-time steps were selected, corresponding to the years 2001, 2011 and 2021. The best cloud-free scenes of Landsat imagery were selected. These were, Landsat 5 and 8, Thematic Mapper (2001 and 2011) and Operational Land Imager-OLI (2021). Landsat datasets were used considering their free access, and compatible resolution of 30 m as well as data availability for the entire study period. To avoid the impacts of seasonal changes, only images for the summer

periods were used (months between August - March). From the Landsat Images and ground truth data, the land cover classification was done and the maps of the two gradients.

3.6.2 Land Cover Classification

All the satellite images were processed using the ArcGIS software, the images were classified into four land cover classes namely, built-up, green space, bare land and water (Table 2). Supervised image classification was done, where training sites were selected as references for the categorisation. In this study, 50 geospatial coordinates were used as training samples for the classification of the Landsat images. Each of the 50 points was classified into the different Land cover types within ArcGIS. The maximum likelihood classifier method (Platt and Goetz, 2004) was adopted for classification, this is a method used to classify pixels of known identity to one of the four different land cover classes identified from the training samples. This classification groups together all the land cover types with the same spectral features and produces a thematic land cover map of the study area.

Table 3: Description of land cover classes identified (as per Rwanga and Ndambuki, 2017)

Land cover Classes	Description
Built-up	Urban land encompasses areas that are developed with human-made structures, such as residential neighbourhoods, commercial buildings, industrial zones, paved surfaces, and road networks.
Green Space	The land is primarily covered by vegetation, such as grassland, trees, and shrubs.
Bare land	Areas characterised by the presence of bare soil, sand, or rocks, with a vegetation cover of no more than 10%. The area consists of uncovered soil, visible rocks, industrial mines, and areas where gravel is extracted.
Waterbody	Interior aquatic formations such as rivers, wetlands, and lakes.

3.6.3 Accuracy assessment

Given the possibility of inaccuracies in land cover classification, the accuracy of the output maps for the years 2001, 2011, and 2021 was evaluated. This phase was performed to evaluate the precision of the classification by comparing the classification of each pixel with the actual land cover conditions acquired from the associated ground truth data. The producer's accuracy quantifies errors of omission, which assesses the effectiveness of classifying real-world land cover categories. The user's

correctness is determined by measuring errors of commission. This refers to the probability of a classified pixel matching the land cover type of its corresponding real-world location (Rwanga and Ndambuki, 2017). The current study utilised an error matrix to evaluate the precision of the classification process, specifically in terms of overall accuracy, user accuracy, and producer accuracy, in comparison to the reference data. The accuracy was determined using ground truth data collected during site inspections. The landcover maps developed for the years 2001, 2011, and 2021 exhibited an overall accuracy of 71%, 78%, and 80% respectively. Basu and Das (2021) define an accuracy value over 70% as acceptable. The landcover maps in this investigation exhibited accuracies ranging from 71% to 80%, which can be considered satisfactory based on the results presented in Tables 4, 5, and 6.

Table 4: Land use classification accuracy for the year 2001

2001	Water bodies	Green space	Bare land	Built-Up	Total(user)	User Accuracy
Water bodies	8	0	0	0	8	100%
Green space	0	5	3	0	8	63%
Bare land	0	3	5	1	9	63%
Built up	0	1	1	4	6	67%
Total (producer)	8	9	9	5	31	
Producer Accuracy	100%	56%	56%	80%		

$$Overall\ accuracy = \frac{Total\ number\ of\ correctly\ classified\ pixels\ (Diagonal)}{Total\ number\ of\ Reference\ pixels} \times 100$$

$$= \frac{8 + 5 + 5 + 4}{31} \times 100$$

$$= 71\%$$

Table 5: Land use classification accuracy for the year 2011

2011	Water bodies	Green space	Bare land	Built-Up	Total(user)	User Accuracy
Water bodies	6	3	0	1	10	60%
Green space	0	13	0	1	14	93%
Bare land	0	2	7	1	10	70%
Built up	0	1	1	9	11	82%
Total (producer)	6	19	8	12	45	
Producer Accuracy	100%	68%	88%	75%		

$$Overall\ accuracy = \frac{Total\ number\ of\ correctly\ classified\ pixels\ (Diagonal)}{Total\ number\ of\ Reference\ pixels} \times 100$$

$$= \frac{6 + 13 + 7 + 9}{45} \times 100$$

$$= 78\%$$

Table 6: Land use classification accuracy for the year 2021

2021	Water bodies	Green space	Bare land	Built-Up	Total (user)	User Accuracy
Water bodies	11	0	0	0	11	100%
Green space	0	9	0	4	13	69%
Bare land	0	1	8	0	9	89%
Built up	1	3	0	8	12	67%
Total (producer)	12	13	8	12	45	
Producer Accuracy	92%	69%	100%	67%		

$$Overall\ accuracy = \frac{Total\ number\ of\ correctly\ classified\ pixels\ (Diagonal)}{Total\ number\ of\ Reference\ pixels} \times 100$$

$$= \frac{11 + 9 + 8 + 8}{45} \times 100$$

$$= 80\%$$

CHAPTER 4: RESULTS

In this study, I set out to assess three ecosystem services, namely temperature regulation, carbon sequestration, and flood regulation, for two urban-rural gradients (A and B) in the greater Johannesburg area. I also assessed the change in the total area covered by green spaces and three other landcover types along the same gradients. In this study, the two gradients A and B are not being compared; rather, they are considered as being distinct. Mapping was done using ArcGIS version 10.5.1 and all statistical analyses were done using the statistical software R version 4.0.3 (R Core Team, 2020). The significance level was set at $p<0.05$.

4.1 Objective 1: Temperature regulation

Figures 6a to 6e show the spatial as well as the temporal distribution of land surface temperatures in the city of Johannesburg, with temperatures increasing gradually over the first 10 years of the assessment period, followed by a slight cooling towards the end of the period. Moreover, the consistent pattern across all the maps is that the most built-up area, the Johannesburg CBD, remains the hottest throughout ($\bar{x}$ = 37,230 °C, 39.383 °C, 39,542 °C for 2001, 2011 and 2021 respectively). According to these maps, the years 2006 to 2016 were the warmest, however, the findings are expanded in Figures 7 to 22.

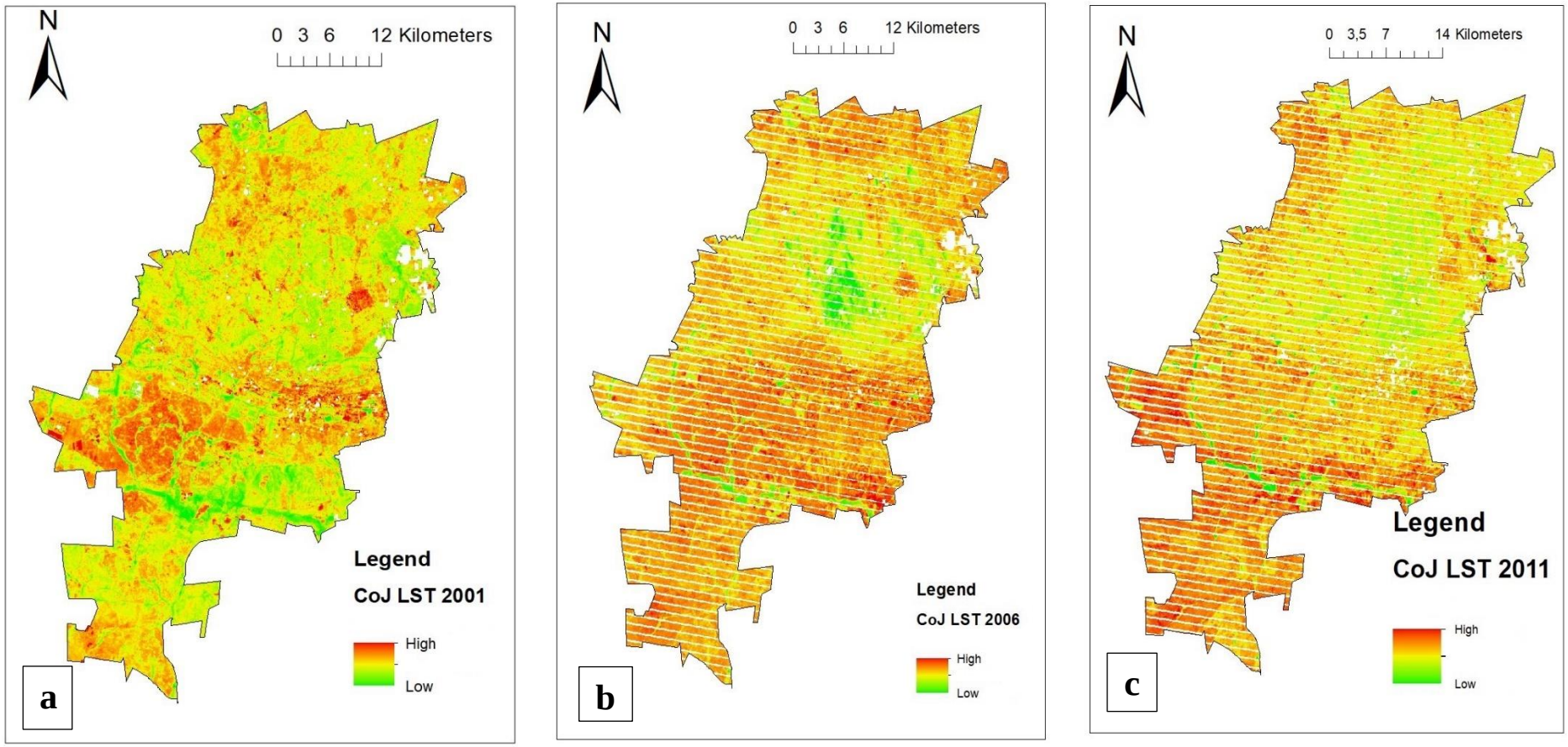

Figures 6a-c: Land Surface Temperature (LST) maps of the city of Johannesburg, South Africa for the years 2001 (a), 2006 (b), and 2011 (c) (the stripes on the two maps are due to the failure of Landsat 7's Scan Line Corrector on the 31st of May 2003. The location of the black stripes varies, and each stripe represents between 390 – 450m of the image; therefore, the US Geological Survey (USGS) estimates that affected images lose about 22% of their data)

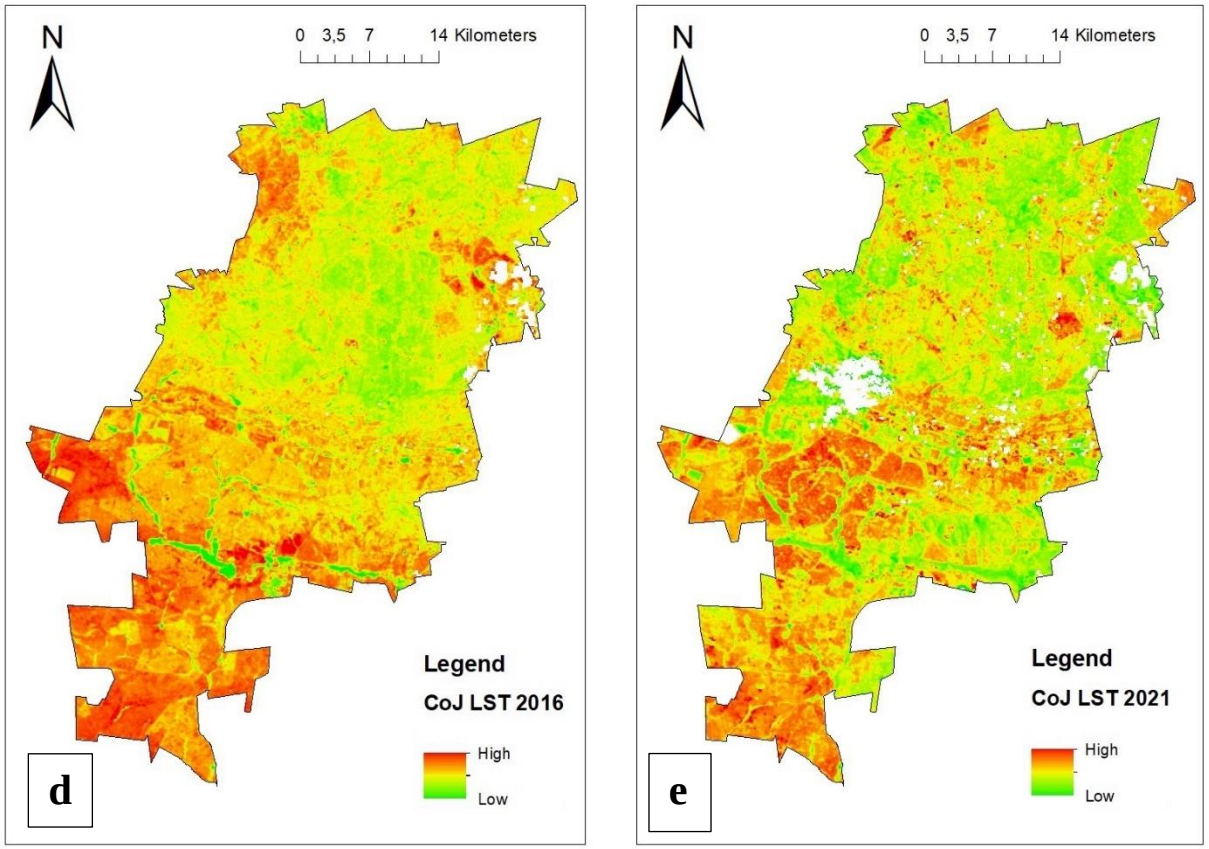

Figures 6d-e: Land Surface Temperature (LST) maps of the city of Johannesburg, South Africa for the years 2016 (d) and 2021 (e) (the stripes on the two maps are due to the failure of Landsat 7's Scan Line Corrector on the 31st of May 2003. The location of the black stripes varies, and each stripe represents between 390 – 450m of the image; therefore, the US Geological Survey (USGS) estimates that affected images lose about 22% of their data)

Along gradient A, the mean land surface temperature (LST) appeared to decrease as the distance from the city centre increased (Figure 7), and the mean LST in the urban extreme in the years 2001, 2011, and 2021 ($\bar{x}$= 38.23 °C, 39.54 °C and 40.44 °C respectively) was higher than the mean LST in the rural end ($\bar{x}$ = 32.70 °C, 36.38 °C and 31.86 °C respectively) (Table7). A linear regression analysis revealed that a large proportion of the variation in LST along the gradients could be explained by the distance from the city centre (R^2= 0.6288, p<0.001). Thus, as the distance from the city centre increases, the land surface temperature (°C) decreases (Figure 8). In the same manner a linear regression analysis indicated that as over the years, the land surface temperature increased (R^2=0.12, p<0.05; Figure 9).

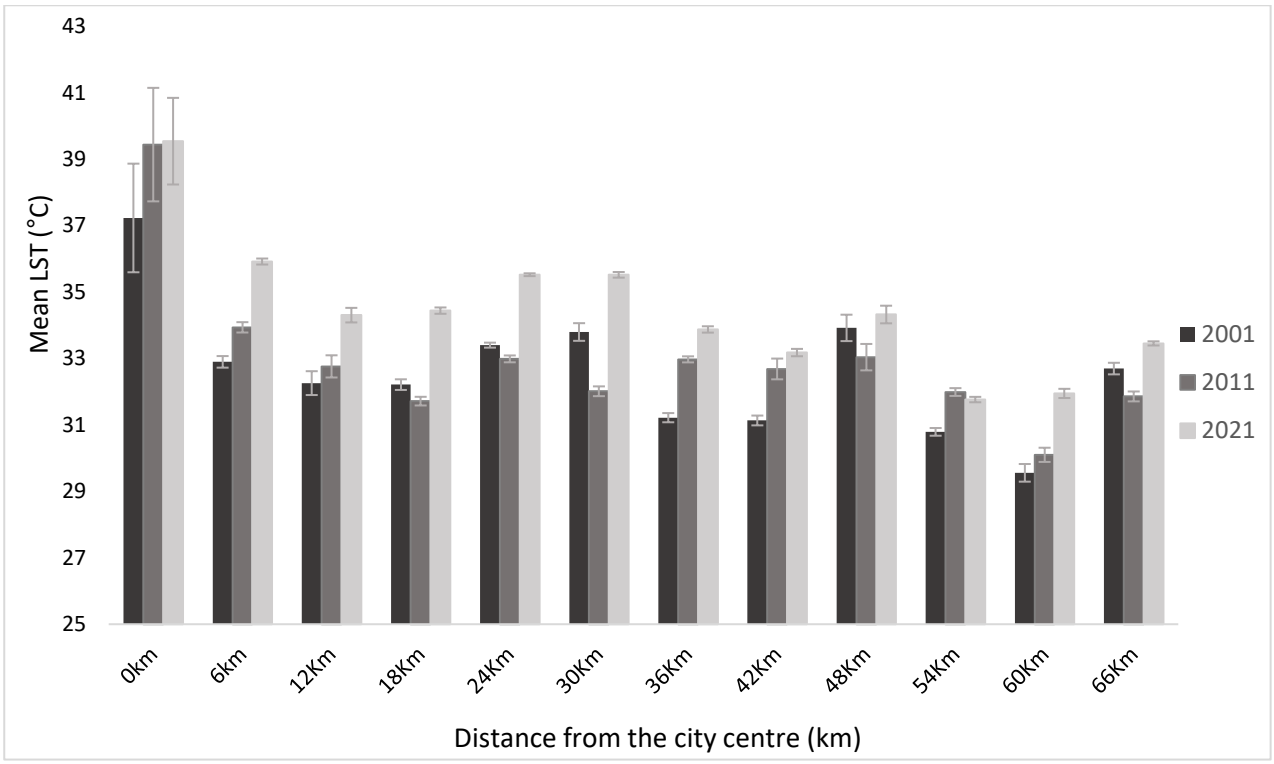

Figure 7: Mean (± SE) land surface temperature along the urban-rural gradient, over a period of two decades

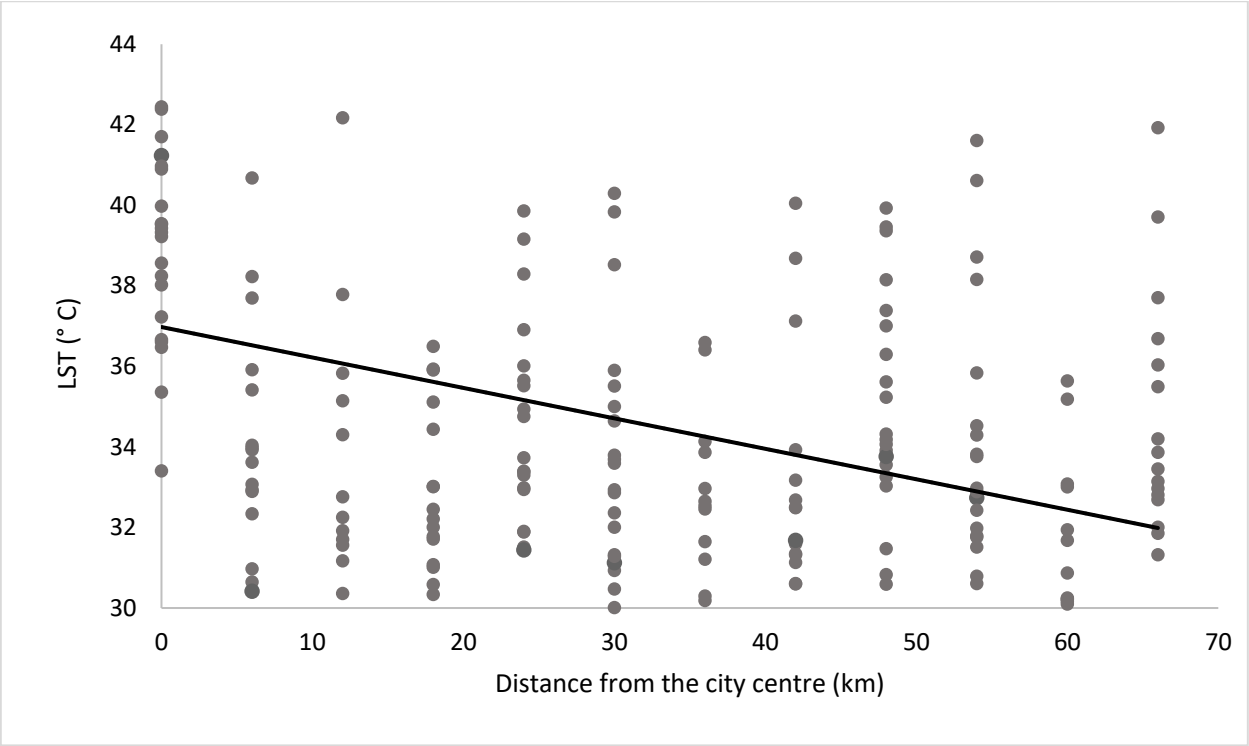

Figure 8: The relationship between the land surface temperature (°C) and the distance from the city centre (km) along gradient A

Table 7: The Kruskal Wallis multiple comparisons post hoc test for LST at different land use types, at the 95% and 99% confidence level

Land use types (site)	P value
CBD (site 1) -Urban Park (sites 2,3&4)	p<0.005
CBD (site 1)-Highway (sites 7,8)	p<0.001
CBD (site 1) - Nature Reserve (sites 9, 10 and 11)	p<0.001
CBD (site 1) - Residential (sites 5,6,12)	p<0.005
Urban Park (sites 2,3&4)-Nature Reserve – (sites 9, 10 and 11)	p<0.005
Residential (sites 5,6,12) -Nature Reserve (sites 9, 10 and 11)	p<0.005
Highway (sites 7,8) -Nature Reserve (sites 9, 10 and 11)	p<0.005

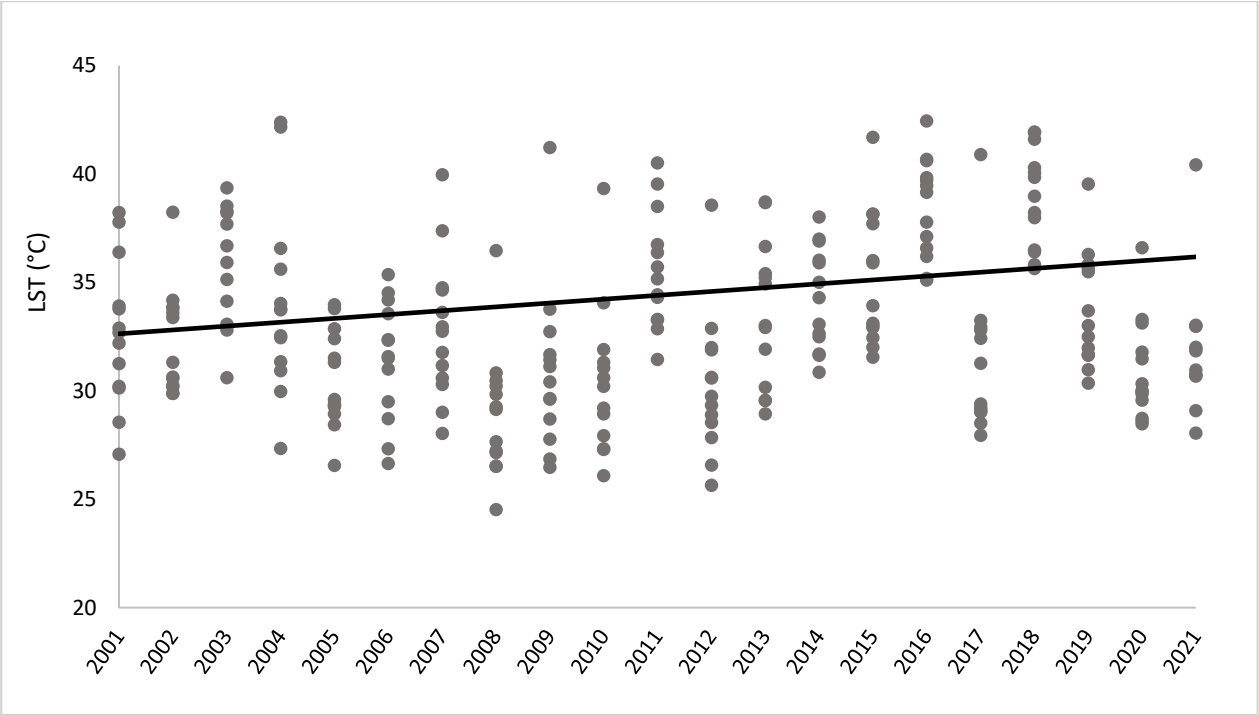

Figure 9: Relationship between the land surface temperature (°C) and time along gradient A

Various land cover and land use types at the time of data collection may also contribute to some of the differences in land surface temperature shown in Figure 7 above, with the more vegetated sites being cooler than the less vegetated sites. Figure 10 indicates the LST observed in each land use type along gradient A. The Kruskal Wallis test revealed a statistically significant difference in the mean LST among the different land use types (X^2_4 = 44.137, p < 0.001). The central business district had the highest mean recorded LST ($\bar{x}$ = 38.890 °C), followed by the Residential ($\bar{x}$ = 33.604 °C). Urban Park was shown to be the coolest land use type among the observed land use type ($\bar{x}$ = 31.895 °C). According to the Kruskal Wallis multiple comparisons post hoc test, a significant difference in the mean LST was found between CBD and the other land use types shown in Figure 10, as well as between Nature Reserve and all the other land use types (Table 7).

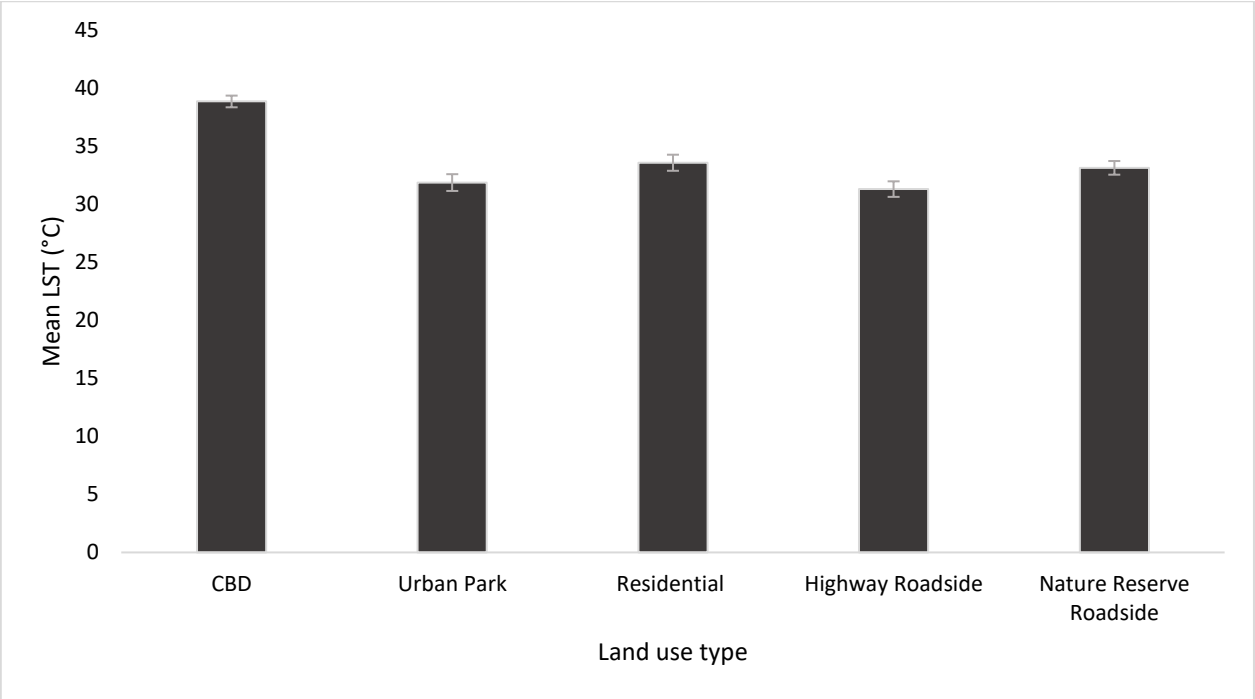

Figure 10: Mean (± SE) land surface temperature(°C) for each land use type along gradient A

Land surface temperature differences between the CBD (site 1) and all other sites (sites 2-12) were assessed using the Kruskal Wallis test, the Δ LST °C was found to differ significantly across the sites (X^2_{10} = 41.733, p<0.001). A fluctuating temperature difference with an upward trend along gradient A was observed (Figure 11). The post hoc test, at 95% and 99% confidence intervals, was performed, the results are shown in Table 8 below.

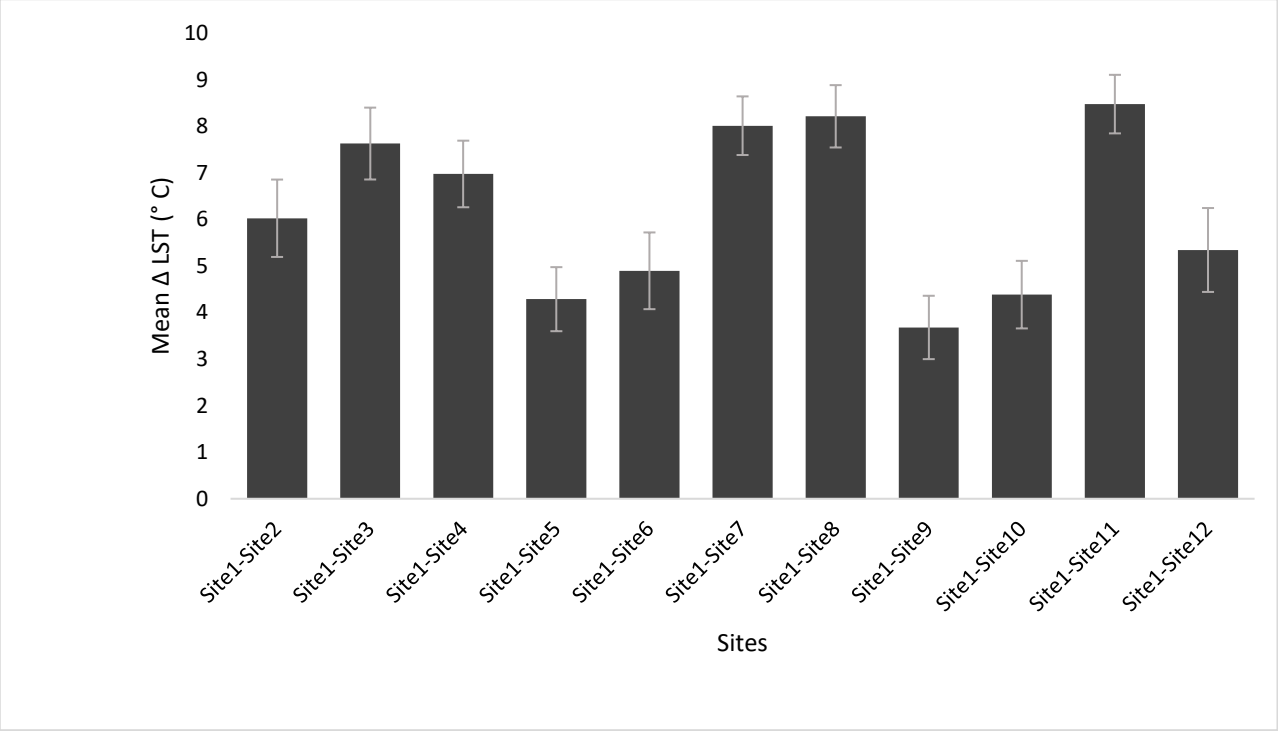

Figure 11: Mean (± SE) land surface temperature difference (°C) between site 1 and all the other sites along gradient A (1= CBD, 2 = Urban Park, 3 = Urban Park, 4 = Urban Park, 5= Residential, 6=Residential, 7 = Highway, 8 = Highway, 9 = Nature Reserve, 10 = Nature Reserve, 11= Nature Reserve, 12 = Residential).

Table 8: Kruskal Wallis Multiple comparison post hoc test for Δ LST °C at a 99% and 95% confidence level

Land use types (site)	P value
Urban Park (site 3) – Nature Reserve (site9, 10, 11)	<0.05
Residential (sites 5,6) - Nature Reserve (site9, 10, 11)	<0.05
Highway (sites 7,8) - Nature Reserve (site9, 10, 11)	<0.01

Similar patterns were observed along gradient B, however, for gradient B the LST data followed a normal distribution, so a one-way ANOVA was performed. The results indicated that the land surface temperature differed significantly across the sites ($F_{12,260}$ = 18.87, p<0.001). LST decreased significantly with the increasing distance from the city (R^2 = 0.9728, p<0.001; Figures 12 and 13). In addition, LST increased as the time increased (R^2=0.39, p<0.05; Figure 14) The results from Tukey's HSD multiple comparisons of means are presented in Table 9.

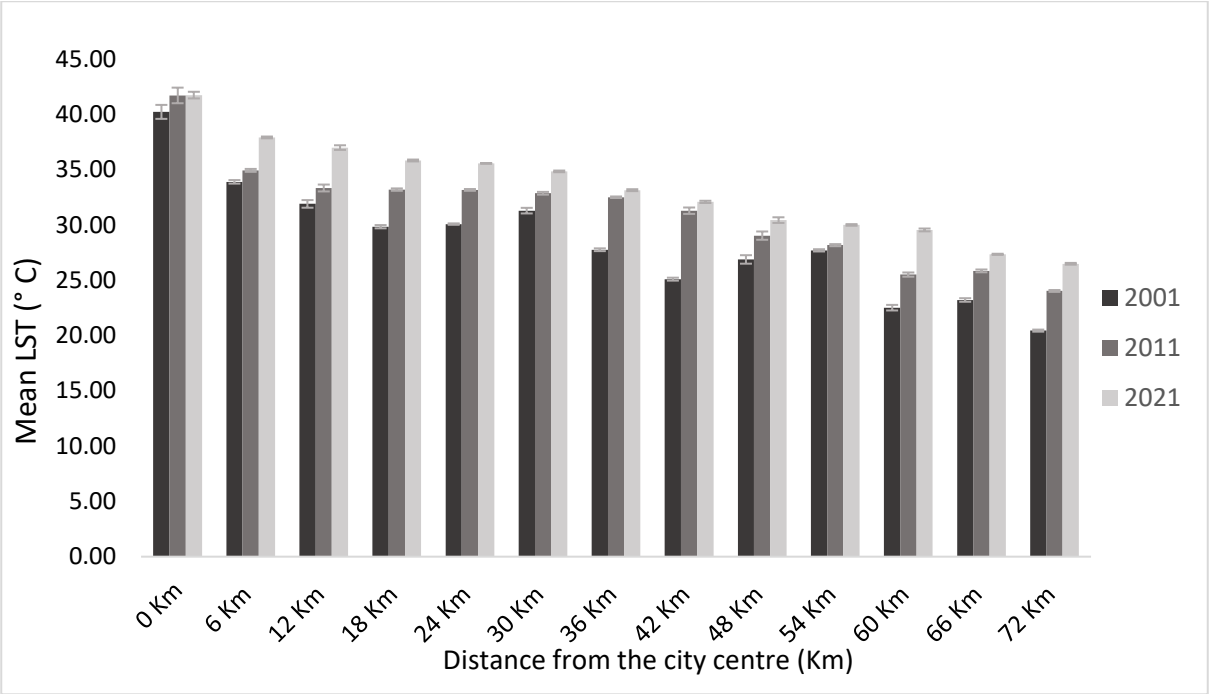

Figure 12: Mean (± SE) land surface temperature (°C) along the urban-rural gradient B for the years 2001, 2011 and 2021

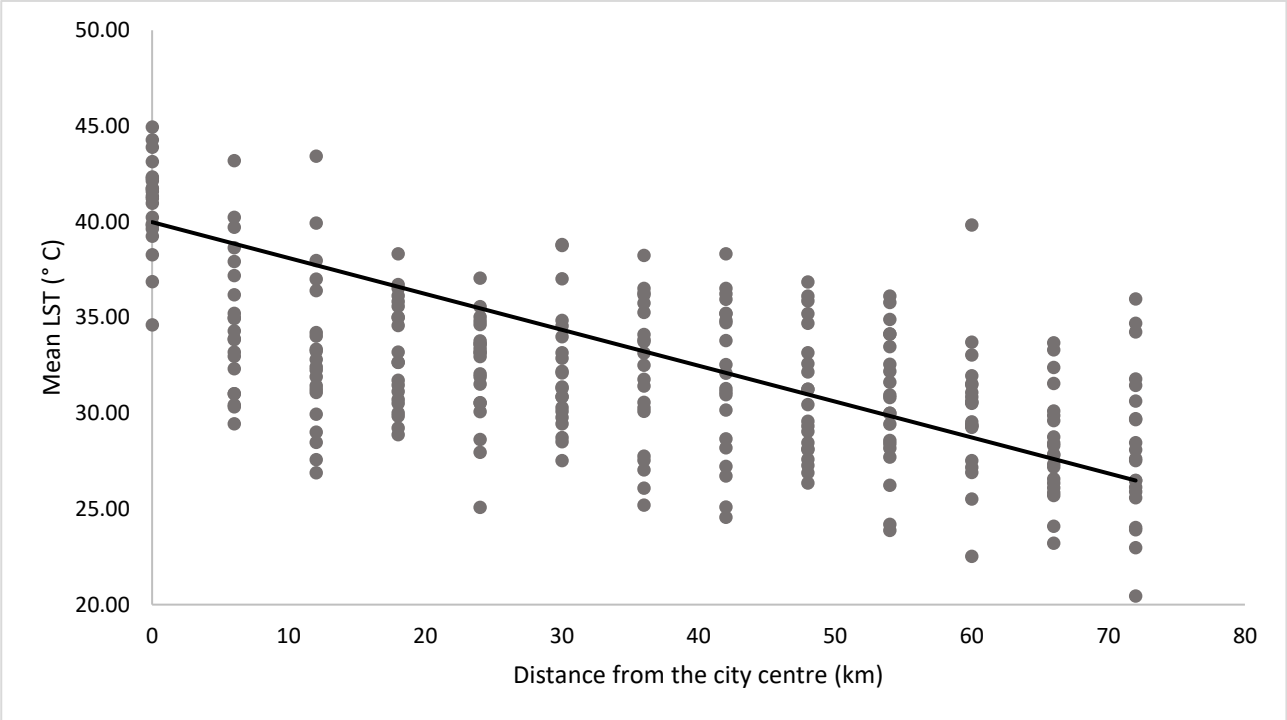

Figure 13: The relationship between the land surface temperature (°C) and the distance from the city centre (km) along gradient B

Table 9: Tukey HSD multiple comparisons of means post hoc test, at 95% confidence level

Land use types (site)	Adjusted p-value
Urban Park (site 4) – CBD (site 1)	<0.001
Roadside (sites 2,3) - CBD (site 1)	<0.001
Highway (sites 5,6) - CBD (site 1)	<0.001
Residential (sites 7,8,9) – CBD (site1)	<0.001
Open Land (sites 10,11,12,13) – CBD (site 1)	<0.001
Open Land (sites 10,11,12,13) - Urban Park (site 4)	<0.001
Open Land (sites 10,11,12,13) - Roadside (sites 2,3)	<0.001
Open Land (sites 10,11,12,13) - Highway (sites 5,6)	0.007

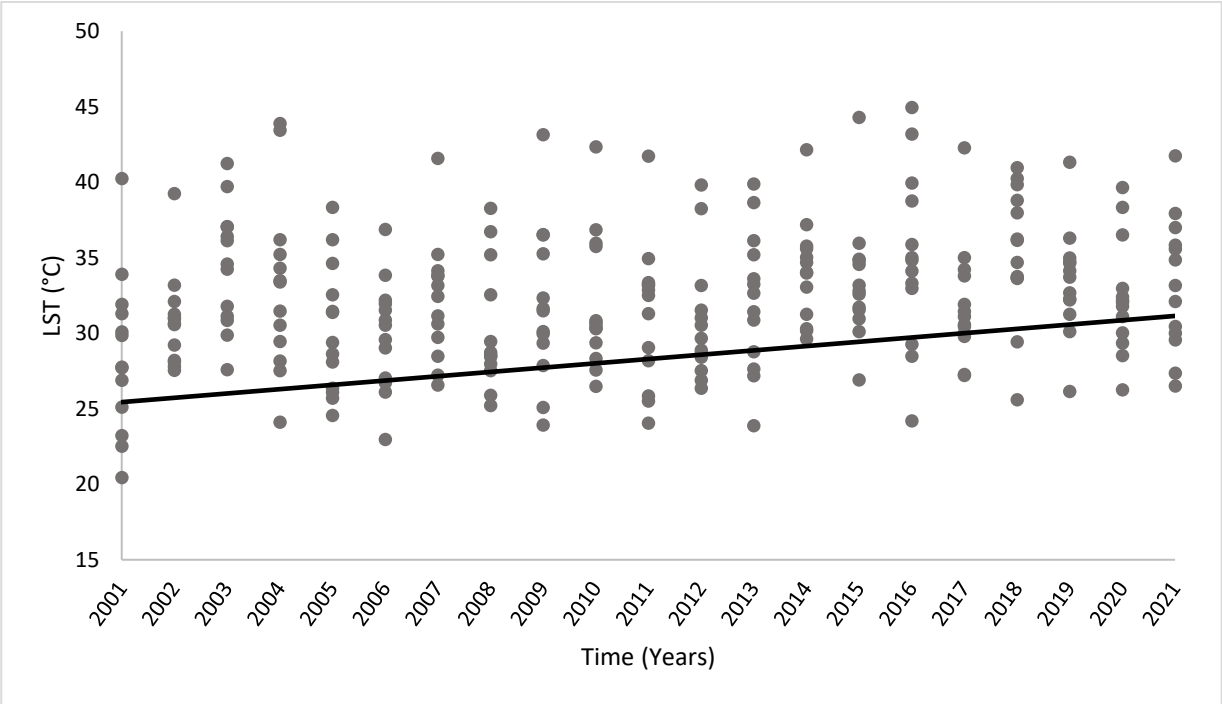

Figure 14: Relationship between the land surface temperature (°C) and time along gradient B

The ANOVA test on the LST at each land use type showed that the land use groups in gradient B had significantly different LSTs ($F_{5,120} = 4.58$, $p<0.001$; Figure 15). The central business district displayed the highest recorded mean LST ($\bar{x}$ = 40.959 °C), followed by the Residential site ($\bar{x}$ = 33.180 °C). Lastly, the Open Land displayed the lowest mean temperature ($\bar{x}$ = 29.297 °C). According to the post hoc test (Table 9), the significant difference was specifically between CBD and all the other land use types shown in Figure 12, as well as between Open Land and all other land use types.

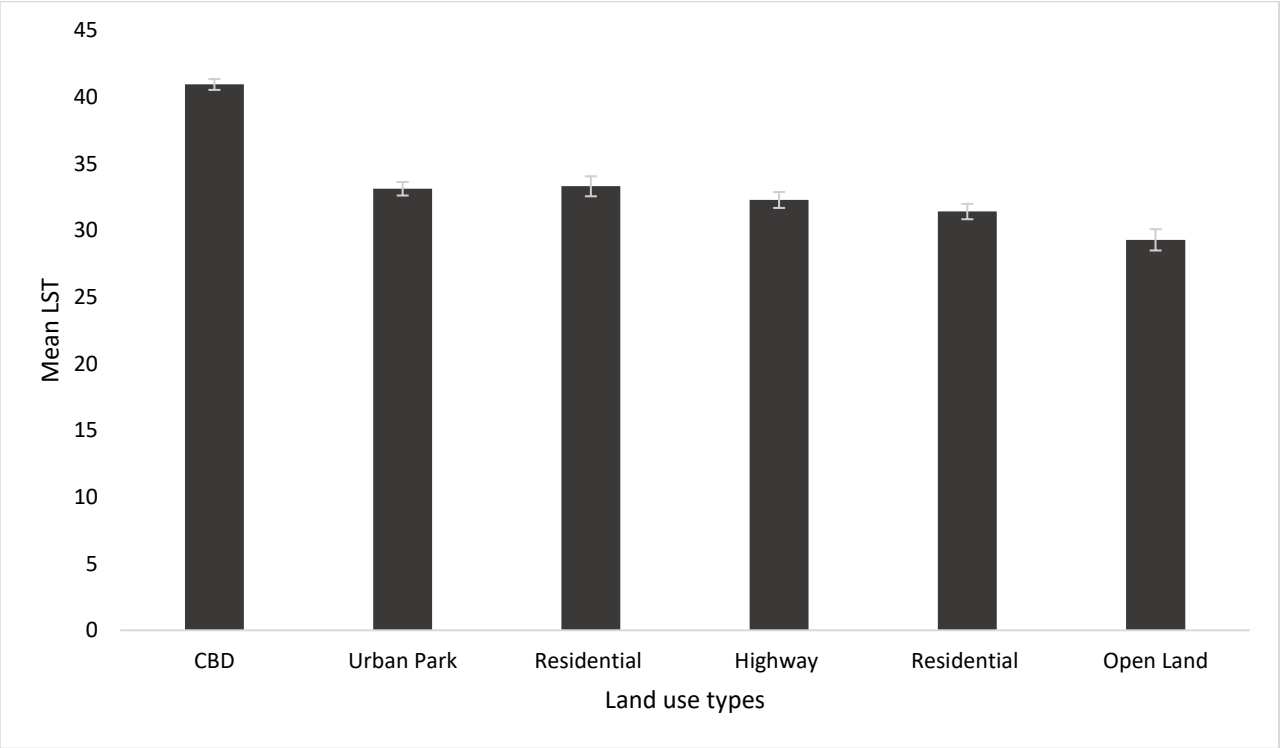

Figure 15: Mean (± SE) Land surface temperature (°C) for each land use type along gradient B

Figure 16 presents the mean LST differences (Δ LST) (°C) between the most urban site (site 1) and all the other sites along gradient B. The Δ LST (°C) indicated an increasing pattern from the urban extreme to the rural extreme of the gradient. According to the ANOVA test, there was a significant difference in the Δ LST (°C) between the sites ($F_{11,240}$ = 6.057, p<0.001). The Tukey HSD Post hoc test results at 95% are shown in Table 10.

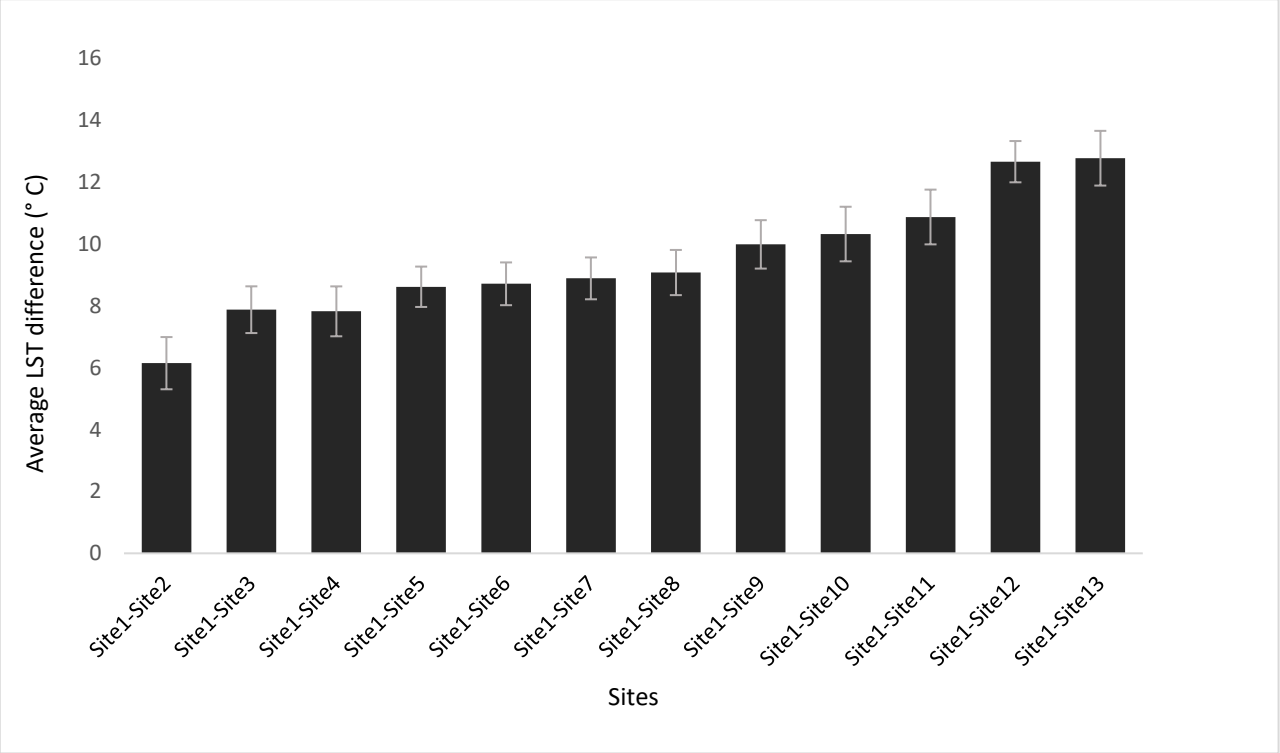

Figure 16: Mean (± SE) land surface temperature difference Δ LST (°C) (between site 1 and all the other sites along the gradient (B), (1 = CBD, 2 = Roadside, 3 = Roadside, 4 = Urban park, 5 = Highway, 6 = Highway, 7 = Residential,8 = Residential, 9 = Residential, 10 = Open Land 11 = Open Land; 12 = Open Land; 13 = Open Land)

Table 10: Tukey HSD multiple comparisons of means post hoc test results for temperature difference, at 95% confidence level

Land use types (site)	Adjusted p-value
Residential (sites 7,8,9) - Roadside (sites 2,3).	0.035
Open Land (sites 10,11,12,13) - Roadside (sites 2,3).	0.004
Open Land (sites 10,11,12,13) - Urban Park (site 4).	0.001
Open Land (sites 10,11,12,13) - Highway (sites5,6).	0.020
Open Land (sites 10,11,12,13) - Roadside (sites 2,3).	0.037

3.1.2 Fractional Vegetation Cover (FVC) versus Land Surface Temperature

Figure 17 presents the mean FVC along gradient A. The vegetation cover along the rural section of the gradient was higher than that of the urban end of the gradient, with cover on the urban end being extremely low, hence it is invisible on the plots. There was a significant difference in the mean FVC between the sites (X^2_{11} = 46.064, p<0.001), with the rural section (site 10 - 13) having a significantly

higher mean FVC ($\bar{x}$ = 0.390 - 0.472) than the urban section (site 1; $\bar{x}$ < 0.001) of the gradient. The Kruskal Wallis Multiple Comparison Post hoc test results are shown in Table 9.

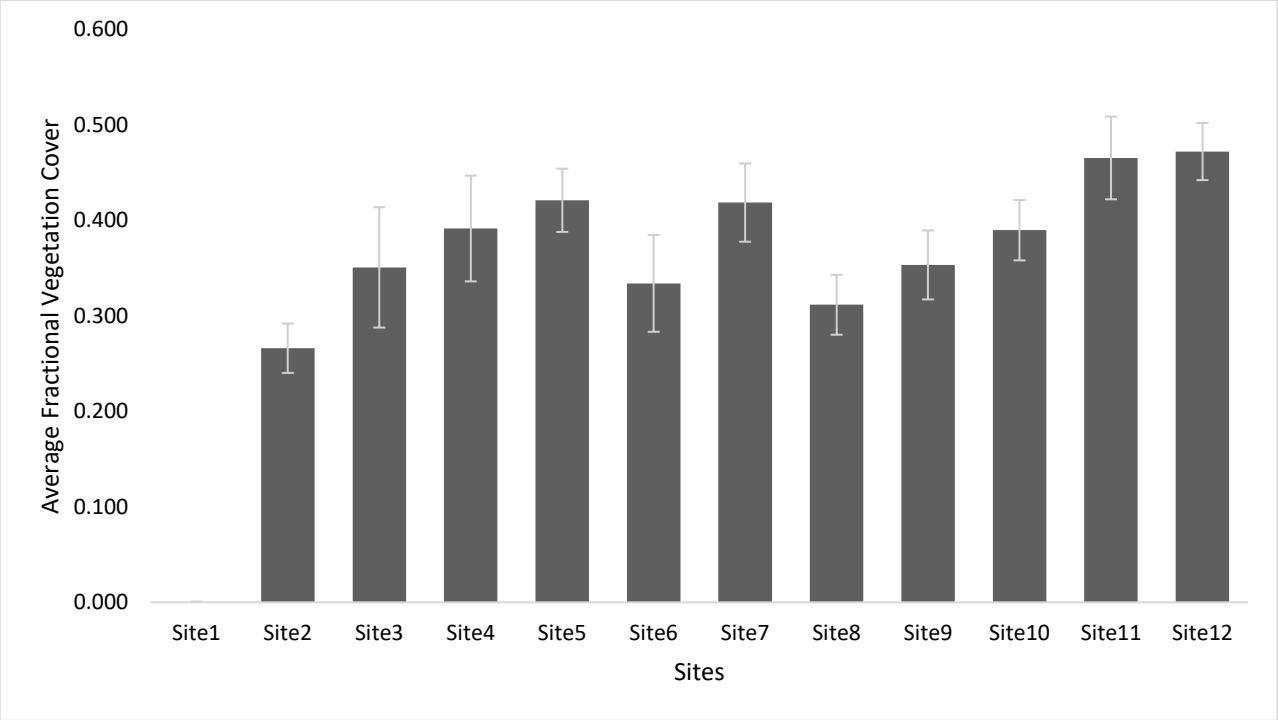

Figure 17: Mean (± SE) fractional vegetation cover across gradient A, (1= CBD, 2 = Urban Park, 3 = Urban Park, 4 = Urban Park, 5= Residential, 6=Residential, 7 = Highway, 8 = Highway, 9 = Nature Reserve, 10 = Nature Reserve, 11= Nature Reserve, 12 = Residential)

Fractional vegetation cover was found to differ significantly between all the assessed land use types (X^2_4 = 20.095, p<0.001). The Urban Park had the highest mean fractional vegetation cover ($\bar{x}$ = 0.395), followed by the Residential ($\bar{x}$ = 0.366), and the CBD had the lowest mean fractional vegetation coverage ($\bar{x}$ = 0.000) (Figure 18). According to the post hoc test, a significant difference in FVC was observed between CBD and all the other land use types along this gradient (Table 11).

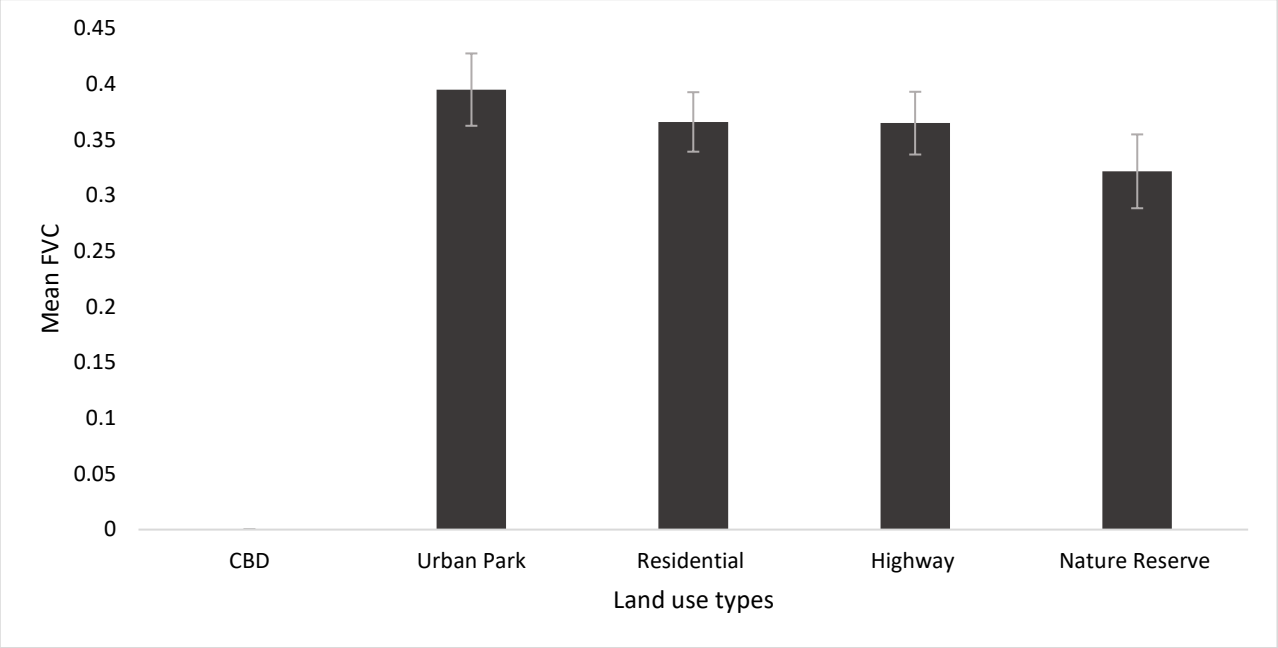

Figure 18: Mean (± SE) fractional vegetation cover at each land use type along gradient A

Table 11: The Kruskal Wallis multiple comparisons post hoc test for FVC, at the 95% and 99% confidence level

Land use types (sites)	P value
CBD (site 1) - Residential (sites 5,6,12	<0.05
CBD (site 1) - Highway (sites 7,8)	<0.05
CBD (site 1) - Urban Park (sites 3,4,5)	<0.05
CBD (site 1) - Nature Reserve (sites 9,10,11)	<0.05

A linear regression analysis between the LST and FVC revealed that a large proportion of the variation in LST could be explained by the variation in FVC (R^2=0.625, p<0.001). Thus, as the vegetation cover increased, the Mean LST decreased in that area (Figure 19).

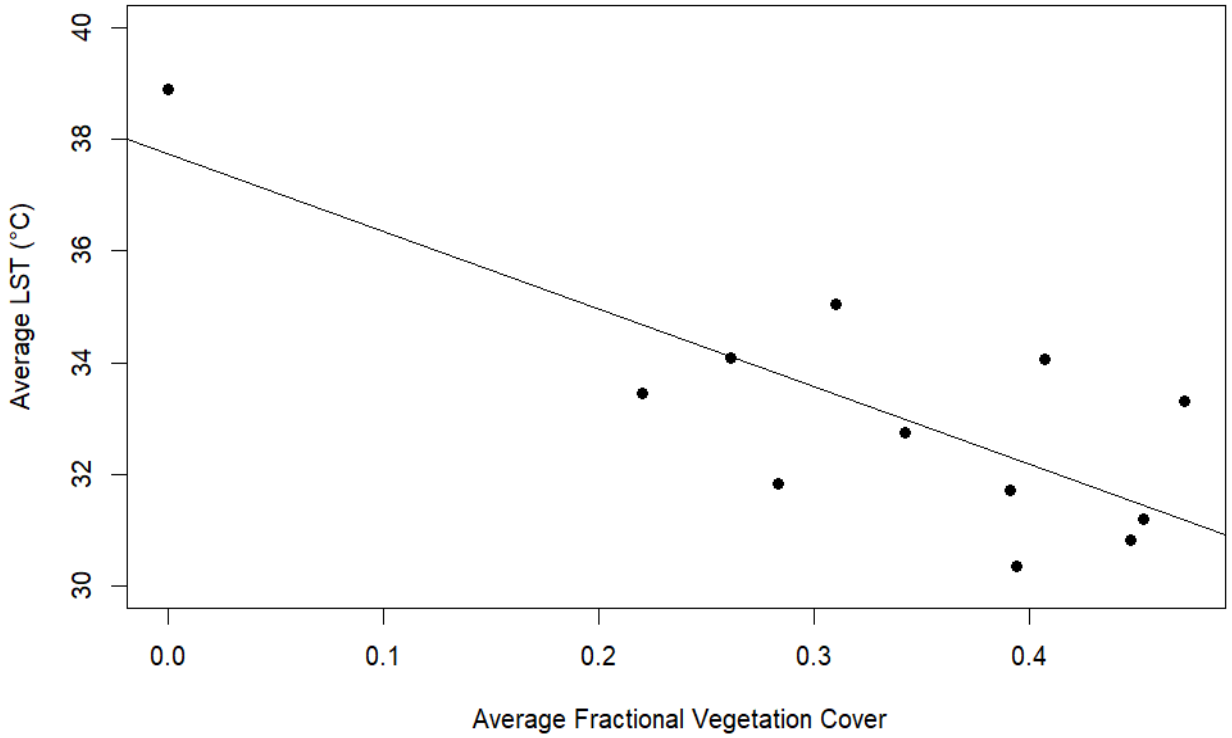

Figure 19: The relationship between fractional vegetation cover on the LST (°C) for gradient A

Figure 20 presents the mean FVC along gradient B. Vegetation cover was shown to increase from the CBD (site 1) to the rural sites (sites 10 - 13). The FVC data were not normally distributed, so a Kruskal Wallis test was performed. The test findings revealed that the FVC differed significantly between the sites (X^2_{12} = 60.556, p<0.001), with the rural end having a significantly higher mean FVC ($\bar{x}$ = 0.6863) than the urban end ($\bar{x}$ = 0.0008) of the gradient. The Kruskal Wallis Multiple Comparison Post hoc test results are shown in Table 12.

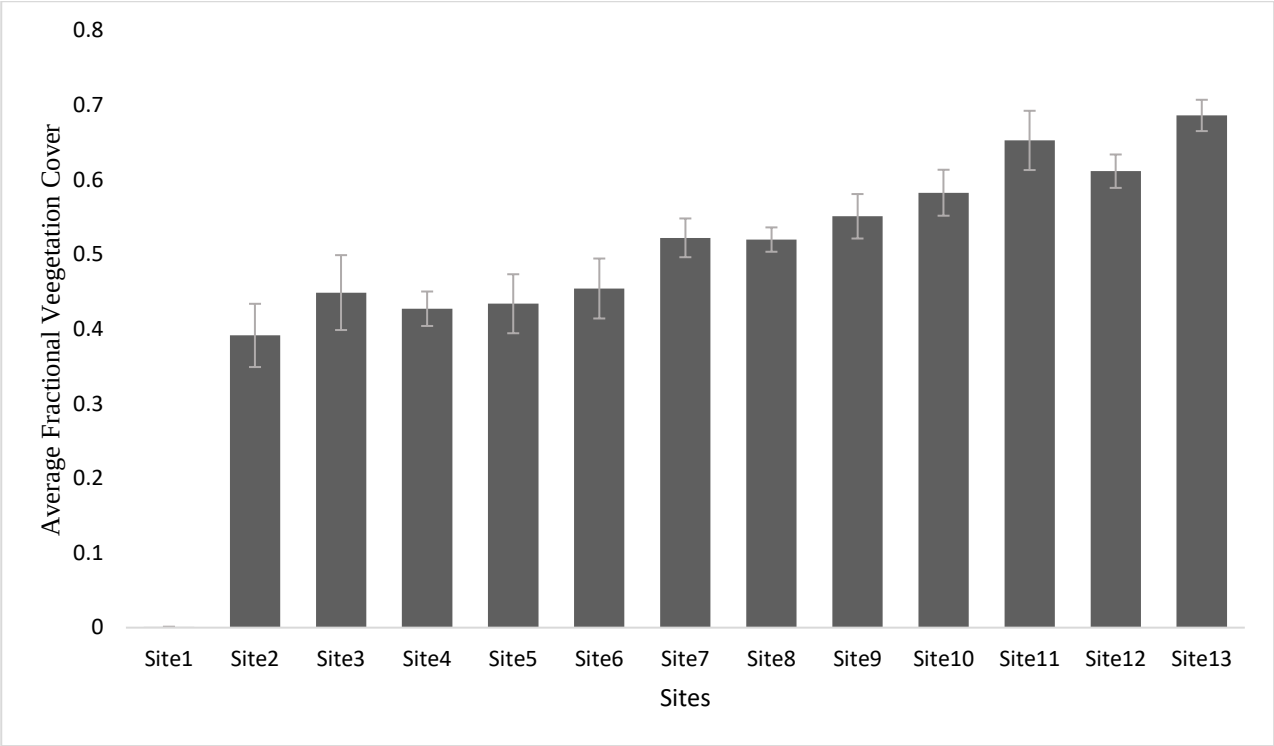

Figure 20: The Mean (± SE) fractional vegetation cover across gradient B, (1 = CBD, 2 = Roadside, 3 = Roadside, 4 = Urban Park, 5 = Highway, 6 = Highway, 7 = Residential,8 = Residential, 9 = Residential, 10 = Open Land 11 = Open Land; 12 = Open Land; 13 = Open Land)

Table 12: The Kruskal Wallis multiple comparisons post hoc test for FVC at the 95% and 99% confidence level

Land use types (site)	P value
CBD (site 1) - Open Land (sites 10, 11, 12, 13)	<0.05
CBD (site 1) – Residential area (sites 7,8,9)	<0.05
Roadside (sites 2, 3) - Open Land (sites 10, 11, 12, 13).	<0.05
Urban Park (site 4) - Open Land (sites 10, 11, 12, 13)	<0.05
Highway (sites 5,6) - Open Land (sites 10, 11, 12, 13)	<0.05

Similar to gradient A, the FVC varied significantly across the land use types in gradient B (X^2_5 = 32.736, p<0.001). The land use type characterised by Open Land exhibited the highest mean fractional vegetation cover ($\bar{x}$ = 0.633), while residential displayed the second highest mean fractional vegetation cover ($\bar{x}$ = 0.535). Conversely, the CBD had the lowest fractional vegetation cover among the land use types ($\bar{x}$ = 0.001) (Figure 21). The post hoc results indicated that the FVC at CBD differed significantly from the FVC at the residential areas, as well as at the Open

Land. In addition, a significant difference in FVC was noted between the Open Land land use type and Residential, Urban Park, and Highway land use types (Table 10).

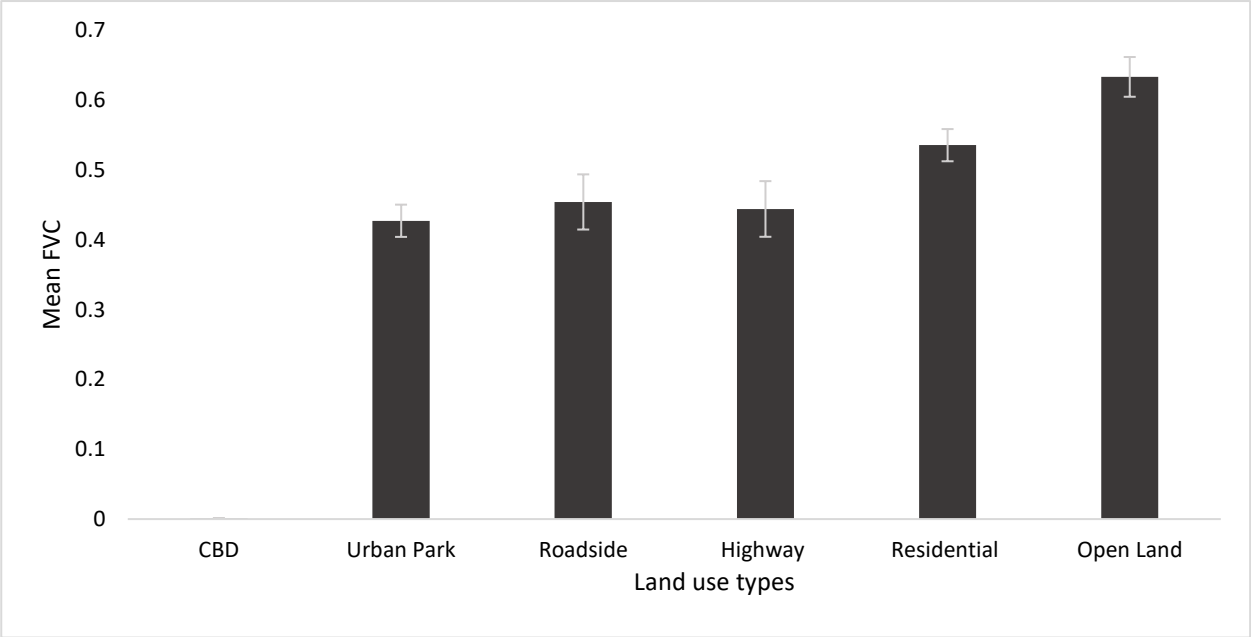

Figure 21: Mean (± SE) fractional vegetation cover for each land use type along gradient B

Along gradient B, the relationship between the fractional vegetation cover and land surface temperature was also assessed, and similar results to gradient A were derived. The linear regression model output provides that a large proportion of the variation in LST could be explained by the variation in FVC ($R^2 = 0.9538$, $p < 0.001$); as the vegetation cover increases, the mean LST decreases (Figure 22).

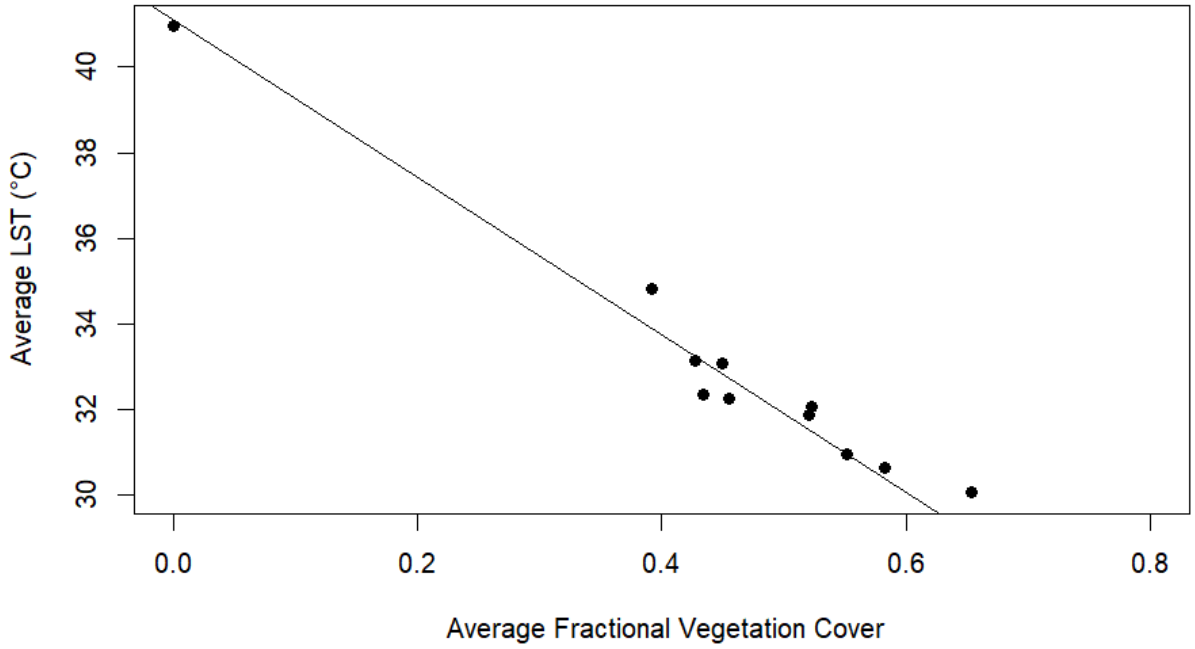

Figure 22: The relationship between fractional vegetation cover and land surface temperature for gradient B

4.2 Objective 2: Carbon sequestration

The estimated carbon storage data along gradient A were analysed using the Kruskal Wallis rank sum test, and the results indicated a significant difference in the stored carbon from site to site (X^2_{11} = 111.7, p<0.001). The stored carbon increased with increasing distance from the city centre (R^2 = 0.2148, p = 0.129; Figure 24), with sites closer to the rural end of the gradient having more estimated stored carbon (sites 10: $\bar{x}$ = 27.489; site 11: $\bar{x}$ = 34.733; site 12: $\bar{x}$ = 16.852) than those that are located towards the urban end of the gradient (Figure 23). To further determine where the significant difference lay, a Kruskal Wallis Multiple comparison post hoc test at a 99% and 95% confidence level was conducted, the results are shown in Table 13.

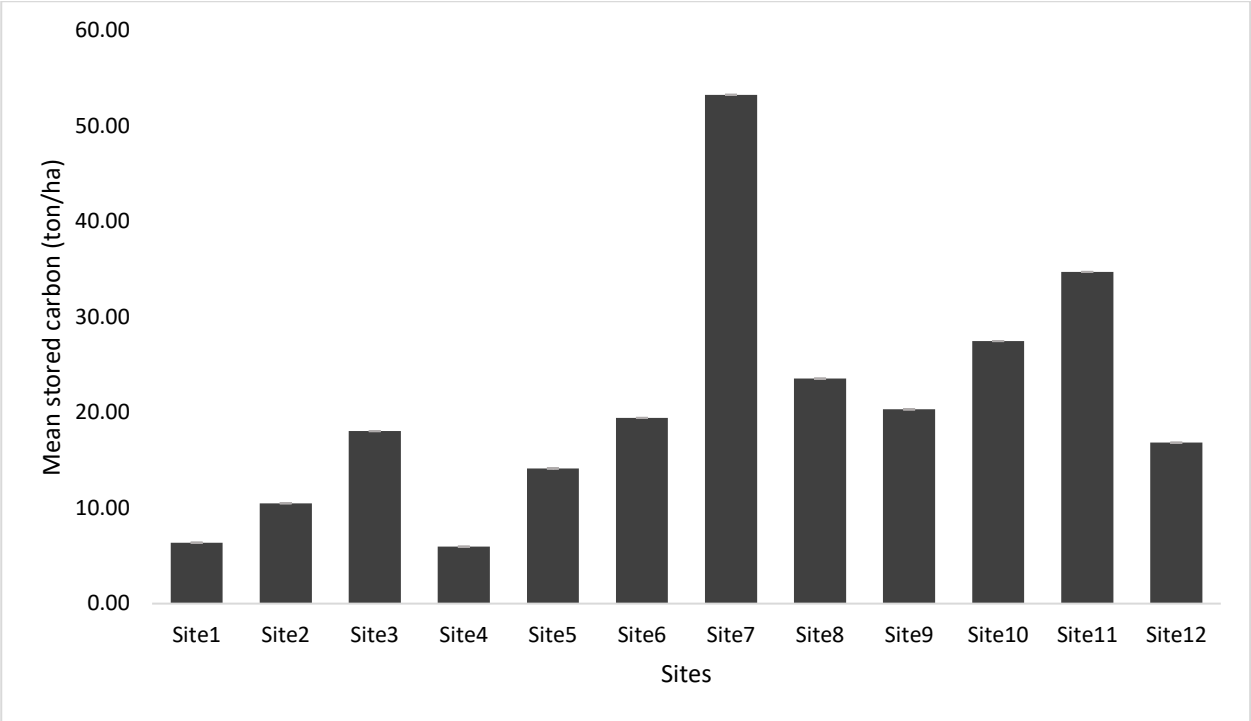

Figure 23: Mean (± SE) stored carbon (ton/ha) along gradient A (1= CBD, 2 = Urban Park, 3 = Urban Park, 4 = Urban Park, 5= Residential, 6=Residential, 7 = Highway, 8 = Highway, 9 = Nature Reserve, 10 = Nature Reserve, 11= Nature Reserve, 12 = Residential)

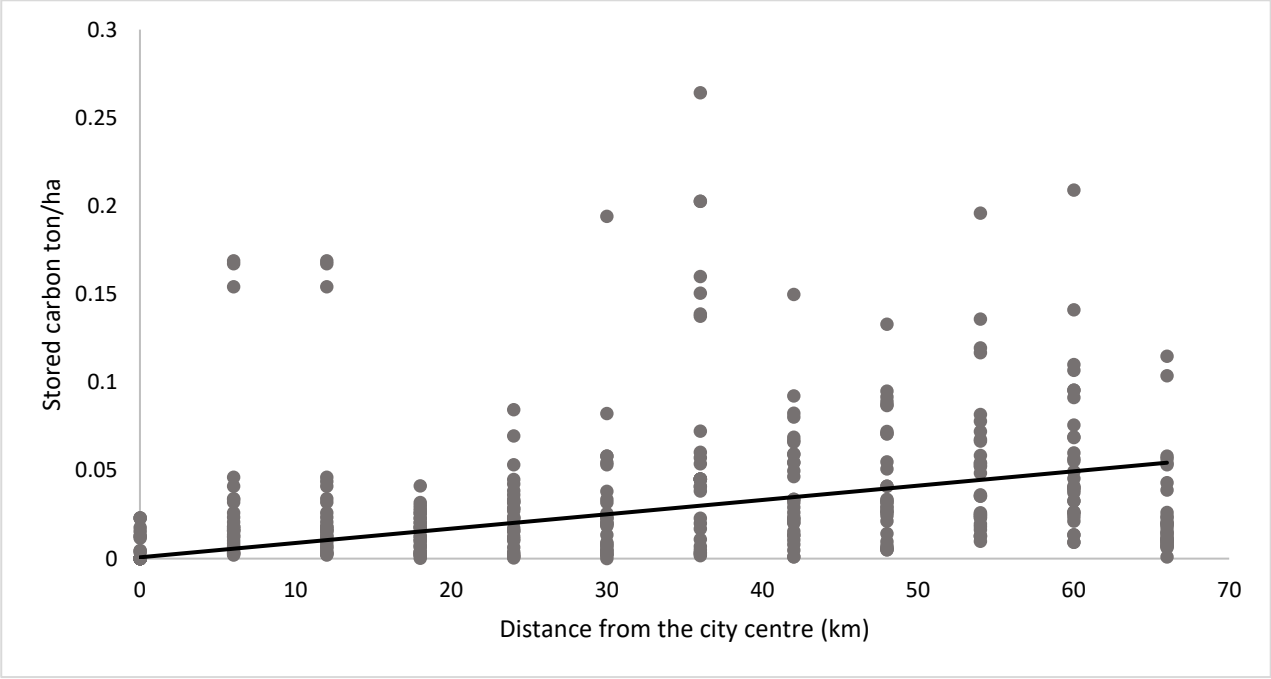

Figure 24: Relationship between stored carbon (ton/ha) and distance from the city centre (km) along gradient A

The stored carbon in the various land use types found along gradient A was assessed using a Kruskal Wallis rank sum test. The results indicated that the amount of stored carbon differed significantly

across the land use types (X^2_4 = 83.032, p<0.001; Figure 25). The highest amount of carbon was stored at the Residential land use type ($\bar{x}$ = 28.961 ton/ha), while the Nature Reserve had he second highest mean stored carbon ($\bar{x}$ = 26.358 ton/ha). The central business district showed the lowest average carbon storage ($\bar{x}$ = 6.380 tons/ha). Following Kruskal Wallis multiple comparisons and a post hoc test (Table 13), it was identified that the significant difference in the amount of carbon stored was between the CBD land use type and all other land use types as shown in Figure 20, as well as, between the Urban Park and the Highway and Nature Reserve, and between Residential and Nature Reserve.

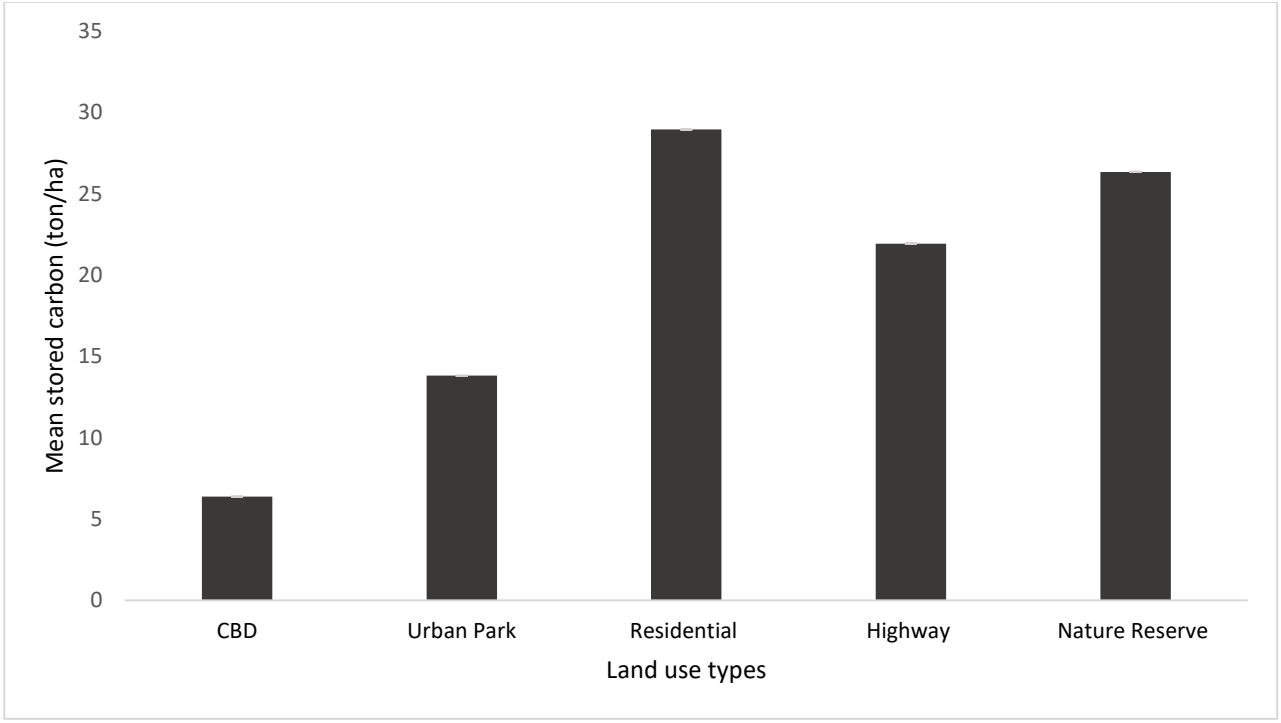

Figure 25: Mean (± SE) stored carbon for each land use type along gradient A

Table 13: Kruskal Wallis multiple comparisons post hoc test, at the 95% and 99% confidence level

Land use type (site)	P value
CBD (site 1) - Urban Park (sites 2, 3, 4)	<0.05
CBD (site 1) - Residential (sites 5,6)	<0.05
CBD (site 1) - Highway (sites 7, 8)	<0.05
CBD (site 1) - Nature Reserve (sites 9, 10, 11)	<0.05
Urban Park (sites 2, 3, 4) - Highway (7, 8)	<0.05
Urban Park (sites 2, 3, 4) – Nature Reserve (9, 10, 11)	<0.05

Residential (sites 5,6) Nature Reserve (9, 10, 11)	<0.05

Carbon storage was also estimated for every fifth year between 2001 and 2021 using Google Earth images to determine tree cover. The mean stored carbon increased from $\bar{x}$ = 1.315 ton/ha in the year 2001 to $\bar{x}$ = 4.413 ton/ha in the year 2021 (Figure 26), thus, a net change of 3.098 ton/ha in stored carbon. The Kruskal Wallis rank sum test also indicated that there was a significant difference in the stored carbon between the years (X^2_4 = 1.9606, p>0.05). According to the Kruskal Wallis multiple comparisons post hoc test, at the 95% confidence level, a significant difference in stored carbon was found between 2001 and 2021.

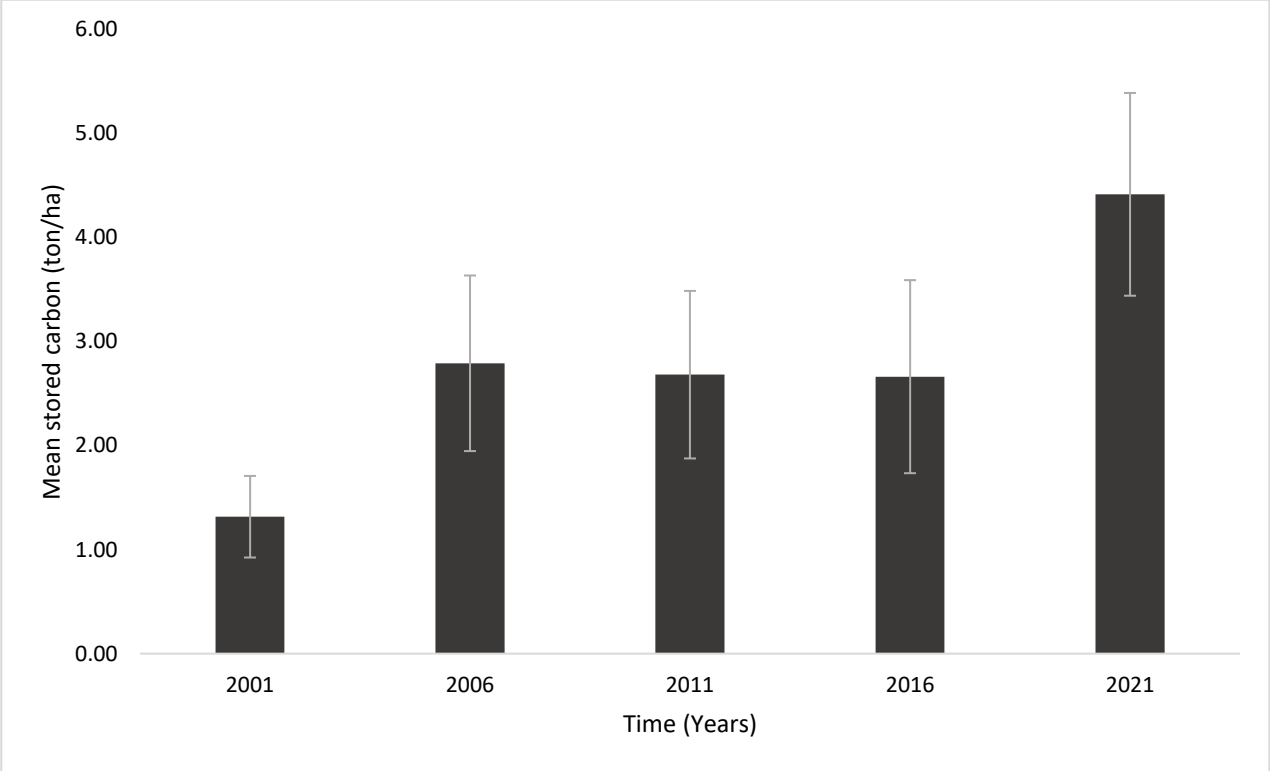

Figure 26: Mean (± SE) stored carbon (ton/ha) for every five years, from 2001 to 2021

Similar to gradient A above, gradient B had variations in the amount of stored carbon. Sites located closer to the rural end of the gradient stored more carbon than the sites closer to the urban end of the gradient. The carbon data were not normally distributed and thus a Kruskal Wallis rank sum test was used for analysis. The test results showed a significant difference in the stored carbon across the sites gradient B (X^2_{12} = 227.03, p<0.001; Figure 27). The stored carbon increased as the distance from the city centre increased (R^2 =0.8486, p<0.001; Figure 28). The post hoc results are shown in Table 14.

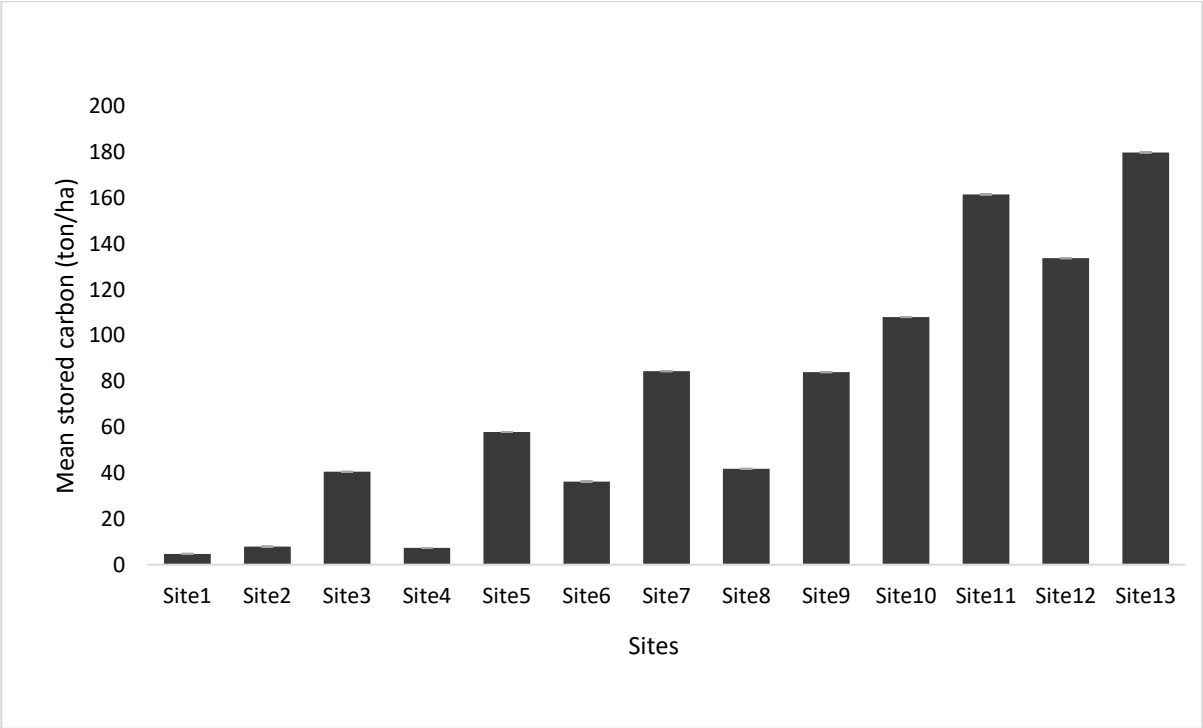

Figure 27: Mean (± SE) stored carbon (ton/ha) along gradient B (1 = CBD, 2 = Roadside, 3 = Roadside, 4 = Urban Park, 5 = Highway, 6 = Highway, 7 = Residential, 8 = Residential, 9 = Residential, 10 = Open Land, 11 = Open Land; 12 = Open Land; 13 = Open Land)

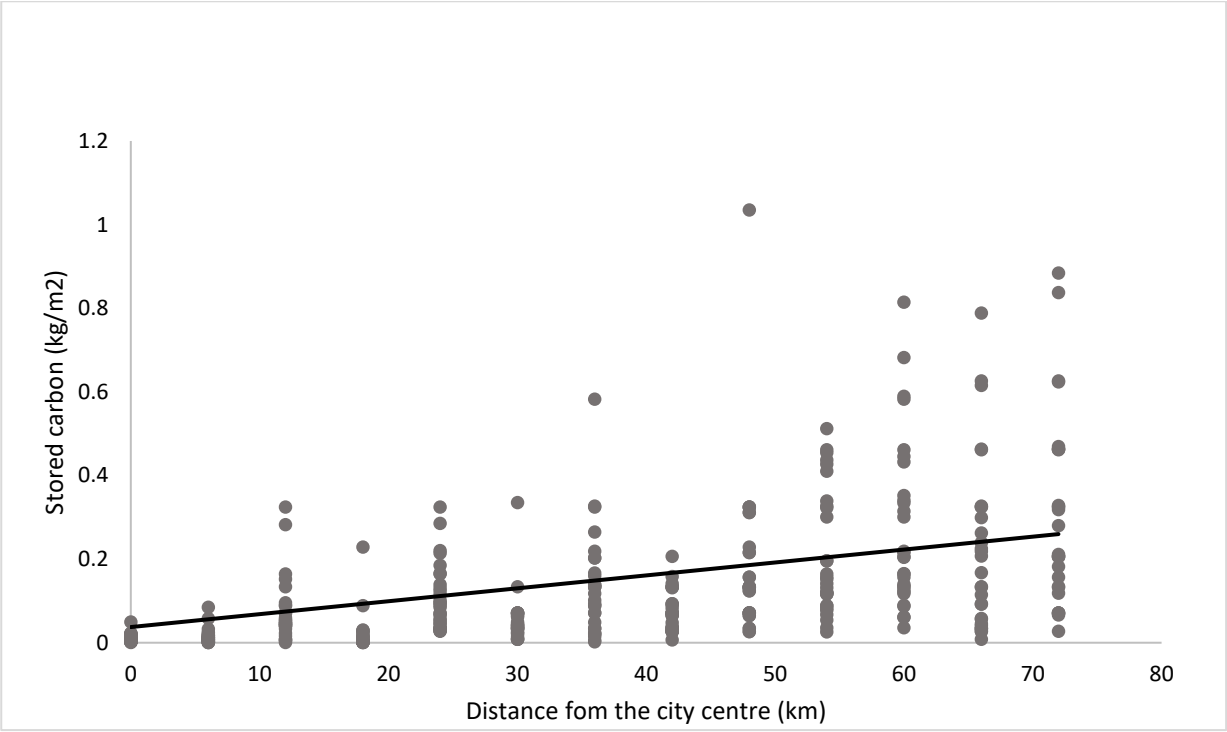

Figure 28: Relationship between stored carbon (ton/ha) and distance from the city centre (km) along gradient B

The stored carbon differed significantly across the various land use types (X^2_5 = 129.28, p< 0.001). The Open Land, land use type stored substantially more carbon ($\bar{x}$ = 145.895 ton/ha), followed by the residential area ($\bar{x}$ = 62.936 ton/ha). CBD again had the least carbon stored compared to all other land use types ($\bar{x}$ = 4.731 ton/ha) (Figure 29). According to the post hoc test, CBD and Urban Park land use types differed significantly from all the other sites, in that the Urban Park had few small trees, and the CBD, had even fewer trees, thus the stored carbon was found to be the lowest in these sites compared to all other sites along the gradient. In Addition, Open Land had significantly more stored carbon than the Residential land use type (Table 14).

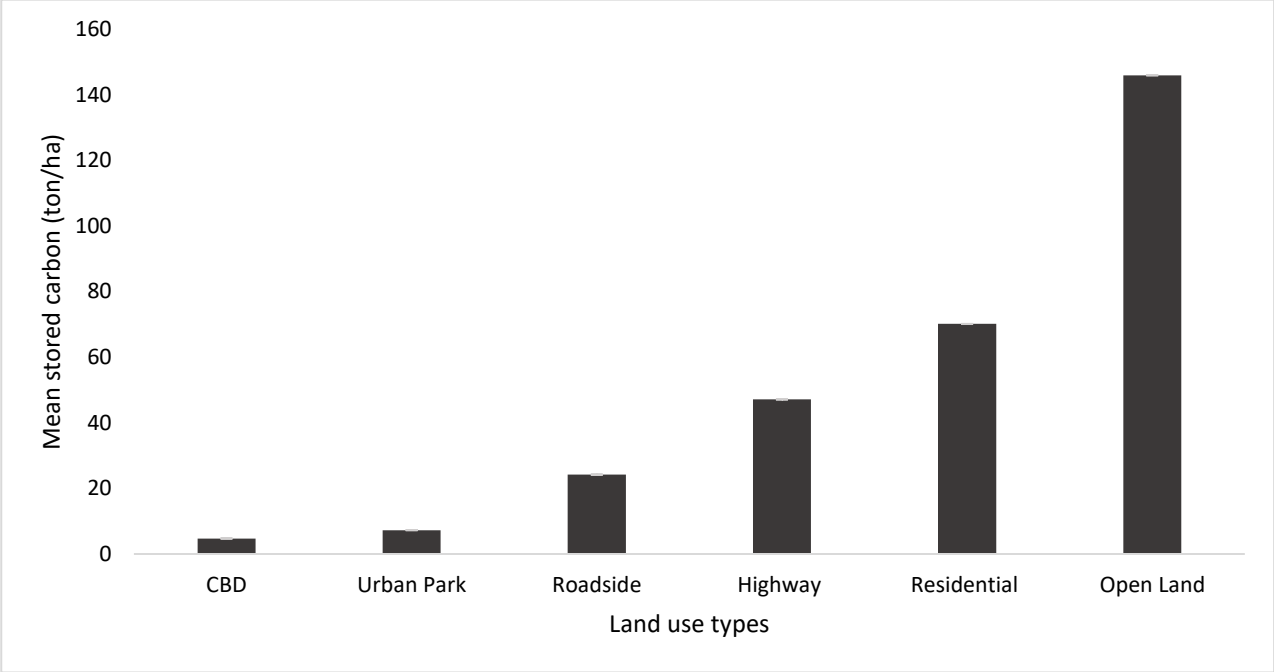

Figure 29: Mean (± SE) stored carbon at each land use type along gradient B

Table 14: Kruskal Wallis multiple comparisons post hoc test, at the 95% and 99% confidence level

Land use types (sites)	P value
CBD (site 1) - Roadside (sites 2,3)	<0.05
CBD (site 1) - Residential (sites 7,8,9)	<0.05
CBD (site 1) - Open Land (sites 10, 11, 12, 13)	<0.05
Highway (site 5,6) - Urban Park (site 4)	<0.05
Residential (sites 7,8,9) - Open Land (sites 10, 11, 12, 13)	<0.05
Urban Park (site 4) - Highway (site 5,6)	<0.05

Urban Park (site 4) - Residential (sites 7,8,9)	<0.05
Urban Park (site 4) - Open Land (sites 10, 11, 12, 13)	<0.05
Highway (site 5,6) - Open Land (sites 10, 11, 12, 13)	<0.05

Along gradient B, carbon storage was estimated for every fifth year during the past two decades. Similar to gradient A, the stored carbon differed significantly between 2001 and 2021 ($X^2_4 = 9.250$, $p < 0.05$). The stored carbon was shown to increase over the years (Figure 30). On average, the stored carbon increased from $\bar{x} = 3.918$ ton/ha in the year 2001 to $\bar{x} = 8.261$ ton/ha in the year 2021. The net change in stored carbon from 2001 to 2021 was a 4.343 ton/ha increase. The Kruskal Wallis multiple comparisons post hoc test, at the 95% confidence level post hoc test indicated that the amount of carbon stored differed significantly between 2001 and 2021.

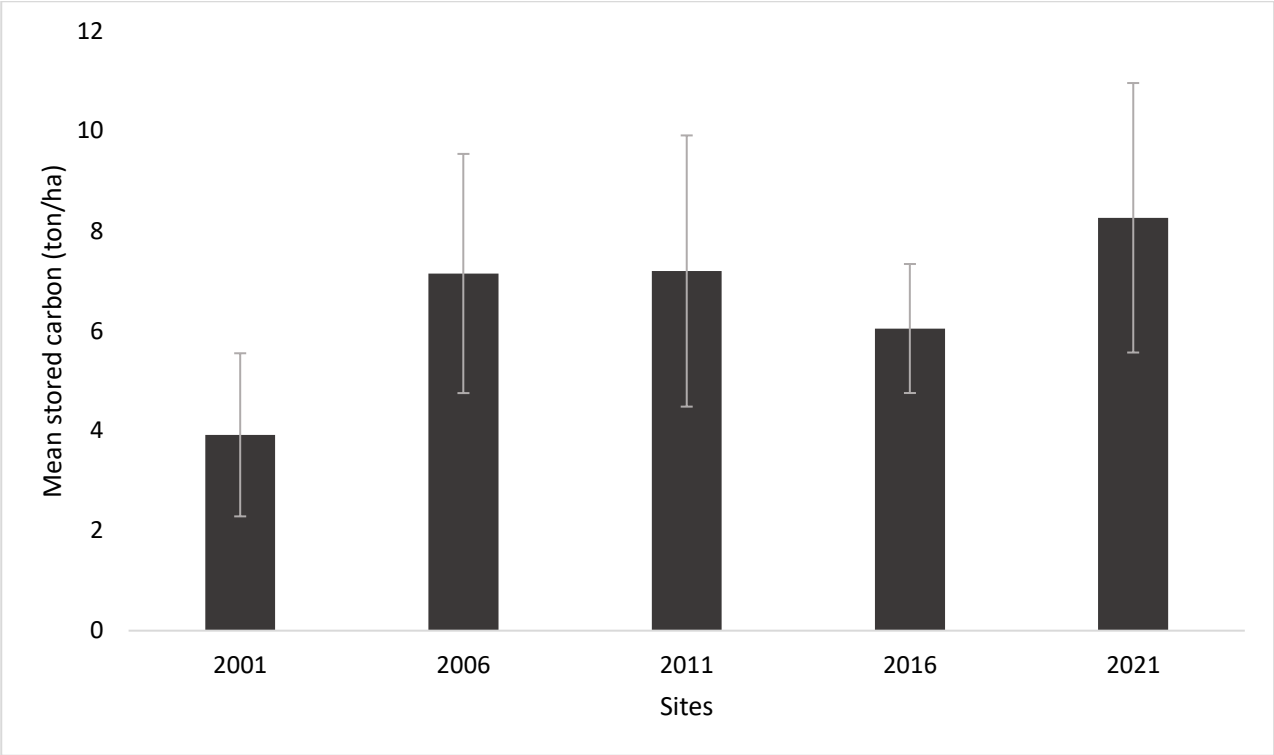

Figure 30: Mean (± SE) stored carbon (ton/ha) along gradient (B) for every five years, from 2001 to 2021

4.3 Objective 3: Flood regulation

The soil compaction data for gradient A did not follow a normal distribution, and accordingly, a Kruskal Wallis rank sum test was used to analyse the data. The results from the test indicated that soil compaction measurements along gradient A differed significantly between the sites ($X^2_{11} = 43.07$, $p < 0.05$; Figure 31). Soil compaction decreased significantly with more distance from the city ($R^2 =$

0.2583, p <0.001; Figure 32). The Kruskal Wallis multiple comparisons post hoc test results are shown in Table 15.

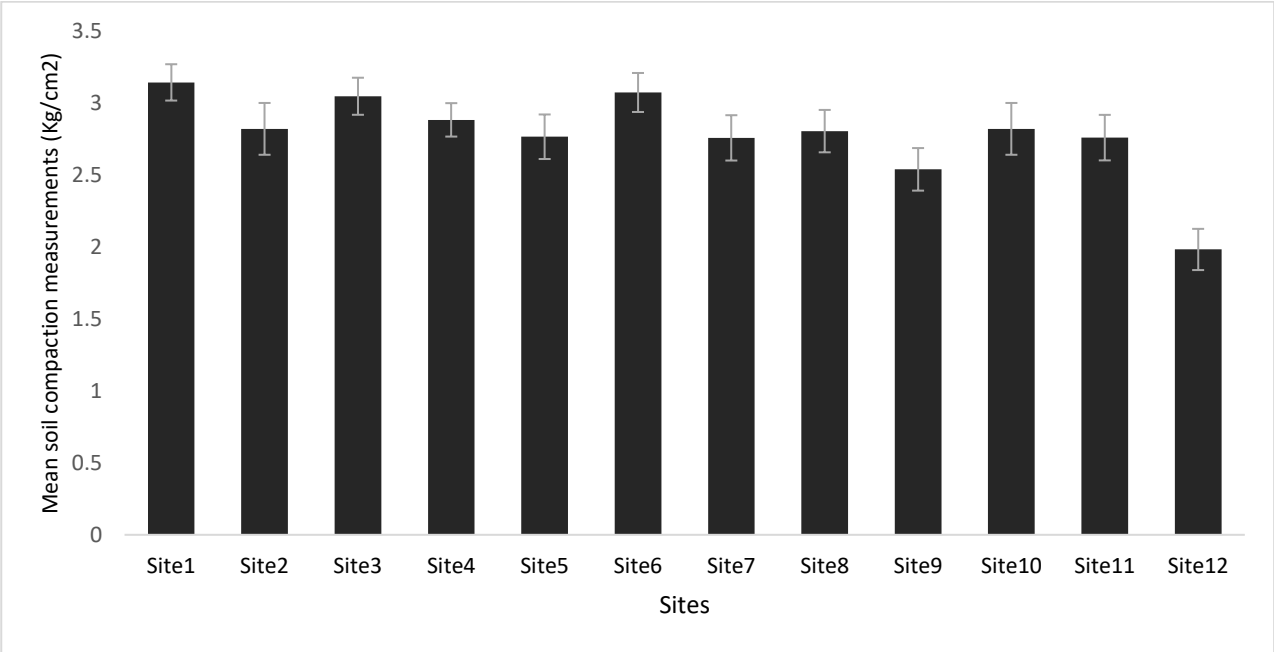

Figure 31: Mean (± SE) soil compaction measurements (kg/cm2) along Gradient A (1 = CBD, 2 = Urban Park, 3 = Urban Park, 4 = Urban Park, 5= Residential, 6=Residential, 7 = Highway, 8 = Highway, 9 = Nature Reserve, 10 = Nature Reserve, 11= Nature Reserve, 12 = Residential)

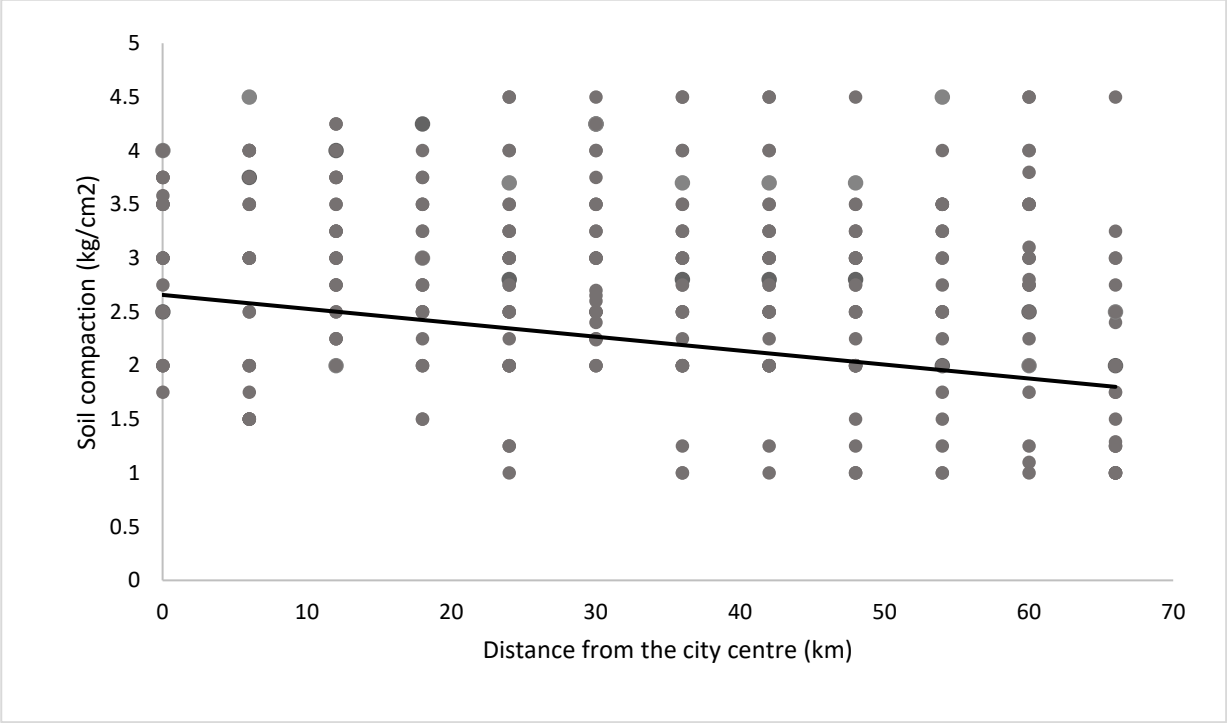

Figure 32: Relationship between soil compaction (kg/cm^2) and distance from the city centre (km) along gradient A

Further analysis showed that there was a substantial variation in soil compaction between the various land use types (X^2_4 = 13.42, p <0.05; Figure 33). The Nature Reserve land use type had the lowest mean soil compaction measurements ($\bar{x}$ = 2.521 kg/cm^2), followed by the Highway land use type ($\bar{x}$ = 2.544 kg/cm^2). The Residential land use type showed the highest mean soil compaction ($\bar{x}$ = 3.206 kg/cm^2). Following the Kruskal Wallis multiple comparisons post hoc test, it is evident that soil compaction in the CBD and Urban Park differed significantly from the soil compaction at the Nature Reserve, more results from the post hoc test are shown in Table 15.

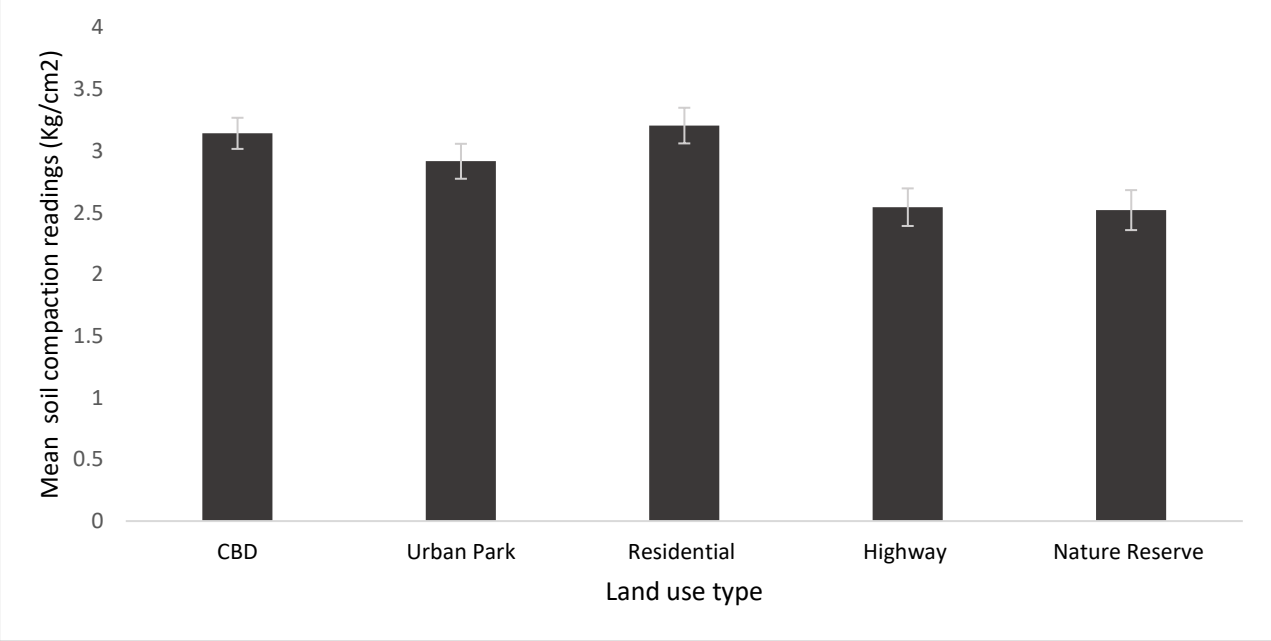

Figure 33: Mean soil compaction readings for each land use type along gradient A

Table 15: The Kruskal Wallis multiple comparisons post hoc test, at the 95% and 99% confidence level for FVC

Land use types (site)	P value
CBD (site 1) -Residential (sites 5,6,12)	<0.05
Urban Park (sites 3,4,5) - Residential (sites 5,6,12)	<0.05
Residential (sites 5,6,12) - Nature Reserve (sites 9,10,11)	<0.05
Highway (sites 7,8) - Nature Reserve (sites 9,10,11)	<0.05
Urban Park (sites 3,4,5) - Nature Reserve (sites 9,10,11)	<0.05
Residential (sites 5,6,12) - Nature Reserve (sites 9,10,11)	<0.05
Highway (sites 7,8) - Nature Reserve (sites 9,10,11).	<0.05
CBD (sites 1) - Nature Reserve (sites 9,10,11)	<0.05

The soil compaction data in gradient B was also not normally distributed, thus it was analysed using a Kruskal Wallis rank sum test. Similar to gradient A, soil compaction varied significantly across the sites (X^2_{12}= 221.74, p < 0.001; Figure 34). The soil compaction significantly decreased as the distance from the city increased. (R^2 = 0.853, p <0.001; Figure 35). Sites proximal to the rural extreme of the gradient had a low soil compaction ($\bar{x}$ = 2,24 kg/cm^2) compared to the sites towards the urban extreme of the gradient ($\bar{x}$ = 3,69 kg/cm^2). The Kruskal Wallis multiple comparisons post hoc test, at the 95% confidence level results are shown in Table 16.

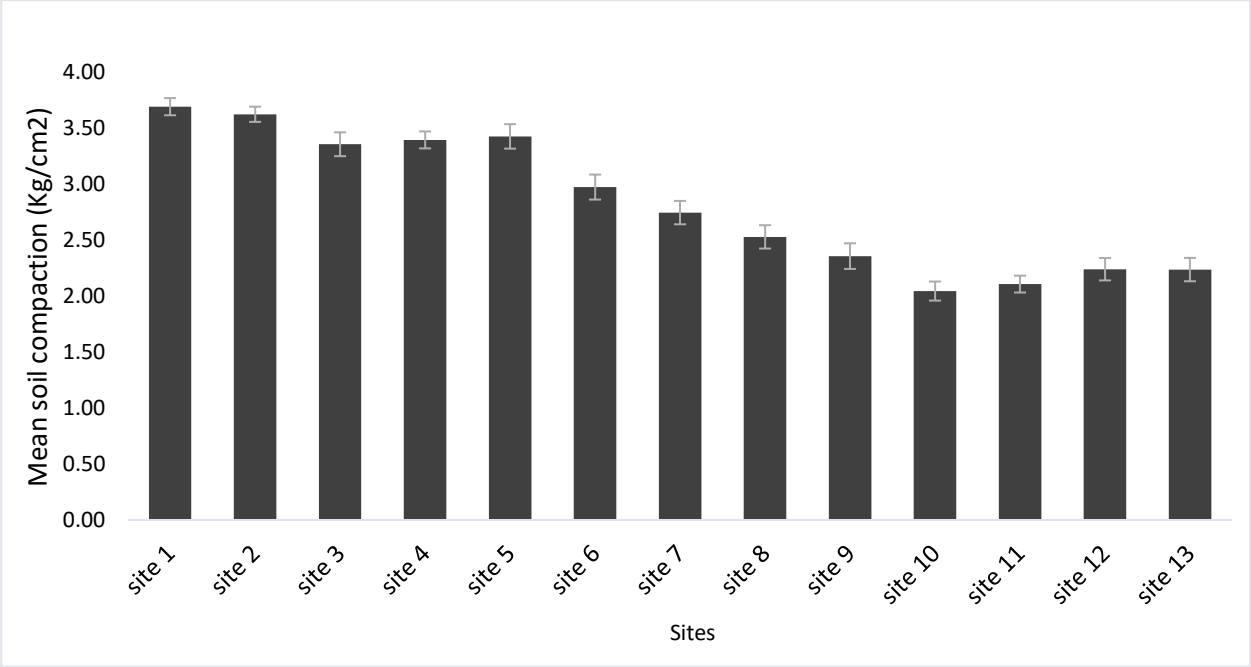

Figure 34: Mean (± SE) soil compaction measurements (kg/cm2) along the urban-rural gradient (B) (with sites being; 1 = CBD, 2 = Roadside, 3 = Roadside, 4 = Urban Park, 5 = Highway, 6 = Highway, 7 = Residential, 8 = Residential, 9 = Residential, 10 = Open Land 11 = Open Land; 12 = Open Land; 13 = Open Land)

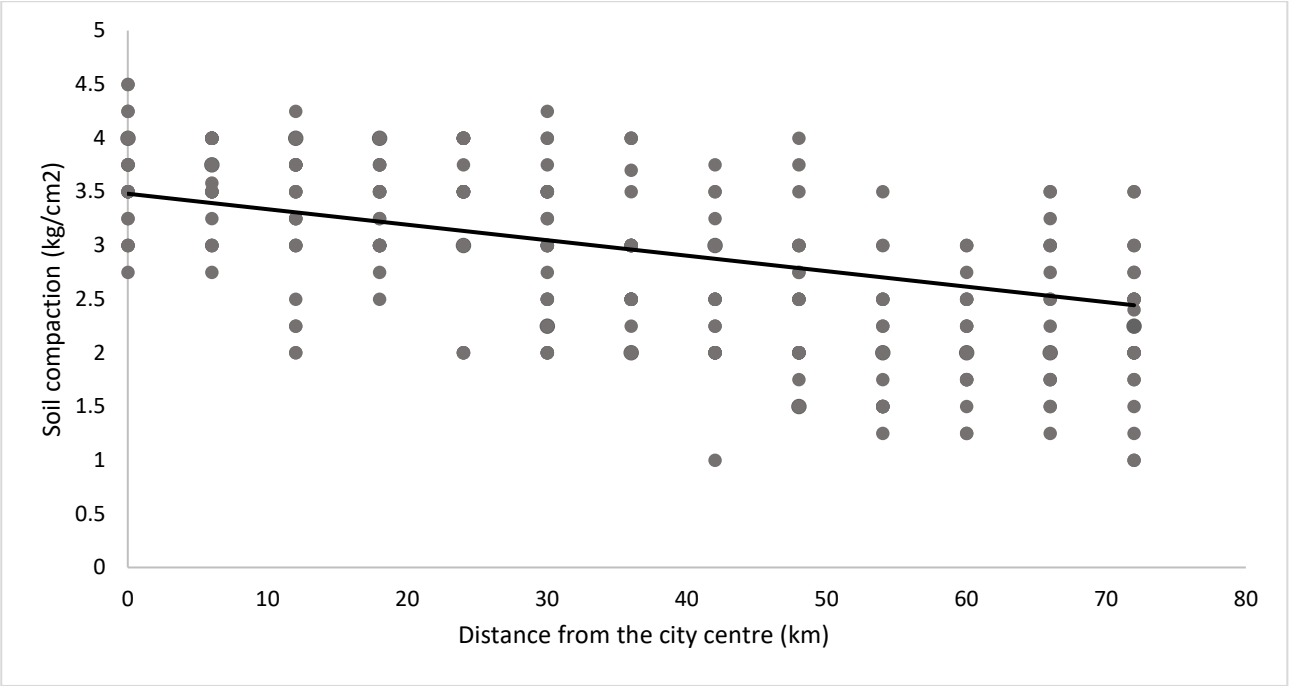

Figure 35: Linear regression showing the change in soil compaction (kg/cm^2) over the distance from the city centre (km) along gradient B

Soil compaction varied significantly across the land use types along gradient B (X^2_5 = 125.8, p < 0.001; Figure 36). Open Land had the least mean soil compaction ($\bar{x}$ = 2.155 Kg/cm^2), followed by the residential land use ($\bar{x}$ = 2.445 Kg/cm^2). The soil in the CBD was the most compacted ($\bar{x}$ = 3.695 kg/cm^2). Table 16 displays the post-hoc results, indicating which land use types had significant differences in soil compaction.

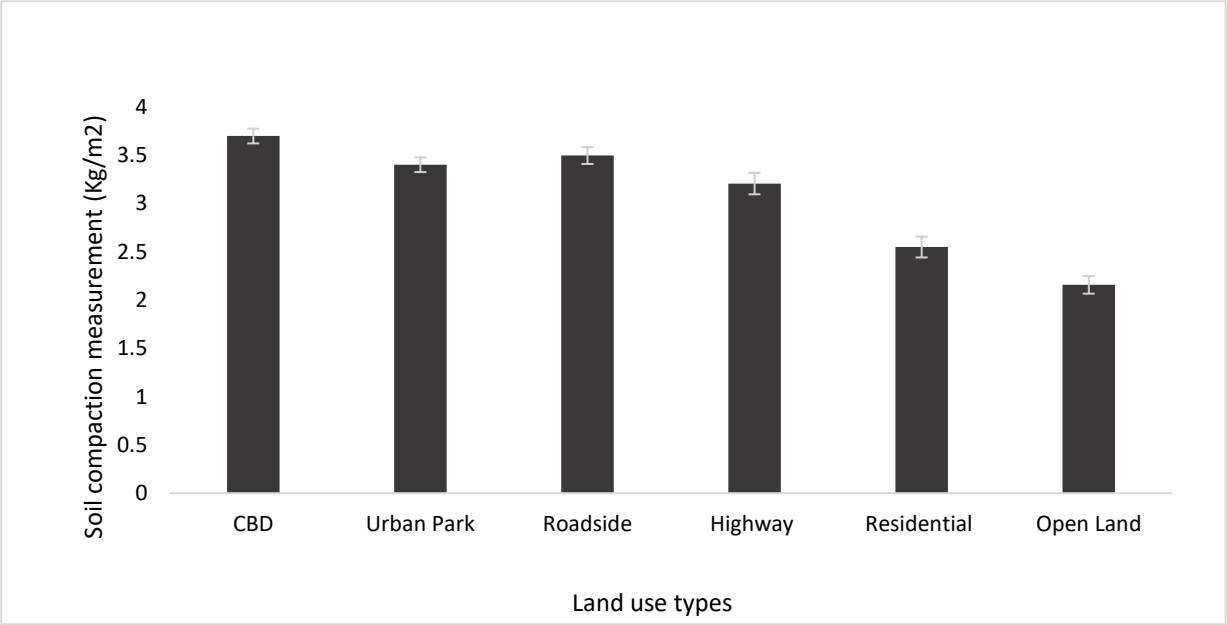

Figure 36: Mean (± SE) soil compaction readings for each land use type along gradient B

Table 16: The Kruskal Wallis multiple comparisons post hoc test, at the 95% and 99% confidence level

Land use types (site)	P value
CBD (site 1) - Highway (site 5,6)	< 0.05
CBD (site 1) - Residential (sites 7,8,9)	< 0.05
CBD (site 1) - Open Land (sites 10, 11, 12, 13)	< 0.05
Roadside (sites 2,3) – Residential (sites 7,8,9)	< 0.05
Roadside (sites 2,3) - Open Land (sites 10, 11, 12, 13)	< 0.05
Urban Park (site 4) - Residential (sites 7,8,9)	< 0.05
Highway (site 5,6) – CBD (site 1)	< 0.05
Urban Park (site 4) - Open Land (sites 10, 11, 12, 13)	< 0.05
Highway (sites 5,6) - Residential sites 7,8,9)	< 0.05
Highway (site 5,6) - Open Land (sites 10, 11, 12, 13)	< 0.05
Residential (sites 8,9) - Open Land (sites 10, 11, 12, 13)	< 0.05

4.4 Objective 4: Land cover change

The landcover maps for gradient A for 2001, 2010, and 2021 show that the city of Johannesburg has grown rapidly over the 20-year sampling period (Figure 36). From 2001 to 2021, the urban green space area along gradient A decreased from 263.84 km^2 to 57.69 km^2, while the areas of built-up land increased from 338.44 km^2 to 486.33 km^2 (Table 17). Therefore, there was a total net loss of ~ 206.15 km^2 in green spaces from 2001 to 2021.

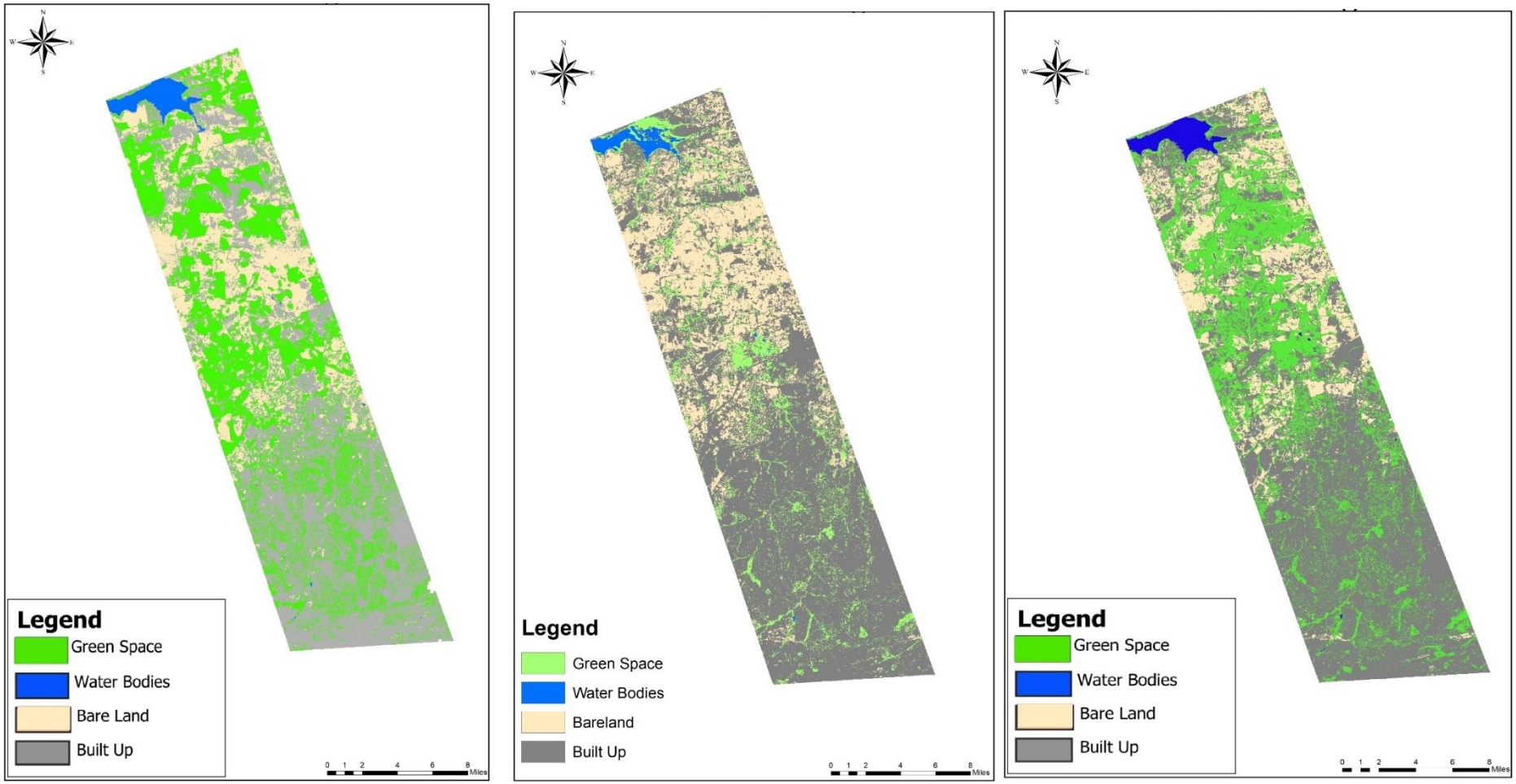

Figure 37: Land cover maps of the northern gradient (gradient A), for the years a) 2001, b) 2011, and c) 2021

Table 17: Changes in land cover area along gradient A

	2001		2011		2021	
Land cover class	**Area (km^2)**	**%**	**Area (km^2)**	**%**	**Area (km^2)**	**%**
Built up	338.44	44.07	410.82	53.95	486.33	65.34
Greenspace	263.84	34.36	206.80	27.16	57.69	7.75
Water	22.50	2.93	15.23	2.00	12.26	1.65
Other	143.13	18.64	128.69	16.90	188.00	25.26

Figure 38 below is a combination of LC maps along gradient B from 2001, 2010, and 2021. These maps show the change in Johannesburg's land cover as a result of urbanisation over the last 20 years. Along gradient B, from 2001 to 2021, the urban green space area within the selected gradient decreased from 261.39 km^2 to 42.4 km^2, while the areas of built-up land increased from 211.88 km^2 to 433.60 km^2 (Table 18). Therefore, there was a total net loss of ~ 219.25 km^2 in the area of green spaces from 2001 to 2021.

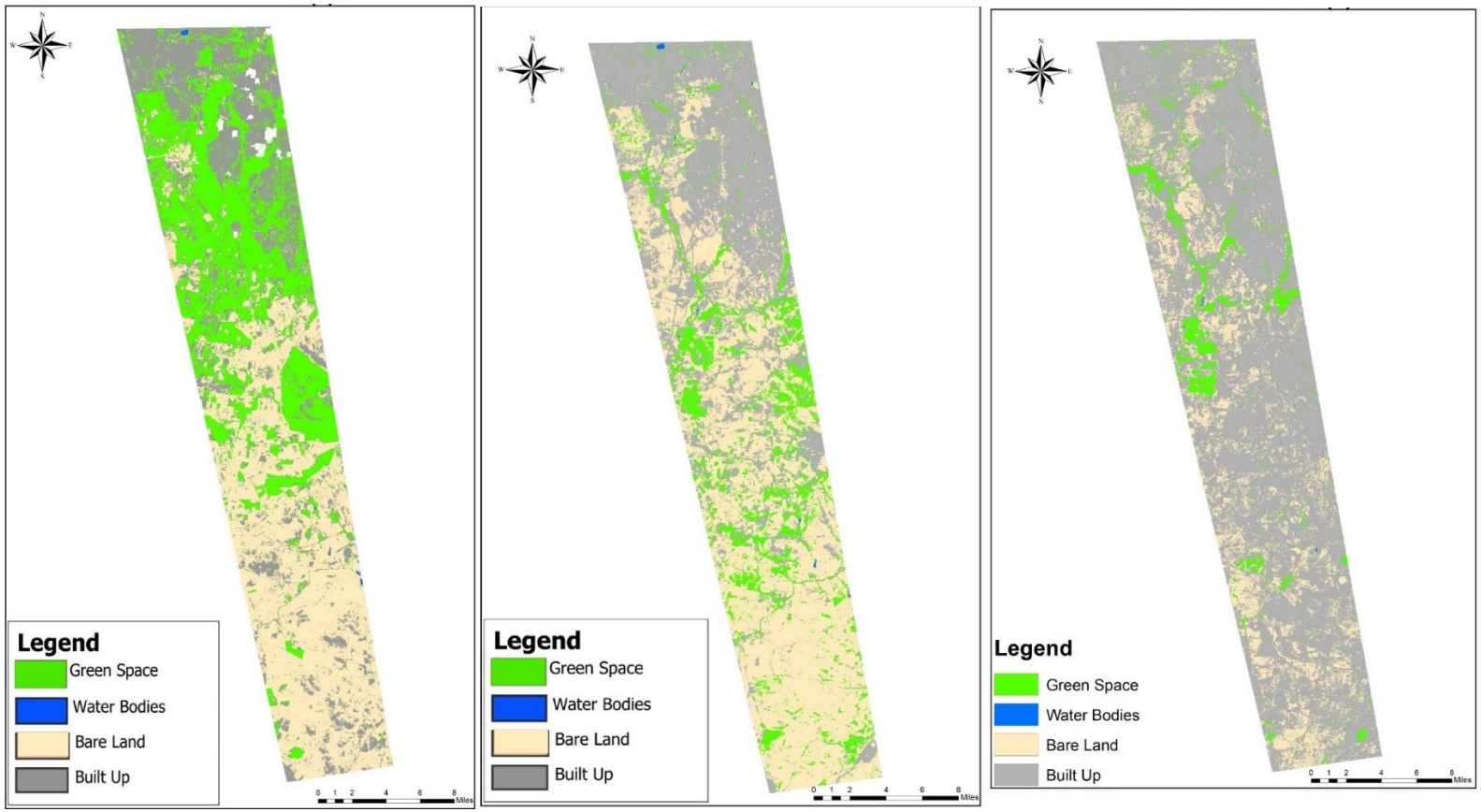

Figure 38: Land cover maps of the southern gradient (gradient B), for the years a) 2001, b) 2011, and c) 2021

Table 18: Area changes in the Land Cover in gradient B

	2001		2011		2021	
Land cover class	**Area (km^2)**	**%**	**Area (km^2)**	**%**	**Area (km^2)**	**%**
Built up	211.88	25.15	310.09	36.86	433.60	67.94
Greenspace	261.39	31.03	100.51	11.95	42.14	6.60
Water	25.51	3.03	18.92	2.25	15.17	2.38
Other	343.54	40.79	411.70	48.94	147.35	23.09

CHAPTER 5: DISCUSSION

The phenomenon of urban heating can be attributed to the increased proportion of impermeable surfaces characterised by low specific heat capacity. This, in turn, results in a reduction in vegetation and permeable surfaces, ultimately resulting in local warming (Zhang *et al*., 2015). Urban areas are facing a significant rise in the likelihood of floods since there has been a reduction in surfaces that allow water to pass through. This has led to a higher amount of water running off the surface and flowing into rivers, hence raising the risk of flooding (Feng *et al*., 2021). The reduction of carbon storage in metropolitan areas due to land conversion is a major concern. According to Kukkonen *et al*. (2022), the amount of urban land in Africa is expected to grow by about six times from 2000 to 2030. This expansion will result in a significant decrease in the amount of carbon stored in the land in African cities.

This study aimed to assess the supply of three ecosystem services, specifically temperature regulation, carbon sequestration, and flood regulation, over two separate urban-rural gradients (A and B) around the city of Johannesburg. Specifically, I set out to assess the land surface temperature, carbon storage, and soil compaction in 12 and 13 sites for gradients A and B respectively. Gradient A runs from the Johannesburg Central Business District (CBD) in a northerly direction towards the Hartbeespoort Dam. Gradient B starts at the Johannesburg CBD and extends in a southward direction towards the Vaal Dam. Furthermore, an evaluation was carried out to analyse the changes in land cover across the urban-rural continuum during a span of 20 years, with a specific focus on the modification of four main land cover classifications (green spaces, water, built-up and bare land).

5.1 Temperature regulation

In this study, I used Landsat 5 TM, 7 ETM+ and 8 OLI datasets to assess the land surface temperature (LST) along the two urban-rural gradients, A and B. The results show that the LST differed significantly from site to site along both gradients. Also, the LST declined with increasing distance from the city, with the more vegetated gradient end having cooler temperatures. This is also reflected in the study by Jia and Zhao (2020), where they found that LST increased with increasing city density along urban-rural gradients in Zhejiang and Anhui provinces, China. Mudede *et al*. (2020), with the use of Landsat 8 satellite data, found that in Soweto, South Africa, areas with a vast tree cover had lower land surface temperatures than highly built-up areas with little to no vegetation. This may be due to the fact that the presence of tree cover and other vegetation types facilitates cooling, hence contributing to the regulation of temperature (Meili *et al*., 2021).

The LST showed changes along gradient A, with a noticeable decrease recorded from the urban to the rural end of the gradient. The examination of Gradient B revealed that it was comparatively cooler than Gradient A. The temperature exhibited a consistent and gradual decline over the gradient, with the urban end being warmer than the rural end. Both gradients had the same pattern: the CBD site consistently recorded the greatest temperature, while the land surface temperature gradually fell from the city centre to the rural end. Furthermore, the correlation between the fractional vegetation cover and the land surface temperature was evaluated in both gradients and consistent patterns were identified. It was found that as the vegetation cover increased, the land surface temperature fell. This could explain why the city centre exhibited the greatest land surface temperature compared to all other locations and land use categories.

Temperature variation in cities is dependent on the land cover and land use types (Ayanlade *et al*., 2021). Gradient A is characterised by multiple urban parks, a substantial residential area that includes an abundance of trees, also known as the urban forest. Towards the rural end, the gradient is dominated by the presence of nature reserves. As a result, the pattern of decrease in gradient A's LST is not steady but fluctuates along the gradient. The CBD, which is the starting point of gradient A, exhibited the highest LST. The impervious surface of the city landscape results in an urban heat island due to the lack of vegetation. Oke *et al*. (2017) showed that urban areas have an average daily air temperature of 1°– 3°C higher than adjacent rural areas, while night-time temperatures can be more than 12°C higher, with much greater disparities in surface temperatures. Gradient A has multiple pockets of urban green spaces, mostly in the form of urban parks. In these sites, the temperature was much lower due to the greenery.

Gradient A is also dominated by residential areas which are slightly warmer than the urban park. The temperature difference may be due to the matrix of impermeable surfaces, mini green spaces and buildings found in the residential areas. As shown in the aerial photographs, there are houses, roads covered in asphalt, large parking areas, convenience stores, fuelling stations and schools. Many of these structures have impervious surfaces that capture and trap heat (Santamouris *et al*., 2019). However, as much as the residential areas are built up, along gradient A they have an extensive tree layer, most houses have large gardens and many trees, and there are also street trees. The presence of this vegetation helps with temperature regulation in these areas.

Trees regulate the temperature in two ways, firstly, trees regulate temperature by shading, and the shade from the tree leaves and branches blocks the energy from the sun from hitting the ground materials such as asphalt that can absorb heat. Thus, from shading there is reduced absorption of the incoming solar radiation by surfaces, which ultimately reduces the surface and air temperature. Secondly, trees regulate the environment through a physiological process of evapotranspiration.

Water is absorbed by the root system, then transported up the tree through the xylem system and then evaporates through leaf stomata. The thermal energy required to evaporate water released by trees, known as latent heat, offsets the thermal energy, known as sensible heat, that would otherwise increase air temperature. Instead, it lowers the temperature of the leaves and the surrounding area (Winbourn *et al*., 2020).

Schwaab *et al*. (2021) also report that the shading from street trees strongly reduces daytime land surface and air temperatures. The extent of temperature reduction depends on the tree's morphological characteristics but has been demonstrated to increase as the leaf area index increases. The sites at the end of gradient A are located on Open Land, along a Highway and a Nature Reserve. In these land cover types, the temperature was the lowest, because the surface is covered by vegetation, and there are minimal built-up structures that can absorb heat.

Gradient B's landscape is characterised by a substantial presence of agricultural lands and open vegetation, the open vegetation, consisting mostly of wetlands, grassland, and agricultural land enhances the cooling effect the cooling effect from evapotranspiration as mentioned above (Nimish *et al*., 2020; Gohain *et al*., 2021). However, the cooling potential of vegetation depends on the vegetation type as well as the climatic context. While natural vegetation has a cooling effect on the surrounding environment, urban green areas without trees are less successful at reducing land surface temperature. The cooling effect of these treeless areas is typically 2-4 times weaker compared to the cooling effect created by urban trees (Schwaab *et al*., 2021). Since there are fewer impervious surfaces and continuous built-up structures, there is less heat loss from traffic and buildings and reduced absorption of heat energy by the concrete and asphalt surfaces (Vujovic et al., 2021).

Lastly, land surface temperature was assessed for three time periods: 2001, 2011 and 2021. For both gradients, the year 2021 was found to be the hottest year, indicating that temperature has increased over the years. Over time, urban areas have been growing, resulting in changes in how land is used and covered, specifically with a significant growth in built-up areas. The Seoul metropolitan area in Korea serves as a distinctive illustration of how urbanisation affects local climate patterns. Observational data spanning 56 years, from 1962 to 2017, indicate a rise in air temperature of around 1.7 °C. Furthermore, it has been determined that urbanisation accounts for 43% of the noted city warming patterns (Hong *et al*., 2019). According to Kafy *et al*. (2020), if the current urbanisation patterns persist, it is anticipated that 70% of the region in Rajshahi, Bangladesh, will have temperatures above 38°C by 2029. Ayanlade *et al*. (2021) recorded alterations in land cover inside Nigerian towns, observing a rise in urbanised and agricultural zones while witnessing a decrease in areas predominantly characterised by vegetation, over the past few years, there has been a substantial rise in land surface temperature due to this alteration. Since trees and other types of vegetation reduce

the effects of heat on urban environments (Mudede *et al*., 2020; Schwaab *et al.,* 2021), the addition of green spaces in cities and towns can help in the mitigation of urban heat (Jia and Zhao, 2020).

5.2 Carbon sequestration

The function of carbon storage within urban ecosystems is crucial. However, modifications to natural habitats in cities caused by urban expansion pose a direct hazard to carbon storage. My objective was to evaluate the capacity of urban trees to store carbon along the urban-rural gradients. The findings revealed notable variations in carbon storage capacity between sites along the urban-to-rural gradients. Specifically, the sites situated in closer proximity to the rural terminus of the two gradients accumulated a greater quantity of carbon than those situated towards the urban end of the gradient.

Along gradient A the Residential area was found to store the highest amount of carbon ($\bar{x}$ = 28.961 tons/ha), followed by the Nature Reserve ($\bar{x}$ = 26.358 tons/ha). Along gradient B, Open Land was found to store the highest amount of carbon ($\bar{x}$ = 145.894 tons/ha) followed by the Residential area ($\bar{x}$ = 62.936 tons/ha). In my analysis, the average stored carbon along gradient A increased by 235% from 2001 to 2021, while along gradient B, there was a 110% increase during the same period. The estimated stored carbon increased over the 20 years, with a greater increase observed in gradient A. As mentioned in the above sections, a significant portion of gradient A is composed of various residential areas. The notable increase in carbon storage along gradient A could then be attributed to the presence of the extensive urban forest that covers the residential area along this gradient. Gradient B's landscape is predominantly covered by open vegetation including vast croplands, wetlands, and open grassland. All the assessed sites along the gradient had large mature trees, except for site 1, the CBD and the urban park, and site 4 which is the aspect that was assessed in this study.

Estimations of the carbon storage capacity can be derived from the quantitative analysis of several factors, including the total number of trees, their dimensions, and the overall land area they occupy. Existing literature indicates that urban green spaces have the potential to increase carbon storage. Research constantly shows that big trees, in particular, are essential for carbon sequestration (Köhl *et al*., 2017). Mildrexler *et al*. (2020) discovered a correlation between significant carbon reserves and the presence of trees with substantial diameters. Pregitzer *et al*. (2021) emphasised that carbon storage is enhanced in native forests with a majority of large and mature trees. Urban trees have the capacity to significantly contribute to the long-term process of carbon sequestration. It is crucial to maintain the long-term survival of urban trees since their ability to store carbon increases as they age (Mildrexler *et al*., 2020). Ariluoma *et al*. (2021), in their study on residential yards in Helsinki, discovered that the presence of trees had a notable impact on the storage of carbon. The implementation of green infrastructure design thus has the potential to enhance the provision and regulation of ecosystem services such as carbon sequestration. Kukonen *et al*. (2022), suggest that

incorporating an urban greenery strategy into development plans is crucial for mitigating and compensating emissions resulting from urban expansion, as well as conserving ecosystem services. Urban green infrastructure encompasses all the interconnected natural, semi-natural, and artificial ecological systems within urban and peri-urban regions. This includes features such as forests, nature reserves, city parks, community gardens, private yards, and street trees (Lähde and Di Marino, 2019).

The literature highlights several factors contributing to the discrepancy in carbon storage between urban and rural areas, including urban expansion, land cover distribution, and management practices (Liu *et al*., 2019). Urbanisation and associated land use changes have been identified as primary drivers of carbon storage depletion (Liu *et al*., 2019). Recent research by Mudede *et al*. (2020) demonstrates how urban growth leads to the conversion of green areas into residential, industrial, and transportation zones, resulting in vegetation loss and reduced carbon sequestration capacity. Studies in various locations, such as Zanzibar City and Xazhou City, China, further underscore the adverse impacts of urban expansion on carbon storage. For instance, research by Kukonen *et al*. (2022) identifies urban expansion as a significant source of greenhouse gas emissions in Zanzibar City, while Li *et al*. (2018) estimated a substantial loss of carbon storage potential in Xuzhou City due to urban expansion from 2000 to 2015. Consequently, ongoing land conversion processes are leading to the degradation or destruction of ecosystems crucial for carbon sequestration.

According to the United Nations, Department of Economic and Social Affairs, Population Division (UNDESA, 2019), the African population is projected to grow from 1.3 to 2.5 billion between 2018 and 2050, all while the rate of urbanisation may go up 43% to 59%. As a result, land covered by cities is projected to increase by over six times from 2000 to 2030. This is anticipated to lead to a significant decrease in the amount of carbon stored in the ground in and surrounding African cities. Moreover, growth in cities in Africa has predominantly been characterised by extensive expansion, lacking in both densification and vertical development in comparison to other continents. Additionally, it is linked to the reduction, deterioration, and division of vegetated areas, resulting in settlements with minimal public vegetation (UNDESA, 2019). Since it is mostly the greenery that stores carbon, this loss of green spaces to urban fabric has a massive impact on carbon storage (Kinnunen *et al*., 2022). According to Estoque and Murayama (2017), there is evidence suggesting that a country experiences a rise of over 11% in its overall carbon dioxide (CO_2) emissions when there is a 10% expansion in its urban land cover. Thus, urban development results in an overall decrease in carbon stocks, it is for this reason the urban end of the gradient was found to lower stored carbon than the rural end, for both gradients.

Research constantly shows that big trees, in particular, are essential for carbon sequestration (Köhl *et al*., 2017). Mildrexler *et al.* (2020) discovered a correlation between significant carbon reserves and

the presence of trees with substantial diameters. Pregitzer *et al*. (2021) emphasised that carbon storage is enhanced in native forests with a majority of large and mature trees. Urban trees have the capacity to significantly contribute to the long-term process of carbon sequestration. It is crucial to maintain the long-term survival of urban trees since their ability to store carbon increases as they age (Mildrexler *et al*., 2020).

While gradient B had less tree cover, its extensive agricultural areas and open grassland would be just as effective at storing carbon. Permanent grasslands store more carbon in the soil due to increased belowground carbon allocation, root turnover, and rhizodeposition (Lorenz *et al*., 2018; Bengtsson *et al*., 2019). As per Jansson *et al*. (2021), agricultural systems have the capacity to store a substantial amount of carbon in the soil, up to one gigaton annually. This amount could compensate for approximately 10% of the eight to ten gigatons of annual greenhouse gas emissions. Crops do this by allocating a significant portion (20–30%) of newly produced sugars to their roots and other belowground parts. Roughly half of the carbon transferred is directed towards root development. A significant portion of this carbon, approximately 30%, is subsequently emitted into the rhizosphere through diverse mechanisms such as root exudation, shedding of root cap cells, interactions with mycorrhizae, or respiratory processes. Plants with extensive and deeper root structures contribute a greater amount of carbon to subterranean environments (Fan *et al*., 2019). Wetlands, located along gradient B, are a type of vegetation noted for having a greater capacity for carbon sequestration compared to all other land-based ecosystems on Earth. This is due to their above-ground productivity, involving the photosynthetic conversion of CO2 into cellulose and other carbon compounds, as well as their below-ground productivity, which involves the transformation of detritus into soil organic matter (Lolu *et al*., 2020). In a recent study conducted by Du *et al*. (2022), it was determined that there was no significant variation in the total storage of soil organic carbon among different types of urban green areas in Guangzhou. Nevertheless, it is observed that there is a positive correlation between the age and size of green spaces and the rise in soil organic carbon content. This suggests that older and larger green spaces have a greater capacity for carbon storage. Consequently, the preservation and upkeep of green spaces hold promise in enhancing carbon sequestration.

Various allometric equations can be used to calculate carbon storage, thus carbon data in this study was validated following the methods by Schaffler and Swilling (2013) as per Els (2018) in the same sites. The carbon data in this study was validated in the same sites using the methods outlined by Schaffler and Swilling (2013) as described by Els (2018). The fluctuations in the stored carbon levels at every site echoed those observed in this study.

5.3 Flood regulation

To better understand the potential for flood regulation along the two sampled gradients, the soil's unconfined comprehensive strength (kg/cm^2), also known as soil compaction was determined at several sites (12 along gradient A and 13 along gradient B). A quantitative estimation of soil compaction was thereby obtained. Soil compaction is the result of external forces compressing soil particles, thereby reducing the interparticle void space. (Correa *et al*., 2019), thereby increasing the soil's resistance to penetration by plant roots. It also causes the micropores to be compacted, reducing water infiltration and permeability (Seraphim *et al*., 2019). As permeability and infiltration are reduced, surface runoff increases, resulting in flooding in urban areas (Abass *et al*., 2020).

In the present study, the soil comprehension strength along both gradients was found to differ significantly from site to site. Sites proximal to the rural extreme of the gradient had a lower mean comprehensive strength (A: $\bar{x}$ = 1.98 kg/cm^2, B: $\bar{x}$ = 2,24 kg/cm^2) compared to the sites towards the urban extreme of the gradient (A: $\bar{x}$ = 3.14 kg/cm^2, B: $\bar{x}$ = 3,69 Kg/cm^2), suggesting that more vegetated sites are less compacted and thus can absorb water for flood mitigation. Flooding can result from urbanisation dynamics in addition to climate change. Even in the absence of climate change, urbanisation alone has the potential to elevate the occurrence of floods in the city (Ahiablame and Shakya, 2016; Ramiaramanana and Teller 2021). Vegetative land cover including urban green spaces can help in reducing surface runoff (Pappalardo *et al*., 2017).

Along Gradient A, soil compaction levels were lowest at the Nature Reserve, followed by the Highway area, and were highest in the Residential area. Gradient B had the lowest soil compaction in Open Land, with residential areas having slightly higher levels. The CBD had the highest level of soil compaction. The results indicate that soil supporting natural vegetation on its own was less compact, but areas that have had human interference such as the CBD as well as residential areas have more compact soils. Numerous academics have researched the influence of land alteration on soil permeability and discovered that soil permeability reduced as forest areas and grassland were converted into cultivated land (Qiu *et al*., 2022). Soil compaction resulting from automated tillage is associated with structural degradation, diminished soil permeability and porosity, compromised soil water retention, and heightened surface discharge (Bogunovic *et al*., 2020). Similarly, Teklay *et al*. (2018) found that the conversion of forest area to agriculture in Ethiopia led to soil compaction, resulting in a 1.1 mm increase in annual surface runoff and peak flow. In their study, Ma *et al*. (2024) also discovered that urbanisation-induced changes in land use and land cover, along with variations in soil properties, led to an increased risk of flooding.

Seraphim *et al*. (2019), found that a reduction in tree cover affects the infiltration rates of the soil; plant roots, insects, and microbes dig, penetrate, and join soil particles in a way that improves the

porosity of the soil. This may explain the results in my study, whereby the areas with tree cover or highly vegetated areas such as the Open Land and Nature Reserve had the lowest soil compaction. Since trees have extensive roots, they are consequently more capable of altering the surrounding soil structure (Vereecken *et al*., 2022).

Soils possess a significant capacity for water retention, enabling them to provide a water supply to plants for their growth while concurrently mitigating the potential for flooding. Nevertheless, the processes of soil compaction and sealing have the adverse effect of reducing or completely eradicating the soil's capacity to retain and regulate water equilibrium. In urban environments, the phenomenon of soil compaction has been observed to have a detrimental impact on several aspects of soil water storage. Specifically, a gradual decline has been observed in the total water-holding capacity, readily accessible water storage capacity, and interim storage of water, meanwhile the insufficient water storage capacity has been observed to gradually increase. The process of soil compaction has the potential to reduce the soil's ability to regulate floods in urban settings (Yang *et al*., 2015).

5.4 Landcover change.

The inclusion of vegetation in cities is a significant aspect of urban planning, this is the impact vegetation has on the societal well-being and the quality of human and animal life at large, the inclusion also serves as a climate mitigation and resilience strategy (Abutaleb *et al*., 2021). Urban green spaces encompass many forms of vegetation within urban areas, such as lawns, grassland, forests, and urban trees (Wang *et al*., 2019). The phenomenon of urban growth has been well-recognised as a significant factor contributing to the deterioration of green spaces within urban centres and their surrounding areas (Abutaleb *et al*., 2021).

This study aimed to provide an analysis of the transformation of green areas in the study region, taking into account the process of urbanisation that has occurred over the years. A landcover analysis focused on four distinct categories, namely green spaces (vegetation), built-up areas, water bodies, and bare ground for the years 2001, 2010 and 2021. The results show that the city of Johannesburg has grown rapidly over the 20-year sampling period. From 2001 to 2021 the urban green spaces area along gradients A and B decreased by about 206.15 km^2 (78.135%) and 219.25 km^2 (83.779%) respectively. Thus, both gradients experienced a substantial loss of green spaces over the 20 years, as the area covered by built-up surfaces increased.

This study substantiates others confirming that urban vegetation has been facing depletion over the years. According to research conducted in Alexandra, one of Johannesburg's townships, findings indicate a significant increase in informal settlement and a corresponding decline in areas

characterised by intact vegetation over 28 years (Mawasha and Britz, 2021). Ruhiiga (2017) posits that there was a significant increase in the expansion of built-up areas in Johannesburg between the years 1990 and 2014, with indications that this trend will persist in the foreseeable future. Similar findings were documented in Nigeria by Ayanlade *et al*. (2021) and Ghana (Abass *et al*., 2018), where built-up and cultivated areas grew significantly over the past 40 years, with a corresponding decline in vegetation cover. In the Gauteng City region, it was found that between 1986 and 2019, there was a 62.5% growth in the built environment, leading to a significant decrease in natural landscapes (Nhamo *et al*., 2021).

The phenomenon of fast urbanisation and its associated changes can be linked to various driving forces, including old and contemporary expansions in the mining industry, government urban policies, rural-urban migration, and changes in the urban land market (Ruhiiga, 2017). The study also highlights the encroachment of urban development on the agricultural lands surrounding the city. Specifically, in the northern region of Johannesburg, the once-existing expansive commercial farms between Johannesburg and Pretoria have been reduced significantly. In their place, a variety of land uses, including residential gated communities, warehouses, factories, and office parks, now coexist (Ruhiiga, 2017). This statement aligns with our study, which indicates that the extent of commercial farming in the northern gradient is no longer as substantial as that observed in the southern gradient.

According to the data provided by Statistics South Africa (2017), Gauteng emerges as the most highly urbanised province in the country. This distinction may be attributed to the presence of two prominent economic centres, namely Johannesburg and Pretoria. Johannesburg, being the economic centre of South Africa, has had significant urban expansion and outward development throughout the years (Gauteng Provincial Government, 2016), leading to the construction of various grey infrastructures such as residential buildings, industrial facilities, healthcare institutions, and transportation networks. These developments are undertaken to accommodate the needs arising from the growing urban population (Busko and Szafranska, 2018).

Estoque and Murayama (2017) reflect that unforeseen and expeditious transformations in urban land use particularly the conversion of undeveloped regions to developed areas, often result in the exhaustion of verdant spaces in the city. Urban green space reduction can lead to the depletion of vital ecosystem services and the deterioration of the urban biosphere, both of which are essential for preserving the ecological integrity and comfort of towns and cities.

Gradient A is defined by an urbanized land cover, large residential areas with multiple pockets of urban green spaces. The ecosystem services such as temperature regulation, carbon sequestration, and flood regulation are not evenly distributed along the gradient due to different land use types that either

support or lack green urban spaces. Gradient B exhibits a greater variety of vegetation cover with less urban development, resulting in more intact vegetation that enhances temperature regulation. The presence of vegetation cover and reduced urban activity create less compact soil, enhancing its ability to regulate floods. Gradient B was determined to be more effective in delivering the evaluated ecosystem service, based on the lower urban development.

CHAPTER 6: CONCLUSION AND RECOMMENDATIONS

Ecosystem services (ESs) have experienced a surge in demand, especially in heavily settled cities, as a result of the disturbance of landscape patterns caused by increased human activity. Ecosystem functionality, structure, and the capacity to provide products and services to society are all influenced by land cover change, subsequent land use, and urbanisation, according to the findings of this study. This study assessed the supply of three ecosystem services along two urban-rural gradients, the findings indicated that, the urban extremities of the urban-rural gradients exhibited higher land surface temperatures than the rural extremes, this was due to the limited to no vegetation cover in these areas. Secondly, there was more carbon storage in the rural end than the urban end of the gradients. This was due to the presence of trees in these landscapes, many of which were large mature trees. Thirdly, the sites located in the urban extreme of the gradient were found to have higher soil comprehensive strength compared to those in the rural extremes, this was again due to the absence of vegetation cover in the urban landscape which would have allowed the soil to be permeable, and control flooding. Lastly, the landcover analysis revealed that the city had experienced a substantial loss of green spaces over the last 20 years as the built-up area increased. These results then, demonstrates the limited capacity of urbanised regions to provide ecosystem services. Conversely, more rural regions retain their ecosystems and hold the capacity to supply ecosystem services to their fullest extent. Consequently, the conservation of ecosystem services is dependent on the preservation of natural areas. The research findings have shown how the green infrastructure enhances the sustainability of cities by supporting the supply of various ecosystem services including flood and climate regulation, carbon sequestration and storage. Therefore, it is recommended that urban areas must consider the valuation of natural systems, open spaces and the ecosystem services that they generate by giving them due cognisance in land-use planning and allocate appropriate resources for their protection, rehabilitation and management. The natural systems in urban areas must be integrated with the urban planning and infrastructure initiatives. Implementing a Green Infrastructure approach can effectively reduce the adverse impacts of urban expansion, including urban heat island effects, noise pollution, air pollution, and the heightened risk of flooding caused by increased runoff. Moreover, it can impact on climate change management by sequestering greenhouse gases and strengthening resistance against climate-related hazards.

It would be of great benefit if urban areas would consider augmenting their green spaces and enhance the overall vegetation coverage by implementing the following strategies: Incorporating green infrastructure into new developments. Modify existing spaces by converting underutilised areas into green parks and installing permeable pavements in parking lots. Initiate habitat restoration, which

involves improving the condition of damaged natural habitats, such as wetlands, rivers, and forests, to promote biodiversity and ecological well-being. Increase the number of street trees to effectively reduce carbon dioxide, dust, and particulate matter in the air, while also improving the regulation of temperature. Enhance flood mitigation measures and promote the implementation of sustainable drainage systems. Lastly, it would be ideal if further research would replicate the analysis done in this study in many more urban-rural gradients whose landscapes include townships and the informal settlements in South Africa to deepen the understanding of ecosystem service provision in these spaces. These findings are essential for informing future decision-making on investments in green infrastructure. These practical recommendations on integrating environmentally friendly assets into municipal accounting systems reinforces the case for investing in and preserving green infrastructure not only in Gauteng cities, but in all the cities around the world.

REFERENCE LIST

Abass, K., Buor, D., Afriyie, K., Dumedah, G., Segbefi, A.Y., Guodaar, L., Garsonu, E.K., Adu-Gyamfi, S., Forkuor, D., Ofosu, A. and Mohammed, A., 2020. Urban sprawl and green space depletion: Implications for flood incidence in Kumasi, Ghana. *International Journal of Disaster Risk Reduction*, 51, p.101915.

Abass, K., Afriyie, K. and Gyasi, R.M., 2018. From green to grey: the dynamics of land use/land cover change in urban Ghana. *Landscape Research*.

Abutaleb, K., Mudede, M.F., Nkongolo, N. and Newete, S.W., 2021. Estimating urban greenness index using remote sensing data: A case study of an affluent vs poor suburbs in the city of Johannesburg. T*he Egyptian Journal of Remote Sensing and Space Science*, 24(3), pp.343-351.

Ahiablame, L. and Shakya, R., 2016. Modeling flood reduction effects of low impact development at a watershed scale. *Journal of environmental management*, 171, pp.81-91.

Alexander, C., 2021. Influence of the proportion, height and proximity of vegetation and buildings on urban land surface temperature. *International Journal of Applied Earth Observation and Geoinformation*, *95*, p.102265.

Anderson, V. and Gough, W.A., 2020. Evaluating the potential of nature-based solutions to reduce ozone, nitrogen dioxide, and carbon dioxide through a multi-type green infrastructure study in Ontario, Canada. *City and Environment Interactions*, *6*, p.100043.

Anderson, V. and Gough, W.A., 2020. Evaluating the potential of nature-based solutions to reduce ozone, nitrogen dioxide, and carbon dioxide through a multi-type green infrastructure study in Ontario, Canada. *City and Environment Interactions*, *6*, p.100043.

Anim, D.O., Fletcher, T.D., Vietz, G.J., Pasternack, G.B. and Burns, M.J., 2018. Effect of urbanisation on stream hydraulics. *River Research and Applications*, 34(7), pp.661-674.

Arehart, J.H., Hart, J., Pomponi, F. and D'Amico, B., 2021. Carbon sequestration and storage in the built environment. S*ustainable Production and Consumption*, 27, pp.1047-1063.

Ariluoma, M., Ottelin, J., Hautamäki, R., Tuhkanen, E.M. and Mänttäri, M., 2021. Carbon sequestration and storage potential of urban green in residential yards: A case study from Helsinki. *Urban Forestry & Urban Greening*, 57, p.126939.

Ayala-Azcárraga, C., Diaz, D. and Zambrano, L., 2019. Characteristics of urban parks and their relation to user well-being. *Landscape and urban planning*, *189*, pp.27-35B

Ayanlade, A., Aigbiremolen, M.I. and Oladosu, O.R., 2021. Variations in urban land surface temperature intensity over four cities in different ecological zones. *Scientific Reports*, 11(1), p.20537.

Baffi, S., Turok, I. and Vacchiani-Marcuzzo, C., 2018. The south African urban system. *International and transnational perspectives on urban systems*, pp.285-314.Balwan, W.K. and Kour, S., 2021. Wetland-an ecological boon for the environment. *East African Scholars Journal of Agriculture and Life Sciences*, 4(3), pp.38-48.

Baró, F., Gómez-Baggethun, E. and Haase, D., 2017. Ecosystem service bundles along the urban-rural gradient: Insights for landscape planning and management. *Ecosystem Services*, 24, pp.147-159.

Beall, J., Crankshaw, O. and Parnell, S., 2014. Uniting a divided city: Governance and social exclusion in Johannesburg. *Routledge*.

Bera, D., Kumar, P., Siddiqui, A. and Majumdar, A., 2022. Assessing impact of urbanisation on surface runoff using vegetation-impervious surface-soil (VIS) fraction and NRCS curve number (CN) model. *Modeling Earth Systems and Environment*, pp.1-14.

Bengtsson, J., Bullock, J.M., Egoh, B., Everson, C., Everson, T., O'connor, T., O'farrell, P., Smith, H.G. and Lindborg, R., 2019. Grasslands—more important for ecosystem services than you might think. *Ecosphere*, *10*(2), p.e02582.

Belay, T., Melese, T. and Senamaw, A., 2022. Impacts of land use and land cover change on ecosystem service values in the Afroalpine area of Guna Mountain, Northwest Ethiopia. *Heliyon*, 8(12).

Bobbins, K., Dunsmore, S., Fitchett, A., Monama, L., Naidu, R., Sykes, G., van den Bussche, J. and Vieira, M., 2019. Towards applying a green infrastructure approach in the Gauteng City-Region (Vol. 11). *Gauteng City-Region Observatory (GCRO)*.

Borsekova, K., Nijkamp, P. and Guevara, P., 2018. Urban resilience patterns after an external shock: an exploratory study. *International journal of disaster risk reduction*, *31*, pp.381-392.

Büyüközkan, G., Ilıcak, Ö. and Feyzioğlu, O., 2022. A review of urban resilience literature. *Sustainable Cities and Society*, *77*, p.103579.

Bustamante, M.M., Silva, J.S., Scariot, A., Sampaio, A.B., Mascia, D.L., Garcia, E., Sano, E., Fernandes, G.W., Durigan, G., Roitman, I. and Figueiredo, I., 2019. Ecological restoration as a strategy for mitigating and adapting to climate change: lessons and challenges from Brazil. *Mitigation and Adaptation Strategies for Global Change*, *24*, pp.1249-1270.

Cao, Y., Kong, L., Zhang, L. and Ouyang, Z., 2021. The balance between economic development and ecosystem service value in the process of land Urbanisation: A case study of China's land Urbanisation from 2000 to 2015. *Land Use Policy*, *108*, p.105536.

Chen, W., Hu, C., Liu, L., Zhang, J., Wang, K. and Liu, S., 2022. Characteristics of built-up land change in resource-based cities and their impact on land surface temperature—Taking Wu'an as an example. *Ecological Informatics*, 68, p.101582.

Cheng, X., Van Damme, S., Li, L. and Uyttenhove, P., 2019. Evaluation of cultural ecosystem services: A review of methods. *Ecosystem services*, *37*, p.100925.

City of Tshwane.2015. Region 7 [Online] Available at: ttps://www.tshwane.gov.za/sites/regions/Pages/Region-7.aspx [Accessed 02 December 2021].

Clinton, P. and Owens, J., 2023. Structure and function of forested soils. Encyclopedia of Soils in the Environment (Second Edition), *Academic Press*.pp.56-57.ISBN 9780323951333. https://doi.org/10.1016/B978-0-12-822974-3.00172-5.

Costanza, R., De Groot, R., Braat, L., Kubiszewski, I., Fioramonti, L., Sutton, P., Farber, S. and Grasso, M., 2017. Twenty years of ecosystem services: how far have we come and how far do we still need to go?. *Ecosystem services*, 28, pp.1-16.

Correa, J., Postma, J.A., Watt, M. and Wojciechowski, T., 2019. Soil compaction and the architectural plasticity of root systems. *Journal of experimental botany*, 70(21), pp.6019-6034.

Cullis, J.D.S., Horn, A., Rossouw, N., Fisher-Jeffes, L., Kunneke, M.M., Hoffman, W., 2019. Urbanisation, climate change and its impact on water quality and economic risks in a water scarce and rapidly urbanising catchment: case study of the Berg River Catchment. *H2Open Journal*. 2, 146–167. https://doi.org/10.2166/h2oj.2019.027

Crookes, D.J., Blignaut, J.N., De Wit, M.P., Esler, K.J., Le Maitre, D.C., Milton, S.J., Mitchell, S.A., Cloete, J., De Abreu, P., Fourie, H. and Gull, K., 2013. System dynamic modelling to assess economic

viability and risk trade-offs for ecological restoration in South Africa. *Journal of environmental management*, 120, pp.138-147.

Deng, C., Liu, J., Liu, Y., Li, Z., Nie, X., Hu, X., Wang, L., Zhang, Y., Zhang, G., Zhu, D. and Xiao, L., 2021. Spatiotemporal dislocation of urbanisation and ecological construction increased the ecosystem service supply and demand imbalance. *Journal of Environmental Management*, *288*, p.112478.

Du, J., Yu, M., Cong, Y., Lv, H. and Yuan, Z., 2022. Soil Organic Carbon Storage in Urban Green Space and Its Influencing Factors: A Case Study of the 0–20 cm Soil Layer in Guangzhou City. *Land*, 11(9), p.1484.

Elmqvist, T., Setälä, H., Handel, S.N., van der Ploeg, S., Aronson, J., Blignaut, J.N., Gómez-Baggethun, E., Nowak, D.J., Kronenberg, J. and de Groot, R., 2015. Benefits of restoring ecosystem services in urban areas. *Current opinion in environmental sustainability*, 14, pp.101-108.

Els, V., 2018. Urban Ecosystem Services in Johannesburg, South Africa. MSc thesis. University of the Witwatersrand, Johannesburg, South Africa.

Estoque, R.C. and Murayama, Y., 2017. Trends and spatial patterns of urbanisation in Asia and Africa: a comparative analysis. In Urban Development in Asia and Africa: Geospatial Analysis of Metropolises. Singapore: *Springer Singapore.* pp. 393-414

Fan, J., McConkey, B. G., Liang, B. C., Angers, D. A., Janzen, H. H., Kröbel, R., Cerkowniak, D. D., & Smith, W. N. (2019). Increasing crop yields and root input make Canadian farmland a large carbon sink. *Geoderma, 336*, 49-58.

Fang, C.L., Cui, X.G. and Liang, L.W., 2019. Theoretical analysis of Urbanisation and eco-environment coupling coil and coupler control. *Acta Geographica Sinica*, 74, pp.2529-2546.

Feng, B., Zhang, Y. and Bourke, R., 2021. Urbanisation impacts on flood risks based on urban growth data and coupled flood models. *Natural Hazards*, *106*, pp.613-627.

Fitchett, J.M. and Raik, K., 2021. Phenological advance of blossoming over the past century in one of the world's largest urban forests, Gauteng City-Region, South Africa. *Urban Forestry & Urban Greening*, 63, p.127238

Folke, C., Polasky, S., Rockström, J., Galaz, V., Westley, F., Lamont, M., Scheffer, M., Österblom, H., Carpenter, S.R., Chapin, F.S. and Seto, K.C., 2021. Our future in the Anthropocene biosphere.

Ambio, 50, pp.834-869.GeoTerraImage (2009). *Gauteng land-cover datase*t. Johannesburg: GeoTerraImage.

Gambe, T.R., Turok, I. and Visagie, J., 2023. The trajectories of urbanisation in Southern Africa: A comparative analysis. *Habitat International*, *132*, p.102747.

Gkatsopoulos, P., 2017. A methodology for calculating cooling from vegetation evapotranspiration for use in urban space microclimate simulations. *Procedia Environmental Sciences*, *38*, pp.477-484.

Gohain, K.J., Mohammad, P. and Goswami, A., 2021. Assessing the impact of land use land cover changes on land surface temperature over Pune city, India. *Quaternary International*, 575, pp.259-269.

Gómez-Baggethun, E. and Barton, D.N., 2013. Classifying and valuing ecosystem services for urban planning. *Ecological economics*, 86, pp.235-245

Gómez-Baggethun, E., Barton, D.N., 2013b. Classifying and valuing ecosystem services for urban planning. *Ecological economics*., Sustainable Urbanisation: A resilient future 86, 235–245. https://doi.org/10.1016/j.ecolecon.2012.08.019

Govindarajulu, D., 2014. Urban green space planning for climate adaptation in Indian cities. *Urban climate*, *10*, pp.35-41.

Güneralp, B., Reba, M., Hales, B.U., Wentz, E.A. and Seto, K.C., 2020. Trends in urban land expansion, density, and land transitions from 1970 to 2010: A global synthesis. E*nvironmental Research Letters*, 15(4), p.044015.

Gupta, A.K., Singh, S., Wajih, S.A., Mani, N. and Singh, A.K., 2017. Urban resilience and sustainability through peri-urban ecosystems: integrating climate change adaptation and disaster risk reduction. *Gorakhpur Environmental Action Group, Gorakhpur (UP) India*, 14, pp.5-28.

Herrero-Jáuregui, C., Arnaiz-Schmitz, C., Herrera, L., Smart, S.M., Montes, C., Pineda, F.D. and Schmitz, M.F., 2019. Aligning landscape structure with ecosystem services along an urban–rural gradient. Trade-offs and transitions towards cultural services. *Landscape Ecology*, *34*, pp.1525-1545.

Hill, M.P., Coetzee, J.A., Martin, G.D., Smith, R. and Strange, E.F., 2020. Invasive alien aquatic plants in South African freshwater ecosystems. In Biological Invasions in South Africa (pp. 97-114). *Cham: Springer International Publishing.*

Holland, R.A., Eigenbrod, F., Armsworth, P.R., Anderson, B.J., Thomas, C.D., Gaston, K.J., 2011. The influence of temporal variation on relationships between ecosystem services. *Biodiversity and Conservation*, *20*, pp.3285-3294.

Hong, J.W., Hong, J., Kwon, E.E. and Yoon, D., 2019. Temporal dynamics of urban heat island correlated with the socio-economic development over the past half-century in Seoul, Korea. *Environmental Pollution*, *254*, p.112934.

Huang, G., 2019. A revisit to impact of urbanisation on flooding. *Urban planning and water-related disaster management*, pp.43-56.

Jaligot, R., Chenal, J. and Bosch, M., 2019. Assessing spatial temporal patterns of ecosystem services in Switzerland. *Landscape ecology*, 34, pp.1379-1394.

Jia, W. and Zhao, S., 2020. Trends and drivers of land surface temperature along the urban-rural gradients in the largest urban agglomeration of China. *Science of the Total Environment*, *711*, p.134579.

Kafy, A.A., Rahman, M.S., Hasan, M.M. and Islam, M., 2020. Modelling future land use land cover changes and their impacts on land surface temperatures in Rajshahi, Bangladesh. *Remote Sensing Applications: Society and Environment*, 18, p.100314.

Kaminski, A., Bauer, D.M., Bell, K.P., Loftin, C.S. and Nelson, E.J., 2021. Using landscape metrics to characterize towns along an urban-rural gradient. *Landscape Ecology*, *36*(10), pp.2937-2956.

Katumba, S. and Everatt, D., 2021. Urban sprawl and land cover in post-apartheid johannesburg and the gauteng city-region, 1990–2018. *Environment and Urbanization ASIA*, 12(1_suppl), pp.S147-S164.

Khatri, N. and Tyagi, S., 2015. Influences of natural and anthropogenic factors on surface and groundwater quality in rural and urban areas. *Frontiers in life science*, 8(1), pp.23-39.

Klein, L.J., Zhou, W. and Albrecht, C.M., 2021. Quantification of carbon sequestration in urban forests. *arXiv preprint arXiv:2106.00182*.

Kinnunen, A., Talvitie, I., Ottelin, J., Heinonen, J. and Junnila, S., 2022. Carbon sequestration and storage potential of urban residential environment–A review. *Sustainable Cities and Society*, *84*, p.104027.

Köhl, M., Neupane, P.R. and Lotfiomran, N., 2017. The impact of tree age on biomass growth and carbon accumulation capacity: A retrospective analysis using tree ring data of three tropical tree species grown in natural forests of Suriname. *Plos one*, *12*(8), p.e0181187.

Kukkonen, M.O., Khamis, M., Muhammad, M.J., Käyhkö, N. and Luoto, M., 2022. Modeling direct above-ground carbon loss due to urban expansion in Zanzibar City Region, Tanzania. *Land Use Policy*, 112, p.105810.

Kuddus, M.A., Tynan, E. and McBryde, E., 2020. Urbanisation: a problem for the rich and the poor?. *Public health reviews*, 41, pp.1-4.

Kuang, W., Du, G., Lu, D., Dou, Y., Li, X., Zhang, S., Chi, W., Dong, J., Chen, G., Yin, Z. and Pan, T., 2021. Global observation of urban expansion and land-cover dynamics using satellite big-data. *Science Bulletin*, *66*(4), pp.297-300.

Larondelle, N. and Haase, D., 2013. Urban ecosystem services assessment along a rural–urban gradient: A cross-analysis of European cities. *Ecological indicators*, 29, pp.179-190.

Lähde, E. and Di Marino, M., 2019. Multidisciplinary collaboration and understanding of green infrastructure Results from the cities of Tampere, Vantaa and Jyväskylä (Finland). *Urban forestry & urban greening*, 40, pp.63-72.

Liu, X., Wang, S., Wu, P., Feng, K., Hubacek, K., Li, X. and Sun, L., 2019. Impacts of urban expansion on terrestrial carbon storage in China. *Environmental science & technology*, *53*(12), pp.6834-6844.

Locatelli, B., 2016. Ecosystem services and climate change. *In Routledge handbook of ecosystem services (*pp. 481-490). Routledge.

Lorenz, K., Lal, R., Lorenz, K. and Lal, R., 2018. Carbon sequestration in grassland soils. *Carbon sequestration in agricultural ecosystems*, pp.175-209.

Lolu, A.J., Ahluwalia, A.S., Sidhu, M.C., Reshi, Z.A. and Mandotra, S.K., 2020. Carbon sequestration and storage by wetlands: Implications in the climate change scenario. R*estoration of wetland ecosystem: A trajectory towards a sustainable environmen*t, pp.45-58.

Luo, Y., Xu, L., Li, Z., Zhou, X., Zhang, X., Wang, F., Peng, J., Cao, C., Chen, Z. and Yu, H., 2023. Air pollution in heavy industrial cities along the northern slope of the Tianshan Mountains, Xinjiang: characteristics, meteorological influence, and sources. *Environmental Science and Pollution Research*, *30*(19), pp.55092-55111.

Lu, J., Li, B., Li, H. and Al-Barakani, A., 2021. Expansion of city scale, traffic modes, traffic congestion, and air pollution. *Cities*, *108*, p.102974.

Ma, X., Wang, C., Dong, B., Gu, G., Chen, R., Li, Y., Zou, H., Zhang, W. and Li, Q., 2019. Carbon emissions from energy consumption in China: its measurement and driving factors. *Science of the total environment*, 648, pp.1411-1420.

Ma, S., Wang, L.J., Jiang, J. and Zhao, Y.G., 2024. Land use/land cover change and soil property variation increased flood risk in the black soil region, China, in the last 40 years. *Environmental Impact Assessment Review*, 104, p.107314.

Mawasha, T.S. and Britz, W., 2021. Hydrological impacts of land use-land cover change on urban flood hazard: A case study of the Jukskei River in Alexandra Township, Johannesburg, South Africa. *South African Journal of Geomatics*, *10*(2), pp.139-162.

Mandle, L., Wolny, S., Bhagabati, N., Helsingen, H., Hamel, P., Bartlett, R., Dixon, A., Horton, R., Lesk, C., Manley, D., Mel, M.D., Bader, D., Myint, S.N.W., Myint, W., Mon, M.S., 2017. Assessing ecosystem service provision under climate change to support conservation and development planning in Myanmar. *PLOS ONE* 12, e0184951. https://doi.org/10.1371/journal.pone.0184951

Mandle, L., Shields-Estrada, A., Chaplin-Kramer, R., Mitchell, M.G., Bremer, L.L., Gourevitch, J.D., Hawthorne, P., Johnson, J.A., Robinson, B.E., Smith, J.R. and Sonter, L.J., 2021. Increasing decision relevance of ecosystem service science. *Nature Sustainability*, *4*(2), pp.161-169.

Ma, S., Wang, L.J., Jiang, J. and Zhao, Y.G., 2024. Land use/land cover change and soil property variation increased flood risk in the black soil region, China, in the last 40 years. *Environmental Impact Assessment Review*, *104*, p.107314.

Mao, D., He, X., Wang, Z., Tian, Y., Xiang, H., Yu, H., Man, W., Jia, M., Ren, C. and Zheng, H., 2019. Diverse policies leading to contrasting impacts on land cover and ecosystem services in Northeast China. *Journal of Cleaner Production*, 240, p.117961.

Marulli, J. and Mallarach, J.M., 2005. A GIS methodology for assessing ecological connectivity: application to the Barcelona Metropolitan Area. *Landscape and urban planning*, 71(2-4), pp.243-262.

Marcotullio, P.J., Keßler, C., Quintero Gonzalez, R. and Schmeltz, M., 2021. Urban growth and heat in tropical climates. *Frontiers in Ecology and Evolution*, *9*, p.616626.

Mandelmilch, M., Ferenz, M., Mandelmilch, N. and Potchter, O., 2020. Urban spatial patterns and heat exposure in the Mediterranean City of Tel Aviv. *Atmosphere*, *11*(9), p.963.

Mayer-Pinto, M., Cole, V.J., Johnston, E.L., Bugnot, A., Hurst, H., Airoldi, L., Glasby, T.M. and Dafforn, K.A., 2018. Functional and structural responses to marine urbanisation. *Environmental Research Letters*, 13(1), p.014009.

Massey, R. and Gunter, A., 2020. Urban geography in South Africa. *Springer*, Johannesburg.

McGrane, S.J., 2016. Impacts of urbanisation on hydrological and water quality dynamics, and urban water management: a review. *Hydrological Sciences Journal*, 61(13), pp.2295-2311.

McKay, T.J.M. and Tantoh, H.B., 2021. A dialogue approach to stakeholder engagement with urban communities: The case of Mofolo Park, Soweto, Johannesburg, South Africa. *Journal of Environmental Planning and Management*, 64(12), pp.2172-2191.

McPhearson, T., Andersson, E., Elmqvist, T. and Frantzeskaki, N., 2015. Resilience of and through urban ecosystem services. *Ecosystem Services*, 12, pp.152-156.

Meili, N., Manoli, G., Burlando, P., Carmeliet, J., Chow, W.T., Coutts, A.M., Roth, M., Velasco, E., Vivoni, E.R. and Fatichi, S., 2021. Tree effects on urban microclimate: Diurnal, seasonal, and climatic temperature differences explained by separating radiation, evapotranspiration, and roughness effects. *Urban Forestry & Urban Greening*, 58, p.126970.

Merwe,J., 2016.The urban structure of South West Africa/Namibia viewed with a Third-world Framework. In *Geography Research Forum.*

Mngadi, M., Odindi, J. and Mutanga, O., 2021. The Utility of Sentinel-2 Spectral Data in Quantifying Above-Ground Carbon Stock in an Urban Reforested Landscape. *Remote Sensing*, 13(21), p.4281.

Miller, J.D. and Hess, T., 2017. Urbanisation impacts on storm runoff along a rural-urban gradient. *Journal of Hydrology*, 552, pp.474-489.

Milliken, S., 2018. Ecosystem services in urban environments. In *Nature based strategies for urban and building sustainability* (pp. 17-27). Butterworth-Heinemann.

Mngumi, L.E., 2020. Ecosystem services potential for climate change resilience in peri-urban areas in Sub-Saharan Africa. *Landscape and Ecological Engineering*, 16(2), pp.187-198.

Mngumi, L.E., 2020b. Ecosystem services potential for climate change resilience in peri-urban areas in Sub-Saharan Africa. *Landscape and Ecological Engineering.* 16, 187198.

Mildrexler, D.J., Berner, L.T., Law, B.E., Birdsey, R.A. and Moomaw, W.R., 2020. Large trees dominate carbon storage in forests east of the cascade crest in the United States Pacific Northwest. *Frontiers in Forests and Global Change*, p.127.

Mudede, M.F., Newete, S.W., Abutaleb, K. and Nkongolo, N., 2020. Monitoring the urban environment quality in the city of Johannesburg using remote sensing data. *Journal of African Earth Sciences*, *171*, p.103969

Nathaniel, S.P., 2021. Natural resources, urbanisation, economic growth and the ecological footprint in South Africa: the moderating role of human capital. *Quaestiones Geographicae*, 40(2), pp.63-76.

Nhamo, L., Rwizi, L., Mpandeli, S., Botai, J., Magidi, J., Tazvinga, H., Sobratee, N., Liphadzi, S., Naidoo, D., Modi, A.T. and Slotow, R., 2021. Urban nexus and transformative pathways towards a resilient Gauteng City-Region, South Africa. *Cities*, 116, p.103266.

Nimish, G., Bharath, H.A. and Lalitha, A., 2020. Exploring temperature indices by deriving relationship between land surface temperature and urban landscape. *Remote Sensing Applications: Society and Environment*, *18*, p.100299.

Nowak, D.J. and Crane, D.E., 2002. Carbon storage and sequestration by urban trees in the USA. *Environmental pollution*, 116(3), pp.381-389.

Oke, T.R., Mills, G., Christen, A. and Voogt, J.A., 2017. Urban climates. *Cambridge University Press*.

Pace, R., De Fino, F., Rahman, M.A., Pauleit, S., Nowak, D.J. and Grote, R., 2021. A single tree model to consistently simulate cooling, shading, and pollution uptake of urban trees. *International Journal of Biometeorology*, 65, pp.277-289.

Pamukcu-Albers, P., Ugolini, F., La Rosa, D., Grădinaru, S.R., Azevedo, J.C. and Wu, J., 2021. Building green infrastructure to enhance urban resilience to climate change and pandemics. *Landscape ecology*, 36(3), pp.665-673.

Pandey, B., Reba, M., Joshi, P.K. and Seto, K.C., 2020. Urbanization and food consumption in India. *Scientific reports*, 10(1), p.17241.

Pascual, A., Giardina, C.P., Selmants, P.C., Laramee, L.J. and Asner, G.P., 2021. A new remote sensing-based carbon sequestration potential index (CSPI): A tool to support land carbon management. *Forest Ecology and Management*, 494, p.119343.

Pascual, A., Giardina, C.P., Selmants, P.C., Laramee, L.J., Asner, G.P., 2021b. A new remote sensing-based carbon sequestration potential index (CSPI): A tool to support land carbon management. *Forest Ecology and Management*. 494, 119343.

Pataki, D.E., Carreiro, M.M., Cherrier, J., Grulke, N.E., Jennings, V., Pincetl, S., Pouyat, R.V., Whitlow, T.H. and Zipperer, W.C., 2011. Coupling biogeochemical cycles in urban environments: ecosystem services, green solutions, and misconceptions. F*rontiers in Ecology and the Environment*, 9(1), pp.27-36.

Pattison-Williams, J.K., Pomeroy, J.W., Badiou, P. and Gabor, S., 2018. Wetlands, flood control and ecosystem services in the Smith Creek Drainage Basin: A case study in Saskatchewan, Canada. *Ecological economic*s, 147, pp.36-47.

Pappalardo, V., La Rosa, D., Campisano, A. and La Greca, P., 2017. The potential of green infrastructure application in urban runoff control for land use planning: A preliminary evaluation from a southern Italy case study. *Ecosystem Services*, 26, pp.345-354.

Pauchard, A., Aguayo, M., Peña, E. and Urrutia, R., 2006. Multiple effects of urbanization on the biodiversity of developing countries: the case of a fast-growing metropolitan area (Concepción, Chile). *Biological conservation*, 127(3), pp.272-281.

Paudel, S. and States, S., 2023. Urban green spaces and sustainability: exploring the ecosystem services and disservices of grassy lawns versus floral meadows. *Urban Forestry & Urban Greening*, p.127932.

Peberdy, S., Harrison, P. and Dinath, Y., 2017. Uneven spaces: Core and periphery in the Gauteng City-Region. Peberdy, S., Philip, H. and Dinath, Y., 2017. Uneven spaces: core and periphery in the Gauteng City-Region (Issue 06). *GCRO*, Johannesburg.

Peng, L., Zhang, L., Li, X., Wang, P., Zhao, W., Wang, Z., Jiao, L. and Wang, H., 2022. Spatio-Temporal Patterns of Ecosystem Services Provided by Urban Green Spaces and Their Equity along Urban–Rural Gradients in the Xi'an Metropolitan Area, China. *Remote Sensing*, *14*(17), p.4299.

Peng, J., Wang, X., Liu, Y., Zhao, Y., Xu, Z., Zhao, M., Qiu, S. and Wu, J., 2020. Urbanisation impact on the supply-demand budget of ecosystem services: Decoupling analysis. *Ecosystem Services*, *44*, p.101139.

Pelorosso, R., Gobattoni, F., Geri, F., Monaco, R., Leone, A., 2016. Evaluation of Ecosystem Services related to Bio-Energy Landscape Connectivity (BELC) for land use decision making across different planning scales. Ecol. Indic. 61, 114–129. https://doi.org/10.1016/j.ecolind.2015.01.016

Piracha, A. and Chaudhary, M.T., 2022. Urban air pollution, urban heat island and human health: a review of the literature. *Sustainability*, *14*(15), p.9234.

Potgieter, L.J., Douwes, E., Gaertner, M., Measey, J., Paap, T., Richardson, D.M., 2020. Biological Invasions in South Africa's Urban Ecosystems: Patterns, Processes, Impacts, and Management, in: van Wilgen, B.W., Measey, J., Richardson, D.M., Wilson, J.R., Zengeya, T.A. (Eds.), Biological Invasions in South Africa, Invading Nature - Springer Series in Invasion Ecology. *Springer International Publishing*, Cham, pp. 275–309. https://doi.org/10.1007/978-3-030-32394-3_11

Portela, C.I., Massi, K.G., Rodrigues, T. and Alcântara, E., 2020. Impact of urban and industrial features on land surface temperature: Evidence from satellite thermal indices. *Sustainable Cities and Society*, 56, p.102100.

Radebe, S.D., 2018. An assessment of amount, distribution and use of urban green spaces in small towns of the Eastern Cape. Unpublished Master's thesis*). Grahamstown: Rhodes University*.

Rahman, M.A., Moser, A., Gold, A., Rötzer, T. and Pauleit, S., 2018. Vertical air temperature gradients under the shade of two contrasting urban tree species during different types of summer days. *Science of the Total Environment*, 633, pp.100-111.

Rahman, M.A., Stratopoulos, L.M., Moser-Reischl, A., Zölch, T., Häberle, K.H., Rötzer, T., Pretzsch, H. and Pauleit, S., 2020. Traits of trees for cooling urban heat islands: A meta-analysis. *Building and Environment*, 170, p.106606.

Ramiaramanana, F.N. and Teller, J., 2021. Urbanization and floods in sub-saharan africa: spatiotemporal study and analysis of vulnerability factors—case of antananarivo agglomeration (Madagascar). *Water*, 13(2), p.149.

Rau, A.L., Burkhardt, V., Dorninger, C., Hjort, C., Ibe, K., Keßler, L., Kristensen, J.A., McRobert, A., Sidemo-Holm, W., Zimmermann, H. and Abson, D.J., 2020. Temporal patterns in ecosystem services research: A review and three recommendations. *Ambio*, 49(8), pp.1377-1393.

Russo, A. and Cirella, G.T., 2021. Urban Ecosystem Services: Current Knowledge, Gaps, and Future Research. Land 2021, 10, 811. *Urban Ecosystem Services II*, p.1.

Saurav, K.C., Shrestha, S., Ninsawat, S. and Chonwattana, S., 2021. Predicting flood events in Kathmandu Metropolitan City under climate change and urbanisation. *Journal of Environmental Management*, 281, p.111894.

Sager, M., 2020. Urban soils and road dust—civilization effects and metal pollution—a review. *Environments*, 7(11), p.98.

Sathyakumar, V., Ramsankaran, R.A.A.J. and Bardhan, R., 2019. Linking remotely sensed Urban Green Space (UGS) distribution patterns and Socio-Economic Status (SES)-A multi-scale probabilistic analysis based in Mumbai, India. *GIScience & remote sensing*, 56(5), pp.645-669.

Salbitano, F., Borelli, S., Conigliaro, M., Yahya, N.A., Sanesi, G., Chen, Y. and Corzo, G.T., 2017. Urban forest benefits in developing and industrializing countries. *In Routledge handbook of urban forestry* (pp. 136-151). *Routledge*.

Sadiq Khan, M., Ullah, S., Sun, T., Rehman, A.U. and Chen, L., 2020. Land-use/land-cover changes and its contribution to urban heat Island: A case study of Islamabad, Pakistan. *Sustainability*, *12*(9), p.3861.

Santamouris, M., Ding, L. and Osmond, P., 2019. Urban heat island mitigation. *Decarbonising the Built Environment: Charting the Transition*, pp.337-355.

Schäffler, A. and Swilling, M., 2013. Valuing green infrastructure in an urban environment under pressure - The Johannesburg case. *Ecological economics*, 86, pp.246-257.

Schüler, G., 2006. Identification of flood-generating forest areas and forestry measures for water retention. *Forest Snow and Landscape Research* 80.

Schütte, S. and Schulze, R.E., 2017. Projected impacts of urbanisation on hydrological resource flows: A case study within the uMngeni Catchment, South Africa. *Journal of environmental management*, 196, pp.527-543.

Seto, K.C., Fragkias, M., 2011. A Meta-Analysis of Global Urban Land Expansion. *PLoS ONE* 6, 9.

Seraphim, A.P.A., Bezerra, M.L. and Oliveira, A.N., 2019. Implication of urban occupation patterns in the natural infiltration. *In Proceedings of the Fábos Conference on Landscape and Greenway Planning* (Vol. 6, No. 1, p. 22).

Schwaab, J., Meier, R., Mussetti, G., Seneviratne, S., Bürgi, C. and Davin, E.L., 2021. The role of urban trees in reducing land surface temperatures in European cities. *Nature communications*, 12(1), p.6763.

Sharma, R., Pradhan, L., Kumari, M. and Bhattacharya, P., 2020. Assessment of carbon sequestration potential of tree species in Amity University Campus Noida. *Environmental Sciences Proceedings*, 3(1), p.52.

Shafique, M., Xue, X. and Luo, X., 2020. An overview of carbon sequestration of green roofs in urban areas. *Urban Forestry & Urban Greening*, 47, p.126515.

Singh, H., Nielsen, M. and Greatrex, H., 2023. Causes, impacts, and mitigation strategies of urban pluvial floods in India: A systematic review. *International Journal of Disaster Risk Reduction*, p.103751.

Singh, N., Singh, S. and Mall, R.K., 2020. Urban ecology and human health: implications of urban heat island, air pollution and climate change nexus. In *Urban Ecology* (pp. 317-334). Elsevier.

Sobrino, J.A. and Raissouni, N., 2000. Toward remote sensing methods for land cover dynamic monitoring: Application to Morocco. *International journal of remote sensing*, *21*(2), pp.353-366.

Steber, A., Brooks, K., Perry, C.H. and Randy, K., 2007. Surface compaction estimates and soil sensitivity in aspen stands of the Great Lakes States. *Northern Journal of Applied Forestry*, *24*(4), pp.276-281.

Semeraro, T., Scarano, A., Buccolieri, R., Santino, A. and Aarrevaara, E., 2021. Planning of urban green spaces: An ecological perspective on human benefits. *Land*, 10(2), p.105.

Sultana, M., 2020. The effect of urbanisation on environment: with special reference to the city of Guwahati, Assam. P*alArch's Journal of Archaeology of Egypt/Egyptology*, 17(9), pp.98-105.

Symes, C.T., Roller, K., Howes, C., Lockwood, G. and van Rensburg, B.J., 2017. Grassland to urban forest in 150 years: avifaunal response in an African metropolis. *Ecology and conservation of birds in urban environments*, pp.309-341.

Tak, A.A. and Kakde, U.B., 2020. Analysis of carbon sequestration by dominant trees in urban areas of Thane city. *International Journal of Global Warming*, *20*(1), pp.1-11.

Tao, Y., Li, F., Liu, X., Zhao, D., Sun, X. and Xu, L., 2015. Variation in ecosystem services across an urbanization gradient: A study of terrestrial carbon stocks from Changzhou, China. *Ecological Modelling*, 318, pp.210-216.

Tan, P.Y., Zhang, J., Masoudi, M., Alemu, J.B., Edwards, P.J., Grêt-Regamey, A., Richards, D.R., Saunders, J., Song, X.P. and Wong, L.W., 2020. A conceptual framework to untangle the concept of urban ecosystem services. *Landscape and urban planning*, *200*, p.103837.

Totaforti, S., 2020. Urban planning in post-apartheid South African cities: The case of Johannesburg. *Open Journal of Political Science*, 10(3), pp.507-520.

Theodorou, P., 2022. The effects of urbanisation on ecological interactions. *Current Opinion in Insect Science*, p.100922.

Thomas, S.C. and Malczewski, G., 2007. Wood carbon content of tree species in Eastern China: Interspecific variability and the importance of the volatile fraction. J*ournal of Environmental Management*, 85(3), pp.659-662.

Tian, Y., Tsendbazar, N.E., van Leeuwen, E. and Herold, M., 2022. Mapping urban–rural differences in the worldwide achievement of sustainable development goals: land-energy-air nexus. *Environmental Research Letters*, 17(11), p.114012.

Tiwari, A., Kumar, P., Kalaiarasan, G. and Ottosen, T.B., 2021. The impacts of existing and hypothetical green infrastructure scenarios on urban heat island formation. *Environmental Pollution*, 274, p.115898.

Threlfall, C.G. and Kendal, D., 2018. The distinct ecological and social roles that wild spaces play in urban ecosystems. *Urban Forestry & Urban Greening*, *29*, pp.348-356.

Tseane-Gumbi, L.A. and Ojakorotu, V., 2021. Muddling through destination marketing: experiences from the North West Province, South Africa. *African Journal of Hospitality*, pp.592-607.

Turpie, J.K., Forsythe, K.J., Knowles, A., Blignaut, J. and Letley, G., 2017. Mapping and valuation of South Africa's ecosystem services: A local perspective. *Ecosystem service*s, 27, pp.179-192.

Udara Willhelm Abeydeera, L.H., Wadu Mesthrige, J. and Samarasinghalage, T.I., 2019. Global research on carbon emissions: A scientometric review. *Sustainability*, 11(14), p.3972.

United Nations, Department of Economic and Social Affairs, Population Division., 2019. World Urbanisation Prospects 2018: Highlights (ST/ESA/SER.A/421). *United Nations*
ISBN: 978-92-1-148318-5.

Upreti, R., Wang, Z.H. and Yang, J., 2017. Radiative shading effect of urban trees on cooling the regional built environment. *Urban Forestry & Urban Greening*, 26, pp.18-24.

Vakhlamova, T., Rusterholz, H.P., Kanibolotskaya, Y. and Baur, B., 2014. Changes in plant diversity along an urban–rural gradient in an expanding city in Kazakhstan, Western Siberia. *Landscape and urban planning*, 132, pp.111-120.

Vargo, J., Habeeb, D. and Stone Jr, B., 2013. The importance of land cover change across urban–rural typologies for climate modeling. *Journal of environmental management*, 114, pp.243-252.

Vargas-Hernández, J.G., Pallagst, K. and Zdunek-Wielgołaska, J., 2018. Urban green spaces as a component of an ecosystem. *Handbook of engaged sustainability*, pp.1-32.

Vega, K.A. and Küffer, C., 2021. Promoting wildflower biodiversity in dense and green cities: The important role of small vegetation patches. *Urban Forestry & Urban Greening*, 62, p.127165.

Veena, K., Parammasivam, K.M. and Venkatesh, T.N., 2020. Urban Heat Island studies: Current status in India and a comparison with the International studies. *Journal of Earth System Science, 129*, pp.1-15.

Venter, Z.S., Shackleton, C.M., Van Staden, F., Selomane, O. and Masterson, V.A., 2020. Green Apartheid: Urban green infrastructure remains unequally distributed across income and race geographies in South Africa. *Landscape and Urban Planning*, 203, p.103889.

Vereecken, H., Amelung, W., Bauke, S.L., Bogena, H., Brüggemann, N., Montzka, C., Vanderborght, J., Bechtold, M., Blöschl, G., Carminati, A. and Javaux, M., 2022. Soil hydrology in the Earth system. *Nature Reviews Earth & Environment*, *3*(9), pp.573-587.

Vujovic, S., Haddad, B., Karaky, H., Sebaibi, N. and Boutouil, M., 2021. Urban heat island: Causes, consequences, and mitigation measures with emphasis on reflective and permeable pavements. *CivilEng*, *2*(2), pp.459-484.

Wang, R., Bai, Y., Alatalo, J.M., Guo, G., Yang, Z., Yang, Z. and Yang, W., 2022. Impacts of Urbanisation at city cluster scale on ecosystem services along an urban–rural gradient: a case study

of Central Yunnan City Cluster, China. *Environmental Science and Pollution Research*, *29*(59), pp.88852-88865.

Wang, S., Hu, M., Wang, Y. and Xia, B., 2022. Dynamics of ecosystem services in response to urbanisation across temporal and spatial scales in a mega metropolitan area. *Sustainable Cities and Society*, *77*, p.103561.

Wang, J., Hu, C., Ma, B. and Mu, X., 2020. Rapid urbanisation impact on the hydrological processes in Zhengzhou, China. *Water*, 12(7), p.1870.

Wang, X.C., Klemeš, J.J., Dong, X., Fan, W., Xu, Z., Wang, Y. and Varbanov, P.S., 2019. Air pollution terrain nexus: A review considering energy generation and consumption. *Renewable and Sustainable Energy Reviews*, *105*, pp.71-85.

Wang, J., Zhou, W., Wang, J. and Qian, Y., 2019. From quantity to quality: enhanced understanding of the changes in urban greenspace. *Landscape Ecology*, *34*, pp.1145-1160.

Winbourne, J.B., Jones, T.S., Garvey, S.M., Harrison, J.L., Wang, L., Li, D., Templer, P.H. and Hutyra, L.R., 2020. Tree transpiration and urban temperatures: current understanding, implications, and future research directions. *BioScience*, *70*(7), pp.576-588.

Xu, H., Lin, D. and Tang, F., 2013. The impact of impervious surface development on land surface temperature in a subtropical city: Xiamen, China. *International Journal of Climatology*, *33*(8), pp.1873-1883.

Warr, P., 2020. Urbanisation and the Demand for Food. *Bulletin of Indonesian Economic Studies*, 56(1), pp.43-86.

Weiskopf, S.R., Rubenstein, M.A., Crozier, L.G., Gaichas, S., Griffis, R., Halofsky, J.E., Hyde, K.J., Morelli, T.L., Morisette, J.T., Muñoz, R.C. and Pershing, A.J., 2020. Climate change effects on biodiversity, ecosystems, ecosystem services, and natural resource management in the United States. *Science of the Total Environment*, 733, p.137782.

While, A. and Whitehead, M., 2013. Cities, urbanisation and climate change. *Urban Studies*, 50(7), pp.1325-1331.

Wu, Y., Zhang, G., Rousseau, A.N., Xu, Y.J. and Foulon, É., 2020. On how wetlands can provide flood resilience in a large river basin: a case study in Nenjiang river Basin, China. *Journal of Hydrology*, 587, p.125012.

Wu, Y., Wu, Y., Li, C., Gao, B., Zheng, K., Wang, M., Deng, Y. and Fan, X., 2022. Spatial relationships and impact effects between urbanisation and ecosystem health in urban agglomerations along the Belt and Road: a case study of the Guangdong-Hong Kong-Macao Greater Bay Area. *International Journal of Environmental Research and Public Health*, *19*(23), p.16053.

Xia, H., Zhao, J., Qin, Y., Yang, J., Cui, Y., Song, H., Ma, L., Jin, N. and Meng, Q., 2019. Changes in water surface area during 1989–2017 in the Huai River Basin using Landsat data and Google earth engine. *Remote Sensing*, *11*(15), p.1824.

Yang, Y., Liu, Y., Li, Y. and Du, G., 2018. Quantifying spatio-temporal patterns of urban expansion in Beijing during 1985–2013 with rural-urban development transformation. *Land use policy*, 74, pp.220-230.

Yang, J.L. and Zhang, G.L., 2015. Formation, characteristics and eco-environmental implications of urban soils–A review. *Soil science and plant nutrition*, *61*(sup1), pp.30-46.

Yu, D., Xun, B., Shi, P., Shao, H. and Liu, Y., 2012. Ecological restoration planning based on connectivity in an urban area. *Ecological engineering*, 46, pp.24-33.

Yun, X., Shen, G., Shen, H., Meng, W., Chen, Y., Xu, H., Ren, Y., Zhong, Q., Du, W., Ma, J. and Cheng, H., 2020. Residential solid fuel emissions contribute significantly to air pollution and associated health impacts in China. *Science advances*, *6*(44), p.eaba7621.

Zhang, Z., Peng, J., Xu, Z., Wang, X. and Meersmans, J., 2021. Ecosystem services supply and demand response to urbanisation: A case study of the Pearl River Delta, China. *Ecosystem Services*, *49*, p.101274.

Zhang, Y., Harris, A. and Balzter, H., 2015. Characterizing fractional vegetation cover and land surface temperature based on sub-pixel fractional impervious surfaces from Landsat TM/ETM+. *International Journal of Remote Sensing*, 36(16), pp.4213-4232.

Zhou, D., Tian, Y. and Jiang, G., 2018. Spatio-temporal investigation of the interactive relationship between urbanization and ecosystem services: Case study of the Jingjinji urban agglomeration, China. *Ecological indicators*, 95, pp.152-164.

Zhu, G., Qiu, D., Zhang, Z., Sang, L., Liu, Y., Wang, L., Zhao, K., Ma, H., Xu, Y. and Wan, Q., 2021. Land-use changes lead to a decrease in carbon storage in arid region, China. *Ecological Indicators*, 127, p.107770.